



Acceleration of the hydrological cycle and its impact on water availability over land: an adverse effect of climate change

Laraib Ehtasham¹, Sadia Hassan Sherani, Faheem Nawaz

Department of Environmental Science, Balochistan University of Information Technology, Engineering and Management Sciences (BUIITEMS), Quetta, Pakistan

Abstract

The hydrological cycle, or water cycle, is one of the most important geochemical cycles on our planet. Normal functioning of its mechanisms (evaporation/evapotranspiration, condensation, and precipitation) is very important for the well-being of human beings. However, the acceleration of the hydrological cycle, mainly due to global warming, is increasing the frequency and intensity of extreme events (floods, droughts, and alterations in water resources) in many regions around the globe. This acceleration or intensification occurs because of rising temperature, which intensifies and speeds up evaporation (probable increase of 5.2%) and precipitation (probable increase of 6.5%); hence this scenario is escalating climate change. According to the datasets retrieved from the Global Land Data Assimilation System (GLDAS) of NASA, rain precipitation rate has shown changes in various regions of the world. Consequently, extreme and frequent events of heavy precipitation, floods, and droughts are also deteriorating the quality of water and preventing recharge of water reservoirs. Although some regions of the world will experience positive outcomes of this scenario in terms of water availability (due to frequent intense precipitation), most of the world's regions are expected to face the daunting issue of water unavailability, as predicted by many researchers.

Keywords

Hydrological cycle; evaporation; precipitation; water availability; climate change.

Submitted 1 February 2024, revised 15 February 2024, accepted 20 May 2024

DOI: 10.26491/mhwm/188920

1. Introduction

Our Earth is covered by 30% solid land and 70% water. Of the total water content on Earth, 97% is saline water in oceans and seas. The remaining 3% is freshwater, out of which almost 2% is in the form of glaciers and polar ice caps; and the remaining 1% is above ground (streams, lakes, rivers, etc.). Moreover, the fraction of fresh water available for human consumption is only 0.01% (Sherani 2020). In Earth's atmosphere and hydrosphere systems, one of the important phenomena is the continuous circulation of water, which is commonly referred to as the hydrological cycle. The hydrological cycle, or water cycle, is the sum of all processes in which water moves from the land and ocean surfaces to the atmosphere and then back toward the Earth's surface in the form of precipitation. Thus, the hydrological cycle is Earth's water recycling system (Graham et al. 2010).

Generally, in the hydrological cycle, water evaporation from the land and ocean surface is about 496,000 cubic km annually; residence time in the atmosphere is about 10 days before precipitating as either rain or snow (Eki 2017). Half of the total solar radiation received at Earth's surface is expended to evaporate water. Furthermore, one-third of the precipitation falling on land runs off into the oceans (Britannica 2020). Direct

groundwater discharge to the oceans accounts for only 0.6% of the total discharge, and only a small proportion of precipitation is stored in rivers and lakes. The remaining precipitation over land ($73,000 \text{ km}^3/\text{y}$) returns to the atmosphere by evaporation (Britannica 2020). Various studies have revealed that the evaporation process by which water changes from a liquid to a gas from seas, oceans, and other water bodies like rivers, lakes, and streams provides nearly 90% of the moisture in our atmosphere. In addition, the remaining 10% in the atmosphere is released by plants through transpiration. A very small proportion of water vapor enters the atmosphere via the process of sublimation (in which water changes directly from solid snow or ice into a gas) (Graham et al. 2010).

Another process in the water cycle is known as condensation, in which water vapor is transformed into the liquid state (Graham et al. 2010). Water vapor is the primary form of atmospheric moisture in the troposphere at altitudes of 10-13 km. Furthermore, water vapor is very important as a supply of moisture for frost, fog, dew, clouds, and precipitation (Li et al. 2020). Condensation is rapid when air contains more water vapor than it receives from evaporation at the prevailing temperature. This condition occurs due to two phenomena: either cooling or the mixing of air masses of different temperatures. As the condensation process completes, the water vapor in the atmosphere is released in the form of precipitation (the last phase of the water cycle) (Britannica 2020). Through a review of relevant literature, this paper focuses on highlighting the acceleration or intensification of the hydrological cycle around the globe, along with describing its overall potential impact on water availability.

2. Methodology

This study encompasses analysis based on a literature review regarding the topic of hydrological cycle acceleration and water availability over land. Various research papers were searched and reviewed, from research databases like PubMed, Research, Web of Science, JSTOR, ScienceDirect, ResearchGate, etc. Data were also obtained from US-EPA sites. The topic was examined with the help of various studies that have been conducted in various regions around the globe.

For the satellite remote sensing analysis in this study, raster data (in NetCDF format) of rain precipitation rate were obtained from the Global Land Data Assimilation System (GLDAS) of the National Aeronautics and Space Administration (NASA). The specific dataset was GLDAS Land Surface Model L4 Monthly 1.0 x 1.0 degree V2.1 (Rodell et al. 2004; Beaudoin, Rodell 2020). Subsequently, ArcGIS 10.8 software was used to make maps (depicting 6 continents) of 6 different months (January and July of 2000, 2010, and 2020; see Fig. 4). Shapefiles were retrieved from the online database; thus, the coordinate system is not represented in the maps. The midrange formula, derived from the study of Can and Ozsoy (2023), was calculated via spreadsheet from the aforementioned rainfall rate data to analyze the data:

$$\text{Midrange (M)} = \frac{X(\text{max}) + X(\text{min})}{2}$$

3. Results

3.1. Acceleration of the hydrological cycle

The earth's climate has not remained constant. Instead, it has been evolving over millennia. Isotopic studies of ice cores show that there has been a variety of variations and responses induced by different components of the earth system (Farooqi et al. 2005). Moreover, rapid variations in Earth's climate have also occurred due to anthropogenic activities. For instance, since the Industrial Era (beginning in 1750), the concentrations and emissions of greenhouse gases (GHGs) have been increased. This dynamic has strongly affected climatic processes and caused prominent changes in Earth's climate (Allen, Ingram 2002; Ciaia et al. 2013).

Consequently, the global hydrological cycle is accelerating and intensifying due to global warming and climate change; resulting in increased evaporation, evapotranspiration, water vapor content, and precipitation (Huntington 2005). In addition, human activities are also contributing to the acceleration of the hydrological cycle by increasing loads of sulfate, mineral dust, and black carbon aerosols in the atmosphere that have the potential to affect the hydrological cycle in two ways; one is through the suppression of rainfall in polluted areas, and the other is through reducing the solar irradiance reaching the Earth's surface (Wild et al. 2004). The mechanisms of both these effects originate primarily when aerosols increase the concentrations of cloud condensation nuclei, reduce the mean size of cloud droplets, and finally result in less efficient coalescence into raindrops (Ramanathan et al. 2001). Secondly, these aerosols reduce the surface solar irradiance, thus reducing surface evaporation and precipitation (Huntington 2005).

Hydrological cycle acceleration increases the frequency and intensity of extreme events, such as heavy rainfall, major storms, ocean salinity, and droughts, and ultimately increases the rate of soil erosion (Loaiciga et al. 1996; Held, Soden 2000; Chagas et al. 2022). Several impacts on agriculture (heat stress, diseases, nutrient cycling, and insects) are related to high evaporation rates from soil and plants (Huntington 2005). A very dynamic aspect of hydrological cycle acceleration is the more frequent occurrence of extreme events, an alarming threat to human populations. These drastic events affect human welfare directly through catastrophic damage and indirectly through adverse effects on overall crop productivity (Arnell et al. 2001; Manabe et al. 2004).

3.1.1. Acceleration of evaporation

As mentioned above, the major process in the water cycle is the process of evaporation. In this phase, water in the liquid state is transformed into vapor or gas (Graham et al. 2010). The transformation occurs when some molecules in a water mass have attained sufficient kinetic energy to eject themselves from the water's surface.

There is a multitude of factors that affect the evaporation rate in the water cycle; they include humidity, temperature, wind speed, and, most importantly, solar radiation (Britannica 2020). Simulations based on one of about 20 coupled models (ocean–atmosphere–land models) estimated that global mean evaporation will experience an increase of about 5.2% by 2050, which is a clear sign of the acceleration of the water cycle (Wetherald, Manabe 2002). Figure 1 represents the changes in meteorological parameters that have occurred in the past few decades around the globe.

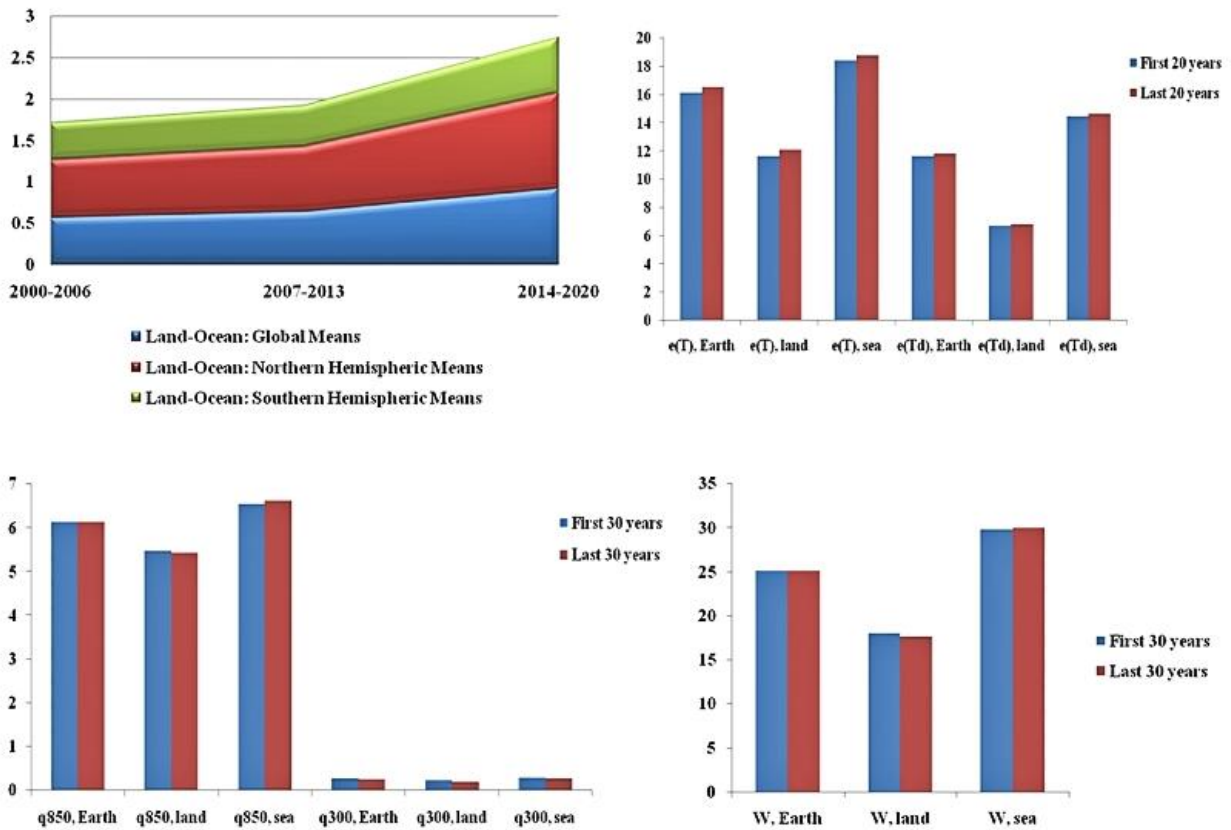


Fig. 1. (a) Global and Hemispheric Monthly Means and Zonal Annual Means based on Land-Ocean Temperature Index or L-OTI (Data source: Lenssen et al. 2019; GISTEMP Team 2023); (b) Water vapor pressures $e(T)$ and $e(Td)$ (Data source: Koutsoyiannis 2020); (c) Specific humidity at 850 hPa and 300 hPa (Data source: Koutsoyiannis 2020); (d) Water vapor amount (Data source: Koutsoyiannis 2020).

3.1.2. Acceleration of precipitation

With the help of precipitation, some amount of water is returned to the atmosphere by evaporation, some is evaporated from the plants by transpiration, some percolates into the soil or ground via infiltration (which may later percolate into streams as groundwater runoff), and the remaining proportion flows directly as surface runoff into the sea (Graham et al. 2010). However, disturbances of all these phenomena related to precipitation are occurring due to the intensification of the water cycle. In this regard, recent modeling studies

suggest that due to increased humidity, precipitation would increase by about 3.4% per degree Kelvin. That amount is less than is suggested by the Clausius–Clayperon relation model that indicates precipitation would increase by about 6.5% because evaporation would be energy-limited as the evapotranspiration rate increases with the rising temperature (Huntington 2005). For instance, Figure 2 shows the precipitation trend (by US-EPA) in the contiguous 48 states of the USA from 1960 to 2020, revealing that these states have been experiencing precipitation increase and hydrological cycle acceleration throughout these years. Moreover, based on climatic changes, changes in the precipitation over small islands have also been estimated (Fig. 3).

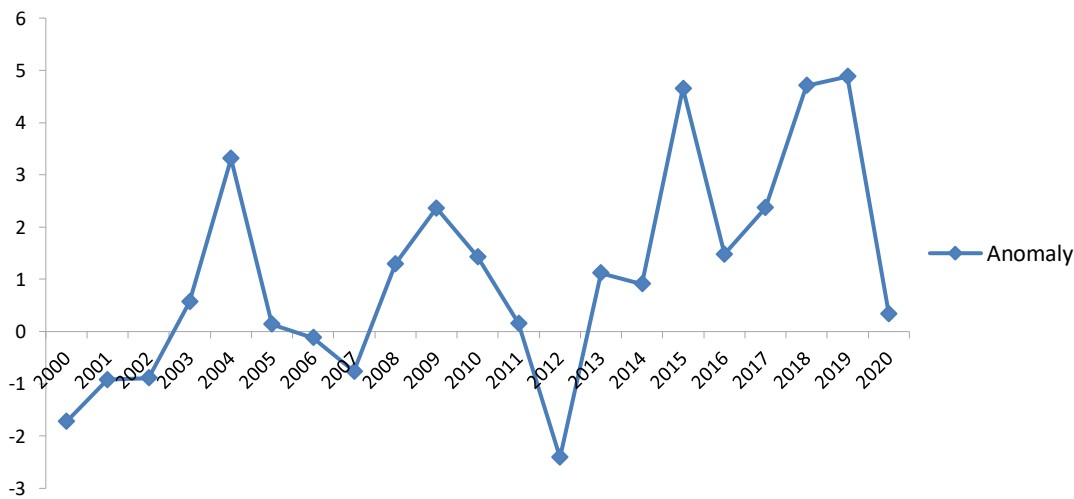


Fig. 2. Precipitation in the contiguous 48 States of USA (1960-2020). Data source: USA-EPA (2021b).

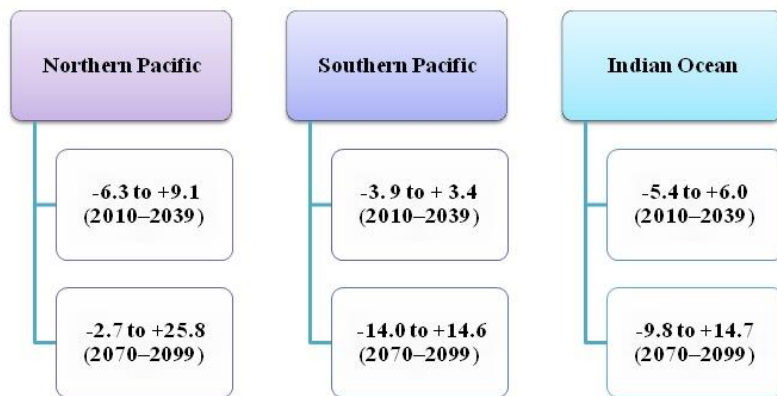


Fig. 3. Projected change in precipitation on small islands (%). Data source: Bates et al. (2008).

Based on the midrange calculation, rainfall rates were $43.096 \text{ kg m}^{-2} \text{ s}^{-1}$ in January 2000, increasing to $43.902 \text{ kg m}^{-2} \text{ s}^{-1}$ in January 2010 (hence representing the changes in the hydrological cycle). The opposite trend was shown for July; midrange values were $42.724 \text{ kg m}^{-2} \text{ s}^{-1}$ (2000), $42.543 \text{ kg m}^{-2} \text{ s}^{-1}$ (2010), and $42.05 \text{ kg m}^{-2} \text{ s}^{-1}$

(2020). These patterns demonstrate that the hydrological cycle has been experiencing changes throughout the world, with either less rainfall and more evaporation or more rainfall and less evaporation. In 2020 (during January), in contrast to 2000 and 2010, the high rainfall rates in areas of Asia near India expanded. Moreover, as compared to 2000 and 2010, the South American region receiving a high rainfall rate expanded in July 2020.

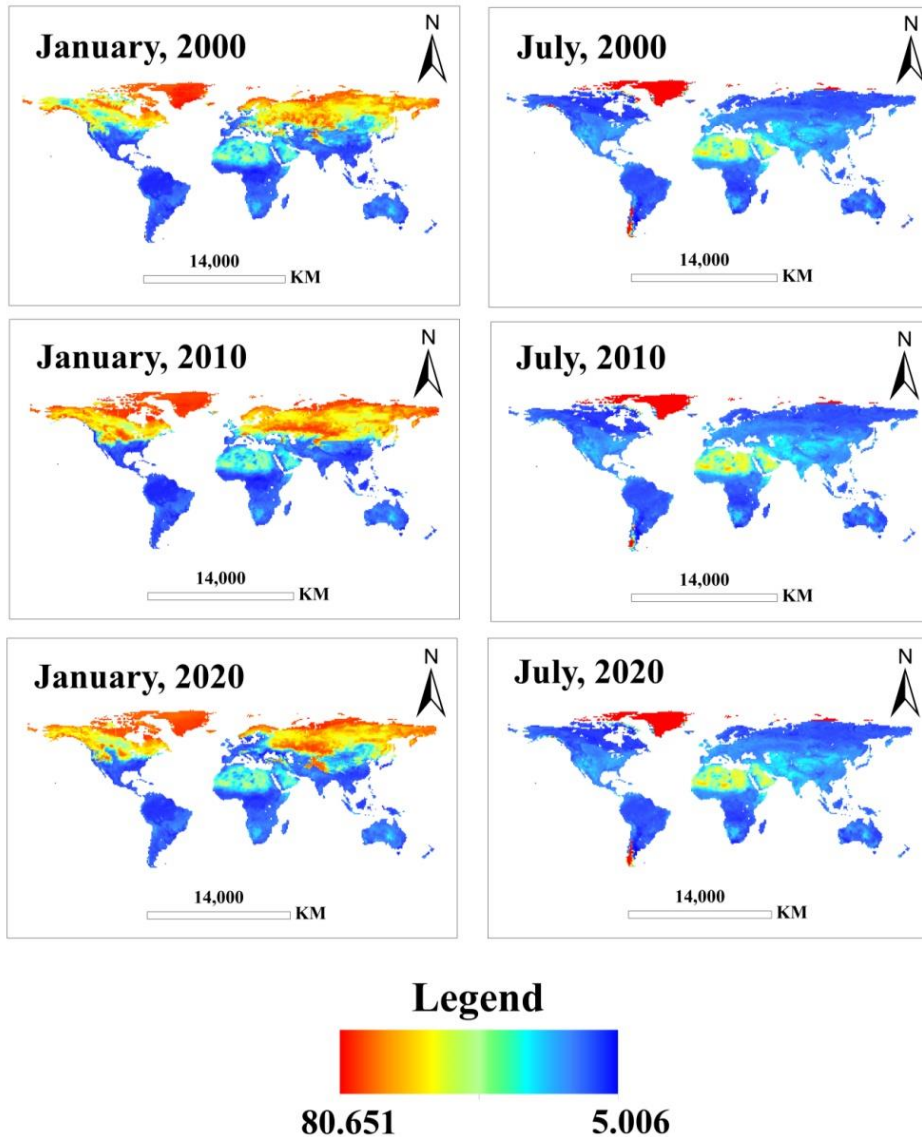


Fig. 4. Maps of rain precipitation ($\text{kg m}^{-2} \text{s}^{-1}$) depicting 6 continents, created in ArcGIS 10.8.

3.2. Evidence from some studies related to acceleration of the hydrological cycle

Following is a brief overview of some studies that can be attributed as evidence of hydrological cycle acceleration. These three studies represent examples of hydrological cycle intensification from three different continents of the world (Asia, North America, and South America).

CHINA

A study indicated an upsurge in precipitation in the regions of Xinjiang, in northwestern China, during 1986-2003. This increasing precipitation was associated with significant warming that occurred during this period, which revealed that the hydrological cycle in Xinjiang region had accelerated. Moreover, it was also found that a significant correlation was present between precipitation and altitude in parts of Xinxiang (including Altay, Tacheng, Tianshan southern slope, Kunlun northern slope, Ili, etc.). At higher altitude stations, there was abundant precipitation (Feng, Wu 2016).

USA

A study in Illinois (midwestern USA) evaluated the acceleration of the terrestrial hydrological cycle over 31 years (1983-2013). The variables that were observed in the study were precipitation, temperature, stream flow, soil moisture, evaporation, and groundwater level. The results showed increasing trends of 8.73 to 9.05 mm/year in precipitation, 6.87 to 7.47 mm/year in evaporation, and 1.57 to 3.54 mm/year in stream flow. Plus, these increasing trends were concurrent with the increasing temperature trend of 0.029 to 0.037°C/year. Consequently, this study provided evidence for the amplification or acceleration of the hydrological cycle as a response to warming in the midwestern USA. Based on the results of this study, Figure 5 depicts the precipitation, evaporation, stream flow, and mean temperature in Illinois (USA) in 1983-2013 and 1992-2013, which portrays an increase in the variables of precipitation, evaporation, and stream flow along with the rise in temperature. Thus, it represents the intensification of the water cycle (Yeh, Wu 2018).

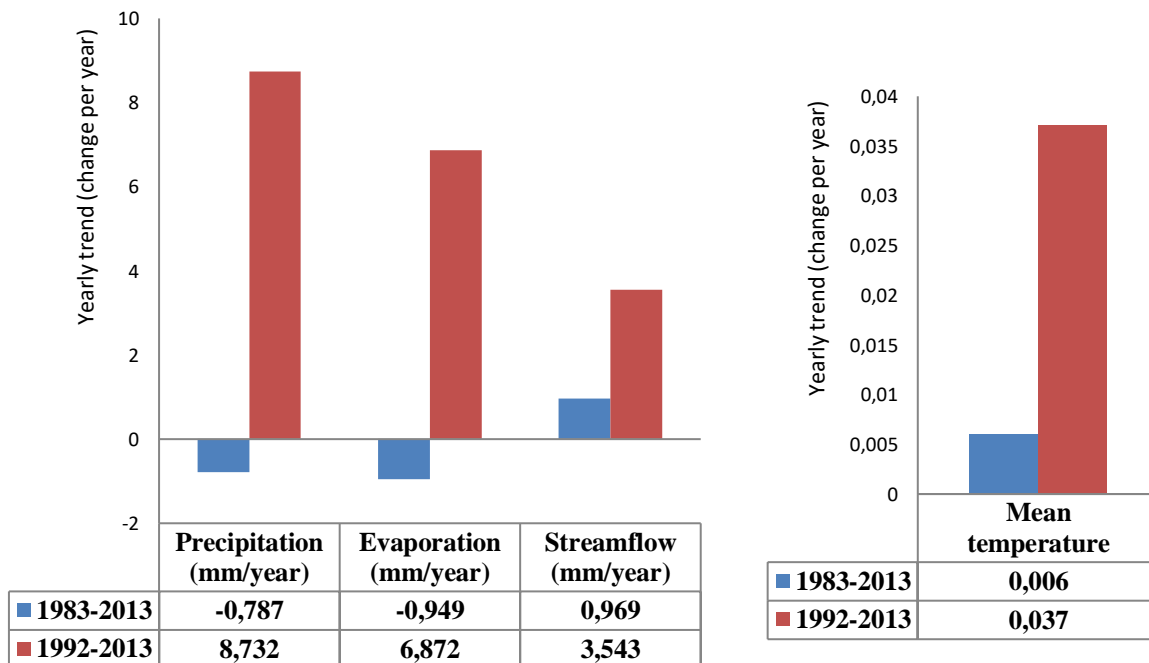


Fig. 5. Yearly trends in precipitation, evaporation, and stream flow (left) and mean temperature (right) in Illinois, USA. Data source: Yeh, Wu (2018).

BRAZIL

A study incorporated data from 886 hydrometric stations to examine the acceleration of the hydrological cycle in Brazil from 1980 to 2015. Annual time series of minimum 7-day, mean daily, and maximum daily streamflow were computed to characterize drought flows, water availability, and flood flows, respectively. The relationships of streamflow changes to their climatic and non-climatic drivers were analyzed by panel regressions. The results represented the acceleration of the hydrological cycle over Southern Amazonia. Specifically in southwestern Amazonia, prolongation of the dry season was found to be connected to a northward shift of the Inter Tropical Convergence Zone (ITCZ), which resulted in increased temperature and evaporation. Moreover, increases in heavy precipitation and floods were found to be linked to the intensification of Walker circulation air masses. Overall, it was found that the acceleration (in terms of more intense and frequent floods and droughts) occurred in over 29% of the Brazilian region and was connected to heavier rainfall (Chagas et al. 2022).

3.3. Effect of acceleration of the hydrological cycle on water availability

As mentioned previously, global warming is associated with acceleration and alteration of the hydrological cycle. This acceleration has the potential to affect and change the availability of water resources (Bates et al. 2008). Any abnormal changes or alterations in Earth's climate result in adverse impacts on human beings (Thomas et al. 2014). As the normal water cycle is disturbed due to global warming and climate change, the surface temperature is increased, and the evaporation rate is disturbed (IPCC 2001; NAST 2001). Increased evaporation rates are expected to reduce water supplies in many regions of the globe. Global water resources are highly sensitive to temperatures, not only through the obvious effects of evaporation, but also because of the effects on rainfall distribution, convection, and wind patterns (IPCC 2008). Variations in evaporation and precipitation patterns due to extreme climate change will elevate water usage to meet human needs, thus fundamentally changing the availability, quality, and timing of water across the globe. Disturbance in the normal water cycle due to climate change results in disturbance in water availability (by reducing supplies of groundwater and surface water), increasing water demand (due to higher temperatures), degrading water quality (increasing runoff resulting in erosion and sedimentation) and overwhelmed water infrastructure (due to flooding). Precipitation is expected to occur more frequently through high-intensity rainfall events, causing increased runoff and erosion (Huntington 2005).

However, the acceleration of the water cycle is not only negative. Instead, it can affect water availability over land in two different ways; either increasing water availability (decreased water stress), or it can decrease water availability (increased water stress). According to SRES (Special Report Emissions Scenarios by IPCC) scenarios (A2 and B2) along with two climate models, water stress will decrease over 20-29% of global land by the 2050s (Bates et al. 2008). In contrast, water stress is projected to increase over 62-76% of global land over the same period. The increase in water availability in a few regions is associated with the upsurge in the frequency

and intensity of precipitation. On the other hand, the projected decrease in water availability in most regions of the world is associated with increasing water withdrawals (Bates et al. 2008).

3.3.1. Increase in water availability due to acceleration of the hydrological cycle

As mentioned previously, hydrological changes (including acceleration of the hydrological cycle) can have positive impacts in terms of water availability. For instance, intensification of precipitation leads to an upsurge in annual runoff, which further increases renewable water resources (if the water is captured and stored in the waterbodies) (Magrin et al. 2005). In regions of the world with adequate infrastructure, this stored water can be beneficial for irrigation. Southern South America is an example, where the flooded area has increased, and crop yields have improved in the Pampas region of Argentina. The increase in flooded land has also provided new opportunities for fishing in the area (Magrin et al. 2005).

3.3.2. Decrease in water availability due to acceleration of the hydrological cycle

Overall, the climate-related projections indicate that the more prevalent impact of intensification of the water cycle will be adverse in the context of decreasing water availability (Bates et al. 2008). For instance, a study conducted in the Llobregat River Basin in Catalonia, northeastern Spain, evaluated the relationships between climate change scenarios and impacts on water availability in the region. Climate change scenarios and hydrological modeling were combined to estimate water availability in the future. AEMET (The Agencia Estatal de Meteorología) and SMC (The Meteorological Service of Catalonia), the Spanish weather agencies, provided the data for climate projections. The results based on AEMET climate scenarios indicated that there would be a decrease of 10% in the annual volume of water available in the future. The results obtained based on SMC scenarios were even more daunting because they revealed the possibility of a 40% decrease in the annual volume of water available in the future due to climate changes (Versini et al. 2016). Figure 6 depicts those factors of the hydrological cycle's acceleration that adversely influence water availability over land.

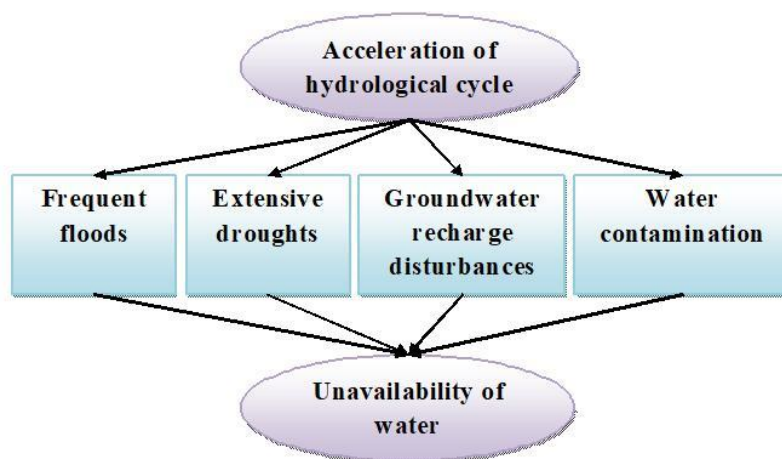


Fig. 6. Factors of the hydrological cycle's acceleration that can cause water unavailability.

3.3.3. Frequent floods

The acceleration of the water cycle has the potential to increase floods. In the 21st century, it is projected that the events of heavy precipitation or intense rainfalls will become more frequent in most of the regions around the globe. This dynamic will eventually result in frequent events of flash flooding (Bates et al. 2008). Moreover, the results of a study based on multi-model analysis projected an upsurge in the risk of very wet winters in central and northern Europe. The reason for this is the intensification of precipitation. For example, it is projected that boreal winter precipitation is prone to increase about five- to seven-fold with likely winter flood hazards. It is also projected that the wet monsoon season will be prolonged and more intense in Asian regions (Palmer, Räisänen 2002). For instance, according to climate models, along with a 2°C rise in global temperature, the flooded area of Bangladesh will increase by 23-29% (Mirza 2003). It is also projected that a traditionally 100-year flood will return more frequently (every 2-5 years) (Zhang et al. 2003). These scenarios of frequent flash floods are mainly negative for those regions of the world that lack the proper infrastructure for water storage. Therefore, such regions are expected to face declining water availability despite experiencing frequent precipitation. Intense floods and runoff often do not fill or recharge water reservoirs, and ultimately the discharge mixes with oceanic water, making it unavailable for use – another negative influence on water availability (Bates et al. 2008). It is estimated that 913 floods have occurred in the world just in the span of 2000-2018, and about 300 million people have been affected by 21st-century floods (Cavallito 2021).

Furthermore, it is crucial to understand flood frequency analysis, because flood frequency indicates the probability of floods occurring at a regional scale in both gauged and ungauged catchments. Flood frequency analysis also helps to assess the risks associated with floods, and to plan appropriate flood mitigation measures. For instance, some studies have used statistical methods for the estimation of flood frequency based on historical data (Acharya, Joshi 2020; Samantaray, Sahoo 2020). These studies provide a clear understanding of flood dynamics in diverse geographical regions. Hence, they provide clarity regarding the intensity and variability of flood incidences from small to larger scales.

Figure 7 represents the statistics given by the US-EPA about the one-day extreme/heavy precipitation events in the contiguous 48 states of the USA from 1960 to 2020. First of all this index shows that 2000-2010 and 2010-2020 decades had prominent difference in terms of precipitation. Secondly, it represents that 2015 was the year when the precipitation in USA was maximum as compared to the rest of the included years.

From the analysis of the flood events from 1973 to 2002, it was found that the proportion of floods among all disasters was 33%. During this time frame, most of the floods (40%) occurred in Asian countries. Moreover, within Asia, most of the flood events occurred in South Asia (Fig. 8) (Dutta, Herath 2004).

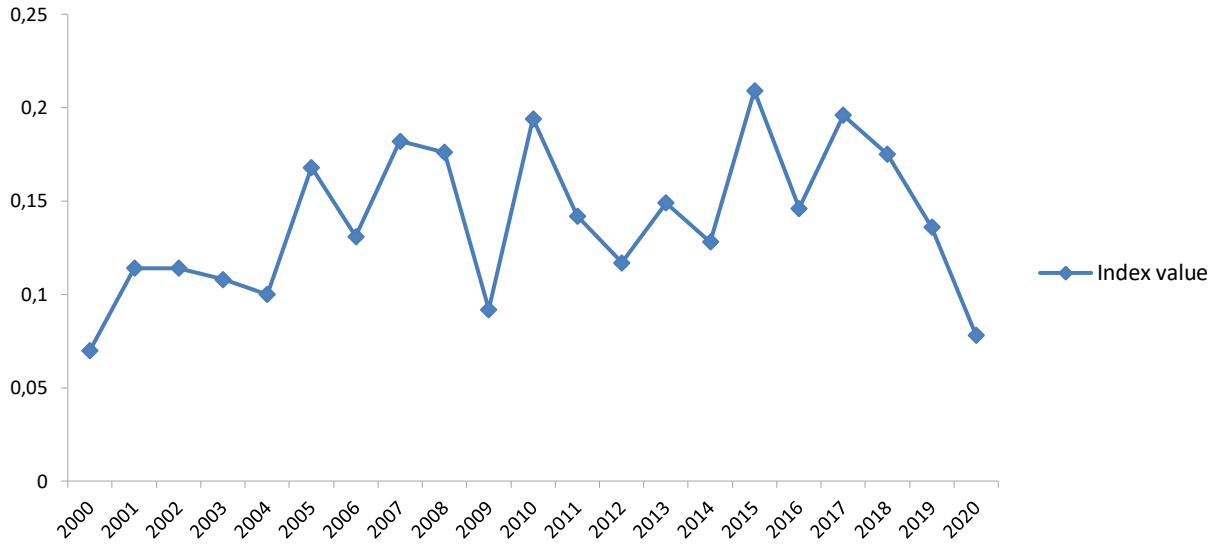


Fig. 7. Extreme One-Day Precipitation Events in the Contiguous 48 States of USA (1960-2020). Data source: USA-EPA (2021a).

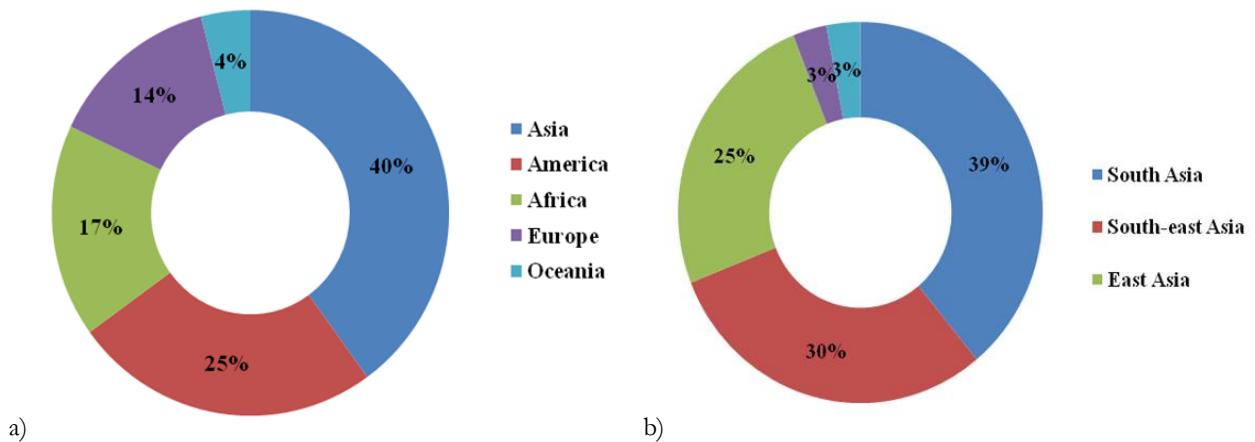


Fig. 8. (a) Flood percentages in the world. (b) Flood percentages in different regions of Asia, Data source: Dutta, Herath (2004).

3.3.4. Disturbance of water quality

Increases in precipitation intensity are expected to cause many forms of water pollution. These include the amplification of nutrients, sediments, salt, dissolved organic carbon, pesticides, pathogens, and thermal pollution. There will be concomitant increases in algal blooms and fungal content in water (Bates et al. 2008). The increased precipitation has the potential to elevate turbidity levels in surface-water sources. For example, heavy precipitation events raised turbidity levels up to a factor of 100 in some of the main reservoirs of New York City, compromising the city's water resources (Miller, Yates 2006). The quality of water is also degraded by flood water because the flowing flood water (having sediments and contaminants) gets mixed with the

clean water of existing reservoirs. Additionally, with increased evapotranspiration, shallow groundwater is prone to salinization in semi-arid and arid areas. Plus, due to decreasing streamflow in semi-arid areas, there is a strong probability of increases in the salinity of rivers and estuaries. For instance, in the headwaters of Australia's Murray-Darling Basin, salinity levels are projected to rise by 13-19% by 2050 (Pittock 2003). Increasing salinity will be accompanied by increasing concentrations of pollutants, such as those mentioned previously, making the water unsuitable for human uses, ultimately decreasing the availability of clean and safe water (Fig. 9) (Bates et al. 2008).

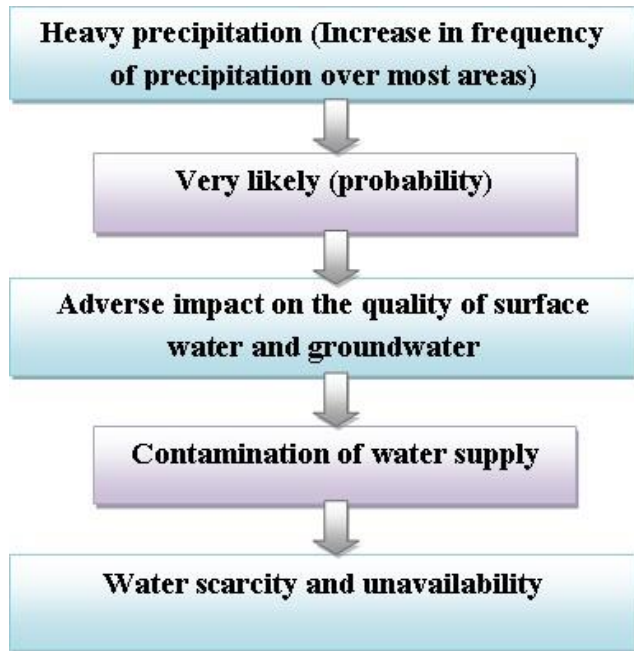


Fig. 9. Flow chart depicting the process of water contamination.

3.3.5. Extensive droughts

On one hand, intense evaporation causes heavy precipitation and floods in some regions of the world. On the other hand, this rapid evaporation makes some regions dry and causes prolonged droughts (Bates et al. 2008). Based on a single-model study of the frequency of drought around the globe, it is projected through various models that the frequency and duration of droughts will increase in the coming decades in many regions of the world. In this regard, the SRES A2 scenario has projected that by the decade of 2090, there will be an increase of 10-30-fold in land experiencing extreme drought, and a 2-fold increase in global drought frequency and mean duration of drought (Burke et al. 2006). It is also projected that by the 2070s, a 100-year drought under today's conditions will return more frequently (10 years) in various countries, including France, Spain, Portugal, Poland, and Turkey (Lehner et al. 2005). These statistics make it clear that areas that are already facing or will face prolonged drought conditions will ultimately face the issue of lacking available water (Bates et

al. 2008). Figure 10 represents the statistical analysis by the US-EPA of drought in the contiguous 48 states of the USA from 1960 to 2020.

Prominent floods have been occurring in Central Europe, South Asia, East Asia, Africa, Oceania and South America (You et al. 2016; Ansah et al. 2020; Chhetri et al. 2020; Mu et al. 2020; Nanditha et al. 2023). Meanwhile, extensive droughts have been taking place in various regions around the world, including Central Asia, South Asia, North America, Oceania, South America, and Africa (Schwalm et al. 2012; Nicholson 2014; Yuan et al. 2018; Garreaud et al. 2020; Tan et al. 2022). Moreover, water contamination, including reduction of dissolved oxygen(DO), rise in temperature, and increase in phosphorus, pathogen contamination, etc., exacerbates water scarcity in the water resources of various regions of the world (Li et al. 2015; Carpenter et al. 2018; Shih et al. 2021; Zhu et al. 2021). The impacts of hydrological cycle acceleration on water availability have been observed and analyzed by many researchers around the world; instances of which are mentioned in Table 1.

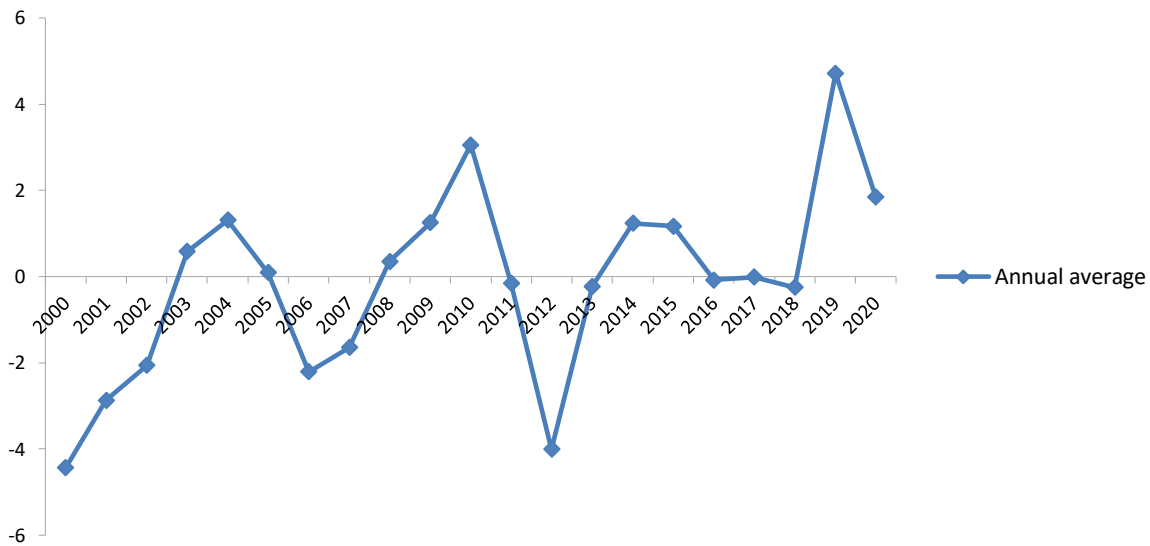


Fig. 10. Average Drought Conditions in the Contiguous 48 States of USA (1960-2020). Data source: US-EPA (2021c).

Table 1. Instances of impacts of hydrological cycle acceleration.

Time	Region	Published sources
Flood events (caused by heavy rainfall)		
2000	South Africa	Dyson, Heerden (2001)
2002	Central Europe (including Austria, Germany and the Czech Republic)	Ulbrich et al. (2003)
2005	Mumbai, Chennai and Bangalore (India)	Guhathakurta et al. (2011)
2002, 2004 and 2007	South Wales, Boscastle and Tewkesbury, respectively (Britain)	Gavin et al. (2011)
2010-2013	Australia	Butler et al. (2015)
2010-2014	Pakistan	Rehman et al. (2015)
2014	South Korea	You et al. (2016)
2016	Hue (Vietnam)	Mu et al. (2020)
2016 and 2017	Nepal	Chhetri et al. (2020)
2015 and 2018	Ghana	Ansah et al. (2020)
2018	Ordu province (Turkey)	Kocaman et al. (2020)
2020	Palermo (Italy)	Francipane et al. (2021)
2021	Brazil	Marengo et al. (2023)
2021	Germany	Fekete, Sandholz (2021)
2022	Pakistan	Iqbal et al. (2022); Nanditha et al. (2023)
Drought events		
1999-2003	Central Asia, Pakistan and China	Zhang, Zhou (2015); Barlow et al. (2016)
2000-2002	Balkans, Greece and Cyprus	Pashiardis (2008)
2003	Various European regions	Rebetez et al. (2006)
2000-2004	Western U.S. and Canada	Woodhouse et al. (2010); Schwalm et al. (2012)
2002-2006	Congo river basin and Tropical Africa	Zhou et al. (2014)
2004-2010	Southwestern China	Yang et al. (2012)
2006-2007	USA and Canada	Basara et al. (2013)
2006-2010	Southern Australia	Van Dijk et al. (2013)
2008-2010	Argentina and Chile	Müller et al. (2014)
2008-2010	Horn of Africa (or Somali Peninsula)	Masih et al. (2014); Nicholson (2014)
2008-2010	Middle-East, India and Central Asia	Neena et al. (2011); Cook et al. (2016)
2013-2016	East Australia	Spinoni et al. (2019)
2015-2016	South Africa	Yuan et al. (2018)
2015-2016	Amazonia	Jiménez-Muñoz et al. (2016); Erfanian et al. (2017)
2010-2018	Chile	Garreaud et al. (2020)
2011-2019	Brazil	Cunha et al. (2019)
2020	Southeastern China	Tan et al. (2022)
Water contamination (due to heavy precipitation)		
Production of high dissolved oxygen (DO) with low phytoplankton concentration (in 2011) and rise in temperature and formation of cyanobacterial blooms (in 2013) in Shibianyu Reservoir	China	Li et al. (2015)
Increase in phosphorus in agricultural watersheds	Upper Midwestern USA	Carpenter et al. (2018)
Increase in emerging contaminants in surface water	Mid-Atlantic USA	Zhu et al. (2021)
Pathogen contamination of Puzi River	Taiwan	Shih et al. (2021)
Increase in <i>E.coli</i> level in drinking water	Rural Kenya	Powers et al. (2023)

3.3.6. Disturbances in groundwater reservoirs

Groundwater is almost 30% of global freshwater, which means that it has a large share of the water usable for human beings. Moreover, the most accessible groundwater is found within 1 km of the surface of the Earth. Groundwater availability and quality decrease below this depth due to high concentrations of minerals (Brands et al. 2016). A very valuable attribute of groundwater aquifers is that they can store water without evaporation losses and in stable condition. Moreover, as water percolates through the ground and soil, the groundwater becomes de-contaminated (Turrall et al. 2011). Almost 24% of the world's groundwater aquifers are already over-exploited, indicating that any further disturbance in groundwater zones will significantly decrease fresh water's availability (Gleeson et al. 2012).

Disturbance and acceleration in the hydrological cycle have adverse impacts on the depth of the groundwater table and recharge rates (Fig. 11). Because many groundwater reservoirs are recharged from precipitation and surface water flow, any change in these processes eventually affects groundwater (Bates et al. 2008). One of the main reasons for the adverse impact on the amount of groundwater is that rainfall has become more flashy (intense) and less predictable in many areas of the world (Brands et al. 2016). Therefore, according to the aforementioned phenomenon of precipitation increase resulting from acceleration of the water cycle, the upsurge in the intensification of rainfall affects the infiltration capacity of the soil, which eventually decreases the groundwater recharge (Bates et al. 2008). However, this is mostly happening in humid areas. In arid and semi-arid regions of the world, on the other hand, more intense rainfall causes fast infiltration and percolation through the ground before evaporating. Plus, alluvial aquifers are mostly recharged by the overflows of floods. Overall, it can be observed that the acceleration of the water cycle that affects groundwater reservoirs in any form ultimately disturbs the very important resources of fresh water present on Earth. Hence, any influence on groundwater influences overall water availability (Bates et al. 2008).



Fig. 11. Groundwater vulnerability to climate change. Data source: Turrall et al. (2011).

4. Discussion and conclusion

Human beings are witnessing a lot of climatic changes around the globe, and intensification or acceleration of the hydrological cycle is one of these changes. It is a fact that global warming (parallel to global average temperature) has been escalating, which in turn increases evaporation and precipitation rates, leading to acceleration of the hydrological cycle. The Clausius–Clapyeron relation suggests that as the temperature increases, the specific humidity should also increase. As the source of the circulation of water from the hydrosphere to the atmosphere and vice versa, it is obvious that any alteration in the hydrological cycle will ultimately influence the water availability over land.

Intense precipitation, rapid evaporation, frequent floods, extensive droughts, and water contamination are some of the prominent outcomes of this accelerating cycle. Even though acceleration of the water cycle is associated with an increase in the amount of available water (mainly by frequent precipitation) in many regions of the world, the risk of water unavailability from acceleration remains an adverse result in other regions. Moreover, the impacts of hydrological cycle intensification extend beyond the direct or immediate concerns of water availability. The alterations in the precipitation patterns have disturbed water quality; ultimately affecting agricultural productivity, ecosystems' well-being, and human health. For example, increased runoff due to heavy precipitation or frequent floods carries pollutants into water bodies.

In a nutshell, human beings need to mitigate and adapt to the root cause of the intensification of this cycle (i.e., global warming) to protect themselves from the associated adversities. Adapting to the abovementioned issues needs interdisciplinary approaches that involve multiple domains (such as hydrology, ecology, climatology, and socio-economic factors). Helpful strategies in this regard include enhancement of infrastructure resilience, implementation of water-saving technologies, and promotion of sustainable land use planning. International cooperation is also crucial in this context. The vulnerable developing and under-developed countries that are facing issues related to the water cycle and climate changes, must be supported by the developed nations.

References

- Acharya B., Joshi B., 2020, Flood frequency analysis for an ungauged Himalayan river basin using different methods: a case study of Modi Khola, Parbat, Nepal, *Meteorology Hydrology and Water Management*, 8 (2), 46-51, DOI: 10.26491/mhwm/131092.
- Allen M.R., Ingram W.J., 2002, Constraints on future changes in climate and the hydrologic cycle, *Nature*, 418, 224-232, DOI: 10.1038/nature01092.
- Ansah S.O., Ahiataku M.A., Yorke C.K., Otu-Larbi F., Bashiru Yahaya P.N.L., Lamptey M., 2020, Meteorological analysis of floods in Ghana, *Advances in Meteorology*, DOI: 10.1155/2020/4230627.
- Arnell N.W., Liu C., Compagnucci R., da Cunha L., Hanaki K., Howe C., Mailu G., Shiklomanov I., Stakhiv E., 2001, Hydrology and water resources, [in:] *IPCC Climate Change 2001: Impacts, Adaptation and Vulnerability, The Third Assessment Report of Working Group II of the Intergovernmental Panel on Climate Change*, J.J. McCarthy, O.F. Canziani, N.A. Leary, D.J. Dokken, K.S. White (eds.), Cambridge University Press, Cambridge, UK, 133-191.

- Barlow M., Zaitchik B., Paz S., Black E., Evans J., Hoell A., 2016, A review of drought in the Middle East and southwest Asia, *Journal of Climate*, 29 (23), 8547-8574, DOI: 10.1175/JCLI-D-13-00692.1.
- Basara J.B., Maybourn J.N., Peirano C.M., Tate J.E., Brown P.J., Hoey J.D., Smith B.R., 2013, Drought and associated impacts in the Great Plains of the United States – a review, *International Journal of Geosciences*, 4 (6B), 72-81, DOI: 10.4236/ijg.2013.46A2009.
- Bates B.C., Kundzewicz Z.W., Wu S., Palutikof J.P. (eds.), 2008, *Climate Change and Water*. Technical Paper of the Intergovernmental Panel on Climate Change, IPCC Secretariat, Geneva, 210 pp.
- Beaudoin H., Rodell M., 2020, GLDAS Noah Land Surface Model L4 monthly 1.0 x 1.0 degree V2.1, Greenbelt, Maryland, USA, Goddard Earth Sciences Data and Information Services Center (GES DISC).
- Brands E., Rajagopal R., Eleswarapu U., Li P., 2016, Groundwater, *International Encyclopedia of Geography*, 3237-3253.
- Britannica T., 2020, Water cycle, *Encyclopedia Britannica*, available online at <https://www.britannica.com/science/water-cycle> (data access 24.05.2024).
- Burke E.J., Brown S.J., Christidis N., 2006, Modelling the recent evolution of global drought and projections for the 21st century with the Hadley Centre climate model, *Journal of Hydrometeorology*, 7, 1113-1125, DOI: 10.1175/JHM544.1.
- Butler I.R., Sommer B., Zann M., Zhao J.X., Pandolfi J.M., 2015, The cumulative impacts of repeated heavy rainfall, flooding and altered water quality on the high-latitude coral reefs of Hervey Bay, Queensland, Australia, *Marine Pollution Bulletin*, 96 (1-2), 356-367, DOI: 10.1016/j.marpolbul.2015.04.047.
- Can A., Ozsoy H., 2023, A different perspective on air pollution measurements, *Journal of Polytechnic*, 26 (1), 329-344, DOI: 10.2339/politeknik.1126580.
- Carpenter S.R., Booth E.G., Kucharik C.J., 2018, Extreme precipitation and phosphorous loads from two agricultural watersheds, *Limnology and Oceanography*, 63 (3), 1221-1233, DOI: 10.1002/lno.10767.
- Cavallito M., 2021, 21st century floods have already affected nearly 300 million people, Re Soil Foundation, available online at <https://resoilfoundation.org/en/environment/world-flood-study/> (data access 20.05.2024).
- Chagas V.B.P., Chaffe P.L.B., Blöschl G., 2022, Climate and land management accelerate the Brazilian water cycle, *Nature Communications*, 13, DOI: 10.1038/s41467-022-32580-x.
- Chhetri T.B., Dhital Y.P., Tandong Y., Devkota L.P., Dawadi B., 2020, Observations of heavy rainfall and extreme flood events over Banke-Bardiya districts of Nepal in 2016-2017, *Progress in Disaster Science*, 6, DOI: 10.1016/j.pdisas.2020.100074.
- Ciais P., Sabine C., Bala G., Bopp L., Brovkin V., Canadell J., Chhabra A., DeFries R., Galloway J., Heimann M., Jones C., Le Quéré C., Myneni R.B., Piao S., Thornton P., 2013, Carbon and other biogeochemical cycles, [in:] *Climate Change 2013: The Physical Science Basis. Contribution of Working Group I to the Fifth Assessment Report of the Intergovernmental Panel on Climate Change*, T.F. Stocker, D. Qin, G.-K. Plattner, M. Tignor, S.K. Allen, J. Boschung, A. Nauels, Y. Xia, V. Bex, P.M. Midgley (eds.), Cambridge University Press, Cambridge, United Kingdom and New York, NY, USA.
- Cook B.I., Anchukaitis K.J., Touchan R., Meko D.M., Cook E.R., 2016, Spatiotemporal drought variability in the Mediterranean over the last 900 years, *Journal of Geophysical Research: Atmosphere*, 121 (5), 2060-2074, DOI: 10.1002/2015JD023929.
- Cunha A.P.M.A., Zeri M., Leal K.D., Costa L., Cuartas L.A., Marengo J.A., Tomasella J., Vieira R.M., Barbosa A.A., Cunningham C., Garcia J.V.C., Broedel E., Alvala R., Ribeiro-Neto G., 2019, Extreme drought events over Brazil from 2011 to 2019, *Atmosphere*, 10 (11), DOI: 10.3390/atmos10110642.
- DelGenio A.D., Lacis A.A., Ruedy R.A., 1991, Simulations of the effect of a warmer climate on atmospheric humidity, *Nature*, 351, 382-385, DOI: 10.1038/351382a0.
- Dutta D., Herath S., 2004, Trend of floods in Asia and flood risk management with integrated river basin approach.
- Dyson L.L., Heerden J.V., 2001, The heavy rainfall and floods over the northeastern interior of South Africa during February 2000, *South African Journal of Science*, 97 (3), 80-86, DOI: 10520/EJC97295.
- Eki R., 2017, Ecology, stormwater management and environmental security in urban centers of developing countries, [in:] *International Youth Peace Conference*, Nigeria, 9-11th October 2017, Godfrey Okoye University: Ugwuomu.

- Erfanian A., Wang G., Fomenko L., 2017, Unprecedented drought over tropical South America in 2016: significantly under-predicted by tropical SST, *Scientific Reports*, 7 (1), DOI: 10.1038/s41598-017-05373-2.
- Farooqi A.B., Khan A.H., Mir H., 2005, Climate change perspective in Pakistan, *Pakistan Journal of Meteorology*, 2 (3), 11-21.
- Fekete A., Sandholz S., 2021, Here comes the flood, but not failure? Lessons to learn after the heavy rain and pluvial floods in Germany, 2021, *Water*, 13 (21), DOI: 10.3390/w13213016.
- Feng G-L, Wu Y-P., 2016, Signal of acceleration and physical mechanism of water cycle in Xinjiang, China, *PLoS ONE*, 11 (12), DOI: 10.1371/journal.pone.0167387.
- Francipane A., Pumo D., Sinagra M., La Loggia G., Noto L.V., 2021, A paradigm of extreme rainfall pluvial floods in complex urban areas: the flood event of 15 July 2020 in Palermo (Italy), *Natural Hazards and Earth System Sciences*, 21 (8), 2563-2580, DOI: 10.5194/nhess-21-2563-2021, 2021.
- Garreaud R.D., Boisier J.P., Rondanelli R., Montecinos A., Sepulveda H.H., Veloso-Aguila D., 2020, The central Chile mega drought (2010-2018): a climate dynamics perspective, *International Journal of Climatology*, 40 (1), 421-439, DOI: 10.1002/joc.6219.
- Gavin N.T., Leonard-Milson L., Montgomery J., 2011, Climate change, flooding and media in Britain, *Public Understanding of Science*, 20 (3), 422-438, DOI: 10.1177/0963662509353377.
- GISTEMP Team, 2023, GISS Surface Temperature Analysis (GISTEMP), version 4. NASA Goddard Institute for Space Studies. Dataset accessed 20th February, 2022.
- Gleeson T., Wada Y., Bierkens M.F., Van Beek L.P., 2012, Water balance of global aquifers revealed by groundwater footprint, *Nature*, 488 (7410), 197-200, DOI: 10.1038/nature11295.
- Graham S., Parkinson S., Chahine M., 2010, The Water Cycle, available online at <https://earthobservatory.nasa.gov/features/Water/page3.php> (data access 27.05.2024).
- Guhathakurta P., Sreejith O.P., Menon P.A., 2011, Impact of climate change on extreme rainfall events and flood risk in India, *Journal of Earth System Science*, 120, 359-373, DOI: 10.1007/s12040-011-0082-5.
- Held I.M., Soden B.J., 2000, Water vapor feedback and global warming, *Annual Review of Environment and Resources*, 25, 441-475, DOI: 10.1146/annurev.energy.25.1.441.
- Huntington T.G., 2005, Evidence for intensification of the global water cycle: review and synthesis, *Journal of Hydrology*, 319 (1-4), 83-95, DOI: 10.1016/j.jhydrol.2005.07.003.
- Iqbal M., Rabbani A., Haq F., Bhimani S., 2022, The floods of 2022: economic and health crisis hits Pakistan, *Annals of Medicine and Surgery*, 84, DOI: 10.1016/j.amsu.2022.104800.
- IPCC, 2001, *Climate Change 2001: The Scientific Basis*, Contribution of Working Group I to the Third Assessment Report of the Intergovernmental Panel on Climate Change Cambridge University Press, Cambridge, UK.
- IPCC, 2008, *Climate Change and Water*. Technical Paper of the Intergovernmental Panel on Climate Change, IPCC Secretariat, Geneva, 210 pp.
- Jiménez-Muñoz J.C., Mattar C., Barichivich J., Santamaría-Artigas A., Takahashi K., Malhi Y., Sobrino J.A., van der Schrier G., 2016, Record-breaking warming and extreme drought in the Amazon rainforest during the course of El Niño 2015-2016, *Scientific Reports*, 6, DOI: 10.1038/srep33130.
- Kocaman S., Tavus B., Nefeslioglu H.A., Karakas G., Gokceoglu C., 2020, Evaluation of floods and landslides triggered by a meteorological catastrophe (Ordu, Turkey, August 2018) using optical and radar data, *Geofluids*, 1, DOI: 10.1155/2020/8830661.
- Koutsoyiannis D., 2020, Revisiting the global hydrological cycle: is it intensifying?, *Hydrology and Earth System Sciences*, 24 (8), 3899-3932, DOI: 10.5194/hess-24-3899-2020.
- Lehner B., Czisch G., Vassolo S., 2005, The impact of global change on the hydropower potential of Europe: a model-based analysis, *Energy Policy*, 33 (7), 839-855, DOI: 10.1016/j.enpol.2003.10.018.
- Lenssen N., Schmidt G., Hansen J., Menne M., Persin A., Ruedy R., Zyss D., 2019, Improvements in the GISTEMP uncertainty model, *Journal of Geophysical Research: Atmospheres*, 124 (12), 6307-6326, DOI: 10.1029/2018JD029522.

- Li X., Huang T., Ma W., Sun X., Zhang H., 2015, Effects of rainfall patterns on water quality in a stratified reservoir subject to eutrophication: implications for management, *Science of the Total Environment*, 521-522, 27-36, DOI: 10.1016/j.scitotenv.2015.03.062.
- Li Y., Aemisegger F., Riedl A., Buchmann N., Eugster W., 2020, The role of dew and radiation fog inputs in the local water cycling of a temperate grassland in Central Europe, *Hydrology and Earth System Sciences*, 25 (5), 2617-2648, DOI: 10.5194/hess-2020-493.
- Loaciga H.A., Valdes J.B., Vogel R., Garvey J., Schwarz H., 1996, Global warming and the hydrologic cycle, *Journal of Hydrology*, 174 (1-2), 83-127, DOI: 10.1016/0022-1694(95)02753-X.
- Magrin G.O., Travasso M.I., Rodríguez G.R., 2005, Changes in climate and crops production during the 20th century in Argentina, *Climatic Change*, 72, 229-249, DOI: 10.1007/s10584-005-5374-9.
- Manabe S., Wetherald R.T., Milly P.C.D., Delworth T.L., Stouffer R.J., 2004, Century-scale change in water availability: CO₂-quadrupling experiment, *Climatic Change*, 64, 59-76, DOI: 10.1023/B:CLIM.0000024674.37725.ca.
- Marengo J.A., Seluchi M.E., Cunha A.P., Cuartas L.A., Goncalves D., Sperling V.B., Ramos A.M., Dolif G., Saito S., Bender F., Lopes T.R., Alvala R.C., Moraes O.L., 2023, Heavy rainfall associated with floods in southeastern Brazil in November–December 2021, *Natural Hazards*, 116, 3617-3644, DOI: 10.1007/s11069-023-05827-z.
- Masih I., Maskey S., Mussá F.E.F., Trambauer P., 2014, A review of droughts on the African continent: a geospatial and long-term perspective, *Hydrology and Earth System Sciences*, 18 (9), 3635-3649, DOI: 10.5194/hess-18-3635-2014.
- Miller K.A., Yates D.N., 2006, *Climate Change and Water Resources: A Primer for Municipal*, Awwa Research Foundation, 83 pp.
- Mirza M.M.Q., 2003, Three recent extreme floods in Bangladesh: a hydro-meteorological analysis, *Natural Hazards*, 28, 35-64, DOI: 10.1023/A:1021169731325.
- Mu D., Luo P., Lyu J., Zhou M., Huo A., Duan W., Nover D., He B., Zhao X., 2020, Impact of temporal rainfall patterns on flash floods in Hue City, Vietnam, *Journal of Flood Risk Management*, 14 (1), DOI: 10.1111/jfr3.12668.
- Müller O.V., Berbery E.H., Alcaraz-Segura D., Ek M.B., 2014, Regional model simulations of the 2008 drought in southern South America using a consistent set of land surface properties, *Journal of Climate*, 27 (17), 6754-6778, DOI: 10.1175/JCLI-D-13-00463.1.
- Nanditha J.S., Kushwaha A.P., Singh R., Malik I., Solanki H., Chuphal D.S., Dangar S., Mahto S.S., Mishra V., 2023, The Pakistan flood of August 2022: causes and implications, *Earth's Future*, 11 (3), DOI: 10.1029/2022EF003230.
- NAST, 2001, *Climate Change Impacts on the United States: The Potential Consequences of Climate Variability and Change: Overview*, A Report of the National Assessment Synthesis Team, US Global Change Research Program, Cambridge University Press, Cambridge, United Kingdom, 620 pp.
- Neena J.M., Suhas E., Goswami B.N., 2011, Leading role of internal dynamics in the 2009 Indian summer monsoon drought, *Journal of Geophysical Research: Atmospheres*, 116 (D13), DOI: 10.1029/2010JD015328.
- Nicholson S.E., 2014, A detailed look at the recent drought situation in the Greater Horn of Africa, *Journal of Arid Environments*, 103, 71-79, DOI: 10.1016/j.jaridenv.2013.12.003.
- Palmer T.N., Räisänen J., 2002, Quantifying the risk of extreme seasonal precipitation events in a changing climate, *Nature*, 415 (6871), 512-514, DOI: 10.1038/415512a.
- Pashiardis S., Michaelides S., 2008, Implementation of the standardized precipitation index (SPI) and the reconnaissance drought index (RDI) for regional drought assessment: a case study for Cyprus, *European Water*, 23 (24), 57-65.
- Pittock A.B. (ed.), 2003, *Climate Change: An Australian Guide to the Science and Potential Impacts*, Australian Greenhouse Office, Canberra, ACT, 239 pp.
- Powers J.E., Mureithi M., Mboya J., Campolo J., Swarthout J.M., Pajka J., Null C., Pickering A.J., 2023, Effects of high temperature and heavy precipitation on drinking water quality and child hand contamination levels in Rural Kenya, *Environmental Science and Technology*, 57 (17), 6975-6988, DOI: 10.1021/acs.est.2c07284.

- Ramanathan V., Krutzen P.J., Kiehl J.T., Rosenfeld D., 2001, Aerosols, climate, and the hydrologic cycle, *Science*, 294 (5549), 2119-2124, DOI: 10.1126/science.1064034.
- Rebetez M., Mayer H., Dupont O., Schindler D., Gartner K., Kropp J.P., Menzel A., 2006, Heat and drought 2003 in Europe: a climate synthesis, *Annals of Forest Science*, 63 (6), 569-577, DOI: 10.1051/forest:2006043.
- Rehman A., Jingdong L., Du Y., Khatoon R., Wagan S.A., Nisar S.K., 2015, Flood disaster in Pakistan and its impact on agriculture growth (a review), *Journal of Economics and Sustainable Development*, 6 (23), 39-42.
- Rodell M., Houser P.R., Jambor U., Gottschalck J., Mitchell K., Meng C., Arsenault K., Cosgrove B., Radakovich J., Bosilovich M., Entin J.K., Walker J.P., Lohmann D., 2004, The Global Land Data Assimilation System, *Bulletin of the American Meteorological Society*, 85, 381-394, DOI: 10.1175/BAMS-85-3-381.
- Samantaray S., Sahoo A., 2020, Estimation of flood frequency using statistical method: Mahanadi River basin, India, *H₂Open Journal*, 3 (1), 189-207, DOI: 10.2166/h2oj.2020.004.
- Schwalm C.R., Williams C.A., Schaefer K., Baldocchi D., Black T.A., Goldstein A.H., Law B.E., Oechel W.C., Paw U.K.T., Scott R.L., 2012, Reduction in carbon uptake during turn of the century drought in western North America, *Nature Geoscience*, 5 (8), DOI: 10.1038/ngeo1529.
- Sherani S.H., 2020, Efficient irrigation practices to minimize water loss, *Pakistan & Gulf Economist*, available online at <https://www.pakistangulfeconomist.com/2020/10/12/efficient-irrigation-practices-to-minimize-water-loss/> (data access 22.05.2024).
- Shih Y.J., Chen J.S., Chen Y.J., Yang P.Y., Kuo Y.J., Chen T.H., 2021, Impact of heavy precipitation events on pathogen occurrence in estuarine areas of the Puzi River in Taiwan, *PLoS ONE*, 16 (8), DOI: 10.1371/journal.pone.0256266.
- Spinoni J., Barbosa P., De Jager A., McCormick N., Naumann G., Vogt J.V., Magni D., Masante D., Mazzeschi M., 2019, A new global database of meteorological drought events from 1951 to 2016, *Journal of Hydrology: Regional Studies*, 22, DOI: 10.1016/j.ejrh.2019.100593.
- Steve G., 2010, The water cycle, Earth Observatory, available online at <https://earthobservatory.nasa.gov/features/Water> (data access 22.05.2024).
- Tan X., Wu X., Huang Z., Deng S., Hu M., Gan T.Y., 2022, Detection and attribution of the decreasing precipitation and extreme drought 2020 in southwestern China, *Journal of Hydrology*, 610, DOI: 10.1016/j.jhydrol.2022.127996.
- Thomas F., Sabel C.E., Morton K., Hiscock R., Depledge M.H., 2014, Extended impacts of climate change on health and wellbeing, *Environmental Science and Policy*, 44, 271-278, DOI: 10.1016/j.envsci.2014.08.011.
- Turrall H., Burke J., Faurè J.M., 2011, *Climate Change, Water and Food Security*, Food and Agriculture Organization of the United Nations.
- Ulbrich U., Brücher T., Fink A.H., Leckebusch G.C., Krüger A., Pinto J.G., 2003, The central European floods of August 2002: Part 1 – Rainfall periods and flood development, *Weather*, 58 (10), 371-377, DOI: 10.1256/wea.61.03A.
- US-EPA, 2021a, Climate Change Indicators: Heavy Precipitation, available online at <https://www.epa.gov/climate-indicators/climate-change-indicators-heavy-precipitation> (data access 22.05.2024).
- US-EPA, 2021b, Climate Change Indicators: U.S. and Global Precipitation, available online at <https://www.epa.gov/climate-indicators/climate-change-indicators-us-and-global-precipitation> (data access 22.05.2024).
- US-EPA, 2021c, Climate Change Indicators: Drought, available online at <https://www.epa.gov/climate-indicators/climate-change-indicators-drought> (data access 22.05.2024).
- Van Dijk, S., Jeffrey J., Katz, M.R., 2013, A randomized, controlled, pilot study of dialectical behavior therapy skills in a psychoeducational group for individuals with bipolar disorder, *Journal of Affective Disorders*, 145 (3), 386-593, DOI: 10.1016/j.jad.2012.05.054.
- Versini P.A., Pouget L., Mcennis S., Custodio E., Escaler I., 2016, Climate change impact on water resources availability: case study of the Llobregat River basin (Spain), *Hydrological Sciences Journal*, 61 (14), 2496-2508, DOI: 10.1080/02626667.2016.1154556.

- Wetherald R.T., Manabe S., 2002, Simulation of hydrologic changes associated with global warming, *Journal of Geophysical Research: Atmospheres*, 107 (D19), DOI: 10.1029/2001D001195.
- Wild M., Ohmura A., Gilgen H., Rosenfeld D., 2004, On the consistency of trends in radiation and temperature record and implications for the global hydrologic cycle, *Geophysical Research Letters*, 31 (11), DOI: 10.11029/2003L091188.
- Woodhouse C.A., Meko D.M., MacDonald G.M., Stahle D.W., Cook E.R., 2010, A 1,200-year perspective of 21st century drought in southwestern North America, *Proceedings of the National Academy of Sciences*, 107 (50), 21283-21288, DOI: 10.1073/pnas.091119710.
- Yang J., Gong D., Wang W., Hu M., Mao R., 2012, Extreme drought event of 2009/2010 over southwestern China, *Meteorology and Atmospheric Physics*, 115 (3-4), 173-184, DOI: 10.1007/s00703-011-0172-6.
- Yeh P.J.-F., Wu C., 2018, Recent acceleration of the terrestrial hydrologic cycle in the U.S. Midwest, *Journal of Geophysical Research: Atmospheres*, 123 (6), 2993-3008, DOI: 10.1002/2017JD027706.
- You C.-H., Lee D.-I., Kang M.-Y., Kim H.-J., 2016, Classification of rain types using drop size distributions and polarimetric radar: Case study of a 2014 flooding event in Korea, *Atmospheric Research*, 181, 211-219, DOI: 10.1016/j.atmosres.2016.06.024.
- Yuan X., Wang L., Wood E.F., 2018, Anthropogenic intensification of southern African flash droughts as exemplified by the 2015/16 season, *Bulletin of the American Meteorological Society*, 99 (1), 86-90, DOI: 10.1175/BAMS-D-17-0077.1.
- Zhang L., Zhou T., 2015, Drought over East Asia: a review, *Journal of Climate*, 28 (8), 3375-3399, DOI: 10.1175/JCLI-D-14-00259.1.
- Zhang Y., Chen W., Cihlar J., 2003, A process-based model for quantifying the impact of climate change on permafrost thermal regimes, *Journal of Geophysical Research: Atmospheres*, 108 (D22), DOI: 10.1029/2002JD003354.
- Zhou L., Tian Y., Myneni R.B., Ciais P., Saatchi S., Liu Y.Y., Piao S., Chen H., Vermote E.F., Song C., Hwang T., 2014, Widespread decline of Congo rainforest greenness in the past decade, *Nature*, 509 (7498), 86-90, DOI: 10.1038/nature13265.
- Zhu L., Jiang C., Panthi S., Allard S.M., Sapkota A.R., Sapkota A., 2021, Impact of high precipitation and temperature events on the distribution of emerging contaminants in surface water in Mid-Atlantic, United States, *Science of the Total Environment*, 755, DOI: 10.1016/j.scitotenv.2020.142552.

“Whiskey is for drinking, water is for fighting:” Colorado River water disputes over the Lake Powell Pipeline

Juan Camilo Perdomo Marin

Abstract

This case study analyzes the history, controversies, implications, and uncertainty in constructing the Lake Powell Pipeline (LPP) to evaluate how the state of Utah has been addressing the larger problem of responding to growing local demands for water within a regional context of reductions and cuts in water allocations. The research uses a multimethod approach, namely, analysis of historical documents, interviews, literature review, and field notes to link this case’s overlapping factors affecting the viability of LPP. The paper is divided into five sections: (1) an introductory review of the political and technological history of the Colorado River; (2) a description of the arguments and controversies related to the construction of LPPs; (3), identifying how the history of the Colorado River and LPP are deeply connected; (4) analysis of the properties of water infrastructure to understand what is at stake in the materialization of this project; and (5) a characterization of the complex political scenarios behind the negotiations over the LPP. The paper concludes with a reflection on how these controversies are part of a worldwide phenomenon: i.e., where building local water infrastructure is prioritized while ignoring the need for more holistic river basin policies.

Keywords

Water scarcity, Colorado River, Utah, drought, Lake Powell, climate change, population growth, infrastructure.

Submitted 18 March 2024, revised 26 May 2024, accepted 28 May 2024

DOI: 10.26491/mhwm/189401

1. Introduction

Water is central in thinking about society, even more so when this substance is scarce, as in Utah. This state is an ideal location for studying the problems related to water access driven by climate change, policy decisions, and demographic factors. Global warming is expected to reduce the region’s yearly snowpack, decreasing water flow in the rivers. Consequently, these changes will diminish the ability of reservoirs to supply the required water, especially in dry seasons. Farmers and urban populations will have less water available to meet their needs. Additionally, drought conditions are expected to contribute to more intense wildfires, expand deserts, desiccate lakes, and foster worsening air quality. These changes will negatively affect the health of humans and animals (EPA 2016; Utah Division of Water Resources 2021).

Nevertheless, the impacts of climate change and natural variability depend not only on physical factors but also on how societies manage their water resources and prepare to face future threats. The southwestern United States is especially vulnerable to water shortages because of the high demand. The states of this region have developed and expanded their cities and economies by consuming more water than is available in the Colorado River basin. Hence, the water crisis is exacerbated by regional environmental planning problems (Kuhn, Fleck 2021; Fleck, Castle 2022; Schmidt et al. 2023). In this panorama, a central question arises: How

can states address growing demands for water in the face of a need to reduce water use throughout the region?

In Utah, construction of the Lake Powell Pipeline (LPP) has been under discussion for several years. The LPP is a water pipeline designed to address water supply problems in rapidly growing communities, such as Washington County, where St. George is located. It is estimated that it will cost about \$2 billion to construct a 225 km, 1.8 m diameter pipeline that would transport approximately 103 million m³ (MCM) per year from Lake Powell to Sand Hollow Reservoir (Lake Powell Pipeline 2022). Numerous Utah officials and planners favor this project, assuring the public that these large-scale interventions are necessary. They indicate that according to hydrological models, there will be a water supply problem in southwestern Utah as the quantity of water in the Virgin River dwindles. Moreover, water demands are expected to increase dramatically due to the area's high population and economic growth (Utah Division of Water Resources 2021; Lake Powell Pipeline 2022). Although water conservation is fundamental, these actors insist that Utah must focus on developing infrastructure to guarantee the region's economic development.

Historically, the state has invested in infrastructure to guarantee water access. Thus, it is contended that the state must follow the same practice to support new citizens. It is also claimed that Utah has the right to take more water from the Colorado River because it has not exercised all of its use rights as established in the Colorado River Compact. Thus, it is argued that Utah can negotiate water withdrawals from the Green River to serve needy communities. Finally, this project will be paid for at meager interest rates, and it will generate a massive number of jobs in the region (Lake Powell Pipeline 2022).

In opposition to this project, critics assert that the scientific models used to justify these engineering works are based on insufficient, outdated, and erroneous data, and thus exaggerate the lack of water in the county, hide the high overconsumption, and do not account for the water that will become available from the transformation of agricultural land for urban expansion (Utah Rivers Council 2022). It is noted that the LPP would negatively affect the water supply of the Colorado River, which is already in a shortage crisis. This group of actors emphasizes that water rights were wrongly distributed among states at a time when the river's water levels were unusually high (Kuhn 2020). It is also stressed that Indigenous nations have legal rights in the water planned for LPP (Penrod 2021).

Critics argue that the future water crisis in Washington County is a scare narrative used to finance costly infrastructure that all the region's citizens will pay for. They argue that "There are many interests who stand to profit immensely from a billion in new spending and are happy to manufacture a fictitious water crisis for legislators" (Frankael 2014, p. 102-103). This project would not benefit all sectors of society, because household water consumption is a low percentage of total water use, which mainly supplies agriculture (Utah Rivers Council 2022). It is also suggested that this pipeline would encourage population growth and, in this way, gen-

erate an increase in the water demand (Smoak 2020). These critics indicate that Utah's current water conservation strategies are minimal. If these efforts were encouraged and expanded, it would be possible to guarantee the water supply in the region without the need to build significant infrastructure (Kuhn 2020; McCool 2021; Olalde 2022; Utah Rivers Council 2022).

In the LPP controversy, actors for and against LPP have differing positions and hence challenge the objectivity of their opponents' positions and data. We find divergent interpretations of the validity of current legal frameworks, the level of water consumption in the state, the effectiveness of the institutional responses to the water crisis, and the environmental and economic impacts of the project. The LPP seems to be a Tower of Babel whose stakeholders speak different languages in which the promises of development and sustainability collide with nightmares of ambition and scarcity.

It is necessary to point out that the groups for and against LPP do not have a final voice in the development of this project. The viability of LPP is not defined simply by the debate of technical and economic factors but by the coming effects of climate change and the political landscape of Utah and the Southwest. The rapid reduction of Colorado River flow, the water cuts of the seven basin states in response to the megadrought, and the upcoming development of a new management framework for the Colorado River Compact by 2026 all greatly influence developments and plans regarding the LPP. The priority of the states is to face the drought, not to increase water use and to further decompensate a system in crisis. For this reason, the future of this infrastructure project is uncertain. If its window of opportunity is currently closing, why should we study an infrastructure project that, at the moment, is only in the imagination of its proponents and critics?

Although LPP is on hold and may end up being buried not in the lands of Washington County but in Utah's history books, this research shows that its controversies have significant intellectual and political relevance. Social theory teaches us that water supply is political and a primary source of conflict; as a well-known saying from the western United States illustrates: "Whiskey is for drinking, water is for fighting." What makes LPP particularly interesting is that it illuminates essential details regarding the political polarization within Utah, as to whether the water crisis should be addressed via infrastructure projects or conservation programs. At the same time, studying the LPP makes it possible to address important questions about present and future challenges facing the design of climate adaptation projects and to draw deep global connections. As river levels decline due to extreme droughts, the political storm over how to govern water increases. The construction of major-scale water pipelines remains a real possibility that water authorities are evaluating worldwide. For this reason, LPP offers insights into Western responses to water access problems that can be useful for policymakers, activists, and researchers. The attendant controversies have essential consequences as they become a historical precedent for political struggles and environmental conflicts. Currently, the eyes of the world are on how Utah responds to the water crisis.

Using a multimethod approach, namely contextual analysis of historical documents, interviews, literature review, and field notes, this case study examines the history, controversies, implications, and uncertainty in the construction of the LPP to show how the state of Utah has been addressing the larger problem: i.e., to respond to growing demands for water in the face of a well-documented need to reduce water use throughout the Colorado River Basin. This paper is divided into five sections to link this case's overlapping contexts: (1) an introductory review of the political and technological history of the Colorado River; (2) a description of the arguments and controversies related to the construction of LPP; (3) identifying how the history of the Colorado River and LPP are deeply connected; (4) analysis of the properties of infrastructures to understand what is at stake in the materialization of this project; and (5) characterization of the complex political scenarios behind the negotiations of LPP between the federal government, the Colorado River basin states, the region's Indigenous nations, and local authorities. Finally, this paper concludes with a reflection on how these controversies are part of a worldwide phenomenon whereby building local water infrastructure is prioritized, ignoring the need for more holistic river basin policies.

2. The control of the Colorado River

Access to water drives social life, so much so that the Colorado River has been the basis of development in the southwestern United States, given that the growth of its cities and industries in the 20th century depended on access to its waters. Starting in the Rocky Mountains, descending the canyons of the Southwest, combining with other important tributaries such as the Green River, and flowing into the Gulf of California in Mexico, the Colorado River has been exploited to boost and sustain the growth of populations in the most arid region of the country. The nation built a complex system of dams, canals, and reservoirs that allowed it to control and transport the river's water to prevent flooding and ensure constant flow of the river throughout the year. Currently, 40 million people in seven states and Mexico depend on the river; its water is used to produce hydroelectric energy, sustain agriculture, and support domestic and industrial consumption in large cities inside and outside its basin (see Fig. 1).

The modern history of the Colorado River Basin is too complex for easy summarization, so this section provides only a brief background. Diverse historical conditions led to the multiplication of hydraulic technology in the United States. In the 19th century, river intervention was required to protect mining infrastructure and workers from natural fluctuations in water levels and flows. As hydraulic systems multiplied in the region, they supported the development of irrigation infrastructure for agriculture, and aqueducts for the growing cities (Isenberg 2006). At the end of the century, the federal government, through land grant laws, encouraged migration to the West using the promise of economic prosperity. Warnings of the danger that there was not enough water to support large populations or extensive irrigation systems in the West were not heeded because it was not politically popular to admit that many of these lands were arid. Many agricultural projects in

the region began to fail. Yet, at the beginning of the 20th century, there was a shift in the technology and politics of the region; the era of large concrete dams for river control and water distribution began with the support of the federal government (Powell 2010). These infrastructure projects allowed the rapid industrialization of the West, so they became symbols of national pride, representing the economic reactivation of the country and the control of nature by human ingenuity.

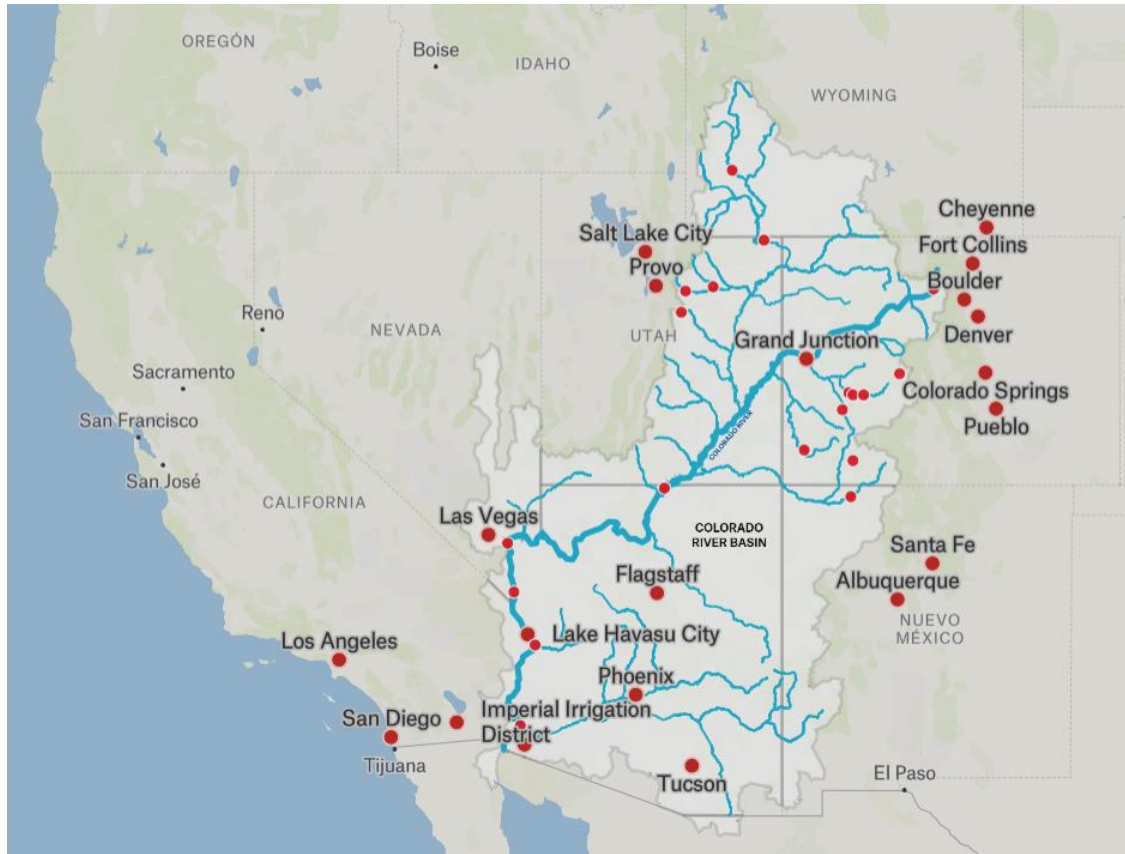


Figure 1. Major Cities that rely on Colorado River water. Source: <https://felt.com/>.

To resolve regional disputes over water rights, in 1922 the seven states of the Colorado River Basin developed the Colorado River Compact to create the legal basis for management of the river. This treaty was designed to formalize water use so that states that did not have the technological capacity to use large amounts of water at the time retained future water rights. This administrative framework assigned different rights and obligations and artificially divided the basin into upper and lower regions accompanied by the implicit promise of upper basin storage at some point (see Fig. 2). In the year of the elaboration of the treaty, the average annual river flow was 20,200 million m³ (MCM) according to historical records of two previous decades. From this total of water, the commissioners defined that each basin had the right to use an annual 9200 MCM. States of the lower basin required those of the upper basin to guarantee their rights of access to water without regard to the variations of the river.

The lower basin's rights to river water were distributed in fixed numbers: California (5400 MCM), Arizona (3500 MCM), and Nevada (370 MCM). The upper basin rights of the Colorado River were divided into percentages: Colorado (51%), Utah (23%), New Mexico (11%), and Wyoming (14%). In addition, a 1944 treaty granted Mexico 1850 MCM. In 1963, the Supreme Court recognized the water rights of Indigenous nations for the first time. However, legal struggles to legalize and enforce these rights, apportioned from state allocations, continue. The laws governing the Colorado River are called the Law of the River. This complex legal framework created the political conditions that in the 1950s led to the construction of the Glen Canyon Dam; the dam was built to accumulate surplus water from the Colorado River so that the Upper Basin states could guarantee the delivery of water to the states of the Lower Basin in times of drought (Powell 2010).

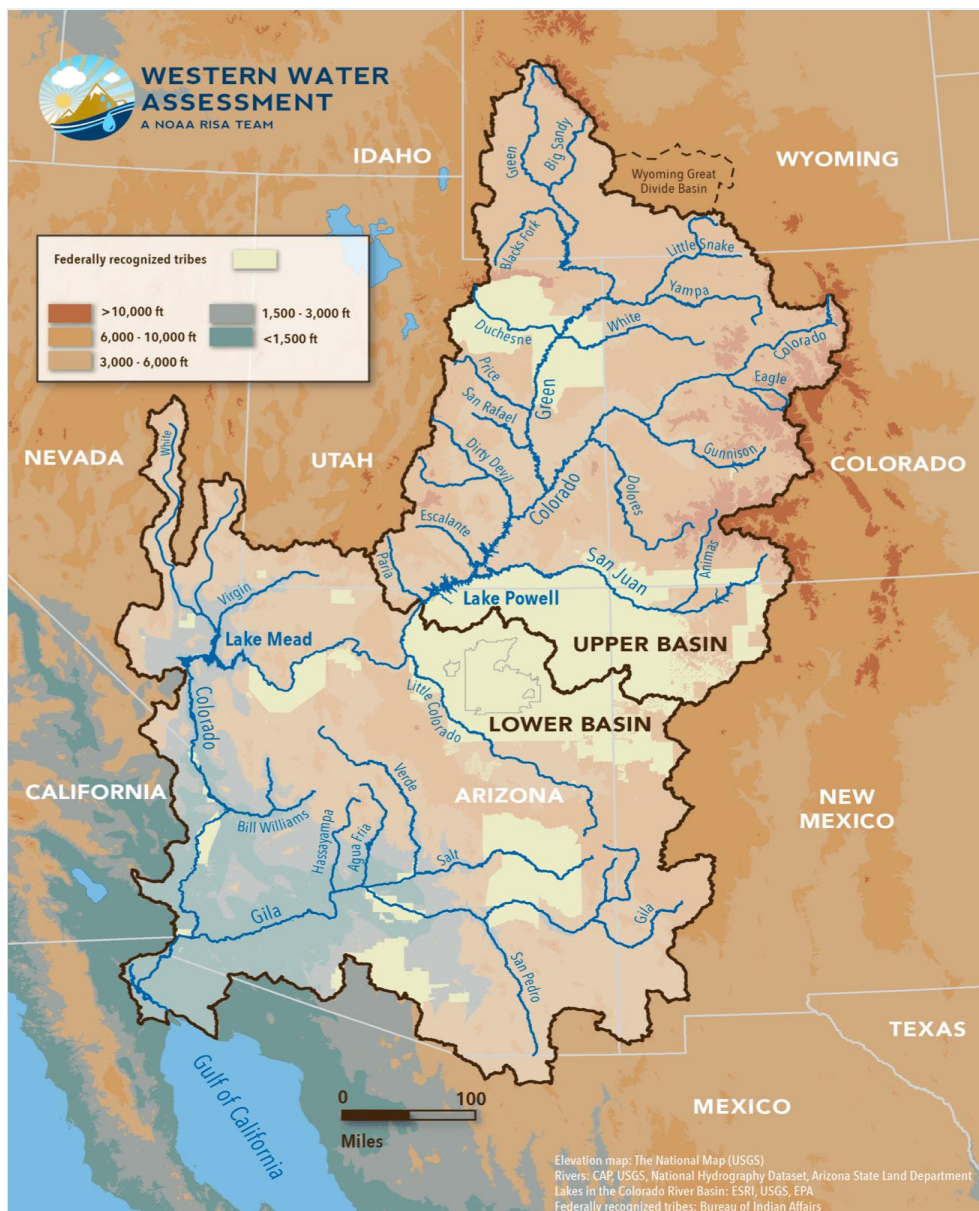


Figure 2. Colorado River Compact (Lukas, Elizabeth 2020, p. 3).

Throughout the world, connecting populations through hydraulic infrastructure is a way of creating and governing them because, as Appel et al. (2018) mention, the design and construction of these projects require imagining and defining a population that materializes from the daily flow of water and shared social aspirations. In this way, “Alignments of the pipes, politics, laws, and policies materially gather, constitute, and manage the population of the city” (p. 22). In the case of the Colorado River Basin, its landscapes have been profoundly modified by human interests, so its history can be seen as a product of the quest to know, predict, and manage the river’s flow, employing large-scale hydraulic technologies and the Law of the River to support and control the economic development of large populations in arid environments.

The shape of the basin landscapes illustrates how the impetus for control of rivers simultaneously drives the economic flourishing of societies and generates new scientific and political challenges that threaten their well-being. The region’s states currently deal with the unexpected material consequences of past political decisions and the effects of anthropogenic climate change. It is estimated that since 1880, the Colorado River has lost 10.3% of its water, and in the past two decades of megadrought, an amount equal to Lake Mead’s capacity (39,400 MCM) (Bass et al. 2023). For this reason, the basin states are faced with complex decisions to reduce water demand.

3. The Lake Powell pipeline controversies

Based on the Law of the River, Utah has argued that because it has rights to 23% of the upper basin allocation, it should still have 493 MCM of undeveloped water. Faced with future threats of water shortages in the center and south of the state, Utah has sought to develop new infrastructure projects to extract water from the Colorado River. In 2006, Utah passed the Lake Powell Pipeline Development Act (Utah Code 73-28). This legislative act justified the need to develop pipelines to transport water from the Colorado River to Washington County and to assign general planning guidelines and institutional responsibility to the Utah Board of Water Resources for constructing this project.

The LPP is designed to ensure Washington County’s medium- and long-term water supply. This infrastructure would consist of a buried 1.8 m diameter, 225 km pipeline transporting 103 MCM of water from Lake Powell in Arizona to the Sand Hollow Reservoir (see Fig. 3). According to its promoters, the approximate cost of this project would be between \$ 1.1 and \$1.7 billion, initially assumed by the State of Utah and repaid in the future with taxes from county citizens. So far, Utah has invested about \$40 million in technical studies for the feasibility and preliminary designs of the project. The Utah Division of Water Resources proposes the development of LPP, and the Washington County Water Conservancy District leads the project. Both institutions, along with stakeholders in favor of this project, argue that it is necessary to build LPP for the four main reasons outlined below.

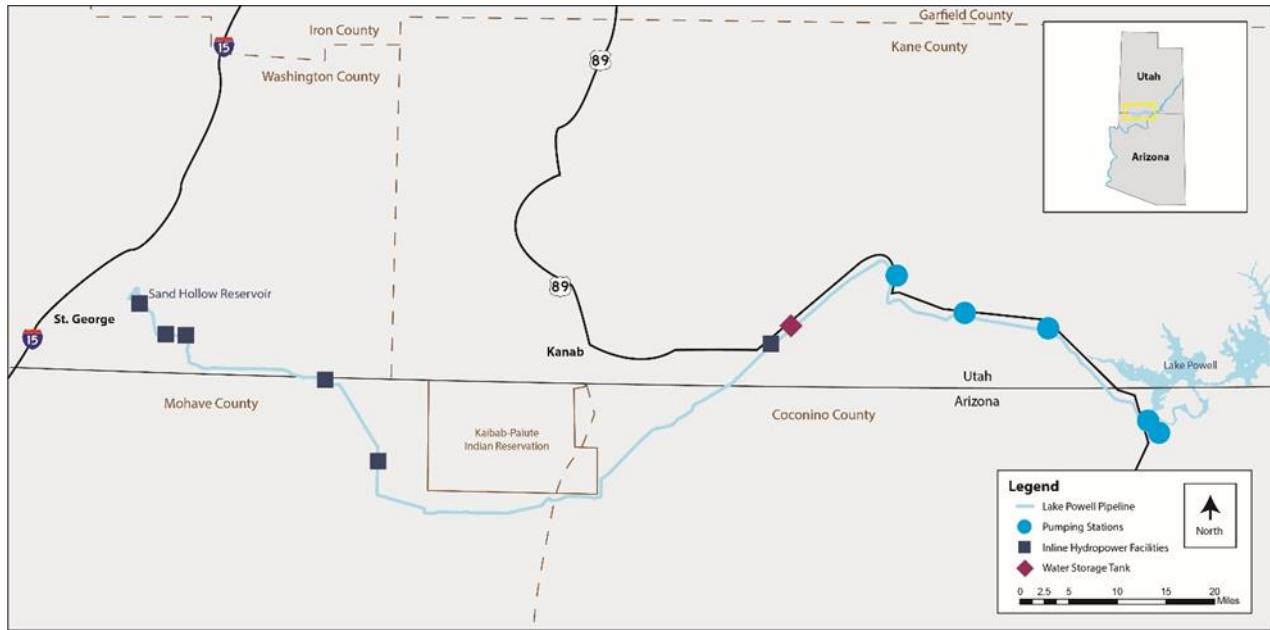


Fig. 3. Proposed Lake Powell Pipeline route. Source: <https://lpputah.org/>.

I. CLIMATE CHANGE

Increasing temperatures threaten to reduce the flow of the Virgin River, on which Washington County depends, so this primary water source will not be sufficient to guarantee the region's water supply in the future. The general manager of the Washington County Water Conservancy District defended the construction of LLP, stating that extreme drought and fluctuations in the local river threaten the social development of its community (Lake Powell Pipeline 2022).

II. POPULATION GROWTH

The county's water sources must be diversified due to its rapid population growth. The Kem C. Gardner Policy Institute (2022) expects Washington County to grow from 200,000 residents in 2020 to 500,000 by 2065. In addition, there is a high population of seasonal residents and tourists who visit its golf courses and the region's national parks. Therefore, water demand will exceed supply in the coming years.

III. CONSERVATION WILL NOT BE ENOUGH

Although Washington County citizens have reduced their water use in recent years, it will only delay water shortages for a few years, even if they meet regional conservation goals (Utah Division of Water Resources 2021).

IV. THE REGION'S ECONOMIC DEVELOPMENT

The only way to ensure Washington County's economic growth is to guarantee a stable water supply. Furthermore, this infrastructure would positively impact the region, reducing the county water consumption by increasing the local cost of water. Moreover, state loans would have low interest rates, and this investment would create numerous jobs throughout the region (Lake Powell Pipeline 2022). In addition to the Utah Division of Water Resources and Washington County Water Conservancy District, there is support from the districts of Central Utah, Jordan Valley, and Weber Basin in a collective organization called Prepare60. This project is also championed by Congress members such as Senator Mike Lee (R-UT), Senator Mitt Romney (R-UT), Representative John Curtis (R-UT), Representative Chris Stewart (R-UT), and Governor Spencer Cox.

The main strategies used by interest groups in favor of LPP have been to elaborate and socialize technical reports on costs and feasibility that justify its development, lobby to gain the support of state legislators and organize events in the local community of Washington County to publicize the benefits of this project. In 2021, *The Spectrum* surveyed 400 city residents about their perceptions of LPP (Meiners 2021). This poll found that 22% did not know about the project, 35% knew a little, 55% knew enough, and only 12% knew the proposal in depth. 59% support it, 35% are very supportive, 35% have some level of opposition, and 19% are very opposed. These figures partially indicate that while most citizens support it, they do not want to pay for it.

LPP is a highly controversial infrastructure project in Utah, as various environmental organizations, academics, Indigenous nations, and states oppose its construction. In recent years, the Utah Rivers Council has led a highly critical citizen study of LPP development, while other environmental organizations such as Conserve Southwest Utah, Glen Canyon Institute, Western Resource Advocates, Center for Biological Diversity, Great Basin Water Network, Save the Colorado, and Sierra Club are also against this project. Renowned academics from the region, such as Eric Kuhn, John Fleck, Daniel McCool, Gabriel Lozada, and Gregory Smoak, have expressed concerns about the negative impacts of this project. In addition, Indigenous nations such as the Ute and Navajo, along with the other six Colorado River Basin states, oppose this project due to legal conflicts over the rights to use the river. In general, there are four significant criticisms of LPP.

I. UTAH HAS NO MORE RIGHTS ON THE COLORADO RIVER

There is a reduction in Colorado River flow because states in the basin have used more water than is available. Therefore, building LPP would further reduce the level of a dwindling river and create more significant supply problems in a system already in crisis.

II. THE JUSTIFICATION FOR THE PROJECT IS BASED ON MISGUIDED FINANCIAL AND SCIENTIFIC DATA

The cost of LPP is higher than the project promoters claim, possibly reaching \$4 billion. The critics also question the validity of model projections of the future demand for water since the models are based on erroneous and old data, and previous models have been wrong (Utah Division of Water Resources 2021). For example,

the Wasatch region was initially projected to need new water supplies by 2015 but is now projected to have sufficient water until 2060. Moreover, the construction and operation of LPP would negatively affect ecosystems and endangered species in the region; the water diversion could also distribute invasive species in Utah.

III. WASHINGTON COUNTY IS NOT TRANSPARENT WITH ITS WATER USE DATA

Washington County has diverse water sources, not only the Virgin River. A drastic reduction in its supply is not expected due to climate change. A high rate of water waste in Washington County needs to be addressed, and its conservation goals need to be more ambitious. In addition, to justify LPP, the county exaggerates its current consumption and future demand, while failing to account for new water available through converting agricultural lands. Likewise, it is not considered that if water demand is reduced, it would not be necessary to build the pipeline (Utah Rivers Council 2022). Critics claim there would be enough water to support population growth with adequate management and water conservation, for example, by increasing the cost of water consumption and eliminating secondary water systems used for landscaping.

IV. UTAH HAS NOT RESOLVED ITS LEGAL PROBLEMS OVER ITS WATER RIGHTS

The State of Utah promised several decades ago to develop the Central Utah Project that would deliver water to the Ute Indian Tribe, but it has not fulfilled that promise and instead has prioritized LPP. If it is possible to obtain new water under the Colorado River Compact, critics affirm that it must be prioritized to comply with agreements with Native American Tribes.

Interest groups opposed to LPP have used various strategies to influence public opinion. They create multiple scientific reports on the shortcomings of the technical justification of LPP, participate in academic events in which they communicate points of view critical of this project, take legal action such as suing water districts that finance lobbies with public funding and have actively expressed their concerns in the open comment sections of federal and state reports related to LPP. Given the problems of water management in Utah, these actors are calling on the state to reject this project, declare a moratorium on diversions and dams, and radicalize the region's conservation goals to respond to the water crisis.

LPP's defenders argue that its critics have engaged in selective readings of their arguments so that they take the data out of context. This is a complex debate because different stakeholders have conflicting ideas about the interpretation of legal frameworks, the political will of Utah water conservation and its achievements, and the future social, ecological, and economic impacts of LPP. The most significant disagreements in this controversy are over water consumption rates in the state and the scale of climate change risk (to explore these controversies in greater detail, see Perdomo 2024a-b). These are the central scenarios defining opinions about whether Utah should prioritize its efforts toward either extensive infrastructure development or water conservation projects.

In 2015, economic studies by Utah professors began to cast doubts on Washington County's financial ability to pay for the construction of LPP. To have more precise criteria when making decisions about the future water infrastructure, Utah state legislators ordered several investigations to evaluate the objectivity of their water data and the economic cost of LPP. In the same year, one independent audit identified that Utah did not have reliable data to project future water demands, and in 2019, another audit found that LPP would be financially sustainable only if taxes were increased and population growth maintained for fifty years. Amid this review of technical data, LPP has slowly advanced in terms of regulatory approvals. At the same time, the gradual reduction of Colorado River flow generates more citizen concern about water use in the region.

In 2016, the Utah Board of Water Resources (UBWR) initiated the process to obtain an approval permit for LPP. Its studies were submitted for evaluation to the Federal Energy Regulatory Commission because multiple hydroelectric stations were planned in the original design. In 2017, the commission accepted the application but stated that it only had jurisdiction over the stations. In 2019, the Department of the Interior, after a request from the UBWR, designated the Bureau of Reclamation as the institution in charge of conducting LPP impact studies, because the UBWR modified its design by eliminating hydropower stations to reduce the project's environmental impacts.

4. The environmental uncertainty of the Colorado River

Over the past two decades, residents of the Colorado Basin have witnessed a gradual reduction in river flow due to climate change, regional planning problems, and population increase. According to the Bureau of Reclamation projections, the river's water supply gap and its demand will increase in the following years (see Fig. 4). An essential aspect that explains the current crisis is that the river's water rights were overallocated. In 1922, the Colorado River Compact commissioners distributed river rights with inaccurate data and ignored scientific precautions, which led them to establish fixed water use figures for the basin despite the river's natural variation (Kuhn, Fleck 2021; McCool 2021). Hence, this legal framework cannot deal with present environmental conditions because it encourages the use of more water than is available. Currently, representatives of the states of the Colorado River Basin recognize this problem and seek to solve it within the legal opportunities of the Law of the River.

In response to the drought at the beginning of the 21st century, the basin states designed technical criteria for coordinated management of the Colorado River reduction at Lake Mead and Lake Powell in the 2007 Colorado River Interim Guidelines. Based on the river's water level decrease, each state of the basin should reduce its water use to keep the dams in operation. Expanding these guidelines, and in response to an increasingly extensive drought, in 2019 the Colorado River Drought Contingency Plan was agreed upon, with the states of the basin and Mexico committing to more conservation strategies (neither of these two plans was designed with the participation of the indigenous communities of the basin). The new environmental conditions of the

21st century are forcing the basin states to develop a more coordinated water management strategy. These immediate actions are planned to keep the dams running until a new management framework for the Colorado River is agreed upon in 2026.

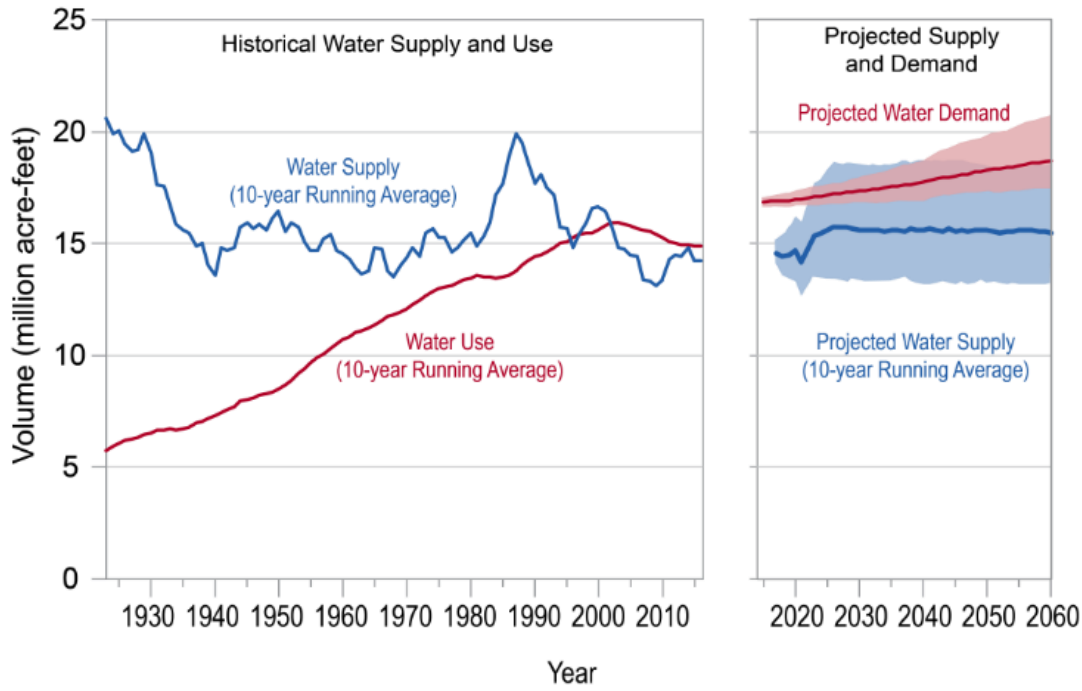


Fig. 4. Historical supply and use and projected future Colorado River basin. Water supply and demand. Source: Bureau of Reclamation (2011).

In June 2020, the Bureau of Reclamation published the Draft Environmental Impact Statement (DEIS) for the LPP and received public comments through September. This document is essential to the approval of LPP because the National Environmental Policy Act (NEPA) requires that infrastructure works on federal lands must evaluate and consider the environmental and socio-economic impacts of these projects along with public comments. Although the draft mentions that construction of LPP is viable and that new water supply sources are needed in Washington County, it also identifies the possible consequences of the different routes LPP can take. This report found that LPP could disturb Indigenous and recreational communities and negatively impact sensitive species in the region.

In mid-2020, the Trump administration ordered federal agencies to speed up the environmental review processes of large infrastructure projects in the nation, such as LPP. In September, a group of environmental organizations named Lake Powell Pipeline Coalition produced a report critical of the DEIS, arguing that it had extensive deficiencies in its analysis that prevented seeing the broad dangers of LPP. In addition, the other six Colorado River Basin states sent a letter to the Department of the Interior requesting that decisions about LPP not be made until their legal and logistical concerns were resolved to avoid legal conflicts. Later, UDWR

asked the Bureau of Reclamation to extend the decision-making process so that it would have time to review the public comments on the draft in more detail.

In mid-2021, the water crisis worsened in the region. The southern part of the Great Salt Lake reached its lowest level in recorded history, and the governor of Utah decreed an emergency drought and asked people to “pray for rain”. In August, the Bureau of Reclamation made the first-ever water shortage declaration for the Colorado River, following the guidelines established in 2007. This action triggered mandatory cuts in the Lower Basin states, and the emergency UDWR Division of Water Resources introduced Utah’s Water Resources Plan, which warns of the dangers of diminishing water supply in the southern part of the state and justifies the urgency of building LPP.

At the beginning of 2022, the media popularized investigations finding that the megadrought in the Western United States between 2000 and 2021 was the worst in 1200 years. In the middle of the same year, further raising regional concerns, the Bureau of Reclamation published the 24-Month Study of water levels in the Colorado River. The worst-case scenario foresees Lake Powell and Lake Mead so low that they could reach dead pool levels in summer 2023. In response to these projections, the Bureau was forced to release more water from upstream reservoirs, hoping to increase the water level of Glen Canyon Dam and encourage more significant conservation by purchasing water rights from the Lower Basin so that Lake Mead water is not used. Amid this environmental crisis scenario, the Utah water authorities recognized that the negotiations on water supply shortages with the other states would affect the development of LPP.

In May 2023, due to institutional pressure from the federal government, the Lower Basin states, after lengthy negotiations, agreed to receive federal funding to conserve 3700 MCM of the Colorado River until 2026. In April, the story of the water crisis in Utah was temporarily inverted by spring melting of a record-breaking snowpack, whence the Governor of Utah declared a state of emergency due to flooding. In June, the Great Salt Lake had risen five feet since November, so boats returned, which had been retired in 2022 due to the drop in lake level. Scientists viewed this water relief with caution. Although the small reservoirs in the country’s Southwest recharged, this winter was abnormal, and there was still a vast water deficit. The annual natural flow of the Colorado River in the past two decades has dropped to 15,400 MCM per year, but the consumptive uses and losses were 18,600 MCM per year (Schmidt et al. 2023). Scientists warn that in the following decades, the basin will tend to become drier and hotter, changes in precipitation are still uncertain, and there will be a further decline in river flows caused by the direct relation between increasing temperature and decreasing runoff (Udall, Overpeck 2017; Bass et al. 2023). In the near future, Lake Powell could be depleted unless water consumption in the region is quickly reduced to extend the functioning of this reservoir. Therefore, new water management strategies, improved hydrological models, expanded conservation strategies, and public education on this topic are needed (Osezua et al. 2023).

There is still no precise date when LPP's Environmental Impact Statement Supplemental Draft will be released or whether it will precede the final report for later obtaining rights to access Green River water stored in Flaming Gorge Reservoir. Scientific and political debates about the Colorado River are focused on taking rapid response actions to avoid reducing the river's water level. These environmental contingencies leave the construction of LPP uncertain. The changes in the Colorado River Compact by 2026 will modify the capacity of Utah to develop water through infrastructure projects.

5. What does infrastructure hide?

The water supply of cities in the southwestern United States depends largely on winter snowfall that recharges the snowpack of the high mountains. The accumulated snow begins to melt in the spring, thus feeding the rivers of the region. Dams store the melted snowpack in reservoirs, making water resources available throughout the year. Although the large dams of the Colorado River were created in the 20th century to regulate variations in water flow throughout the year, produce energy, and distribute water in the region, today, the capacity of this infrastructure to control nature is challenged by the increase in extreme weather events such as intense droughts and floods intensified by anthropogenic climate change.

Faced with the risk of water shortages, states seek to build pipelines to satisfy societal needs, such as in the case of LPP. To study the impact of LPP on the Colorado River Basin, we first need to understand the political nature of infrastructure projects. This section is based on the premise that by identifying the shared qualities of the infrastructure, we can more clearly comprehend the Colorado River's history and what is at stake in the construction of LPP. By placing this specific case within a larger historical and intellectual landscape, it is possible to make apparent the implications of extending water pipelines from Lake Powell to Washington County.

Infrastructure projects the future by embodying the promise of prosperity and economic development. Appel et al. (2018) argue that infrastructure represents the aspirations of progress and the desires for the modernity of nations, "That is why there is always greater investment in future-oriented infrastructures than is justified by their expense" (p. 19). The relevance of infrastructure lies not only in its functionality but also in the promises it embodies, as ideals of modernization of countries that are attractive to citizens. In this way: "Different visions of the future, different aspirations for one's own life, and for the future of the community or nation, play an important role in shaping which infrastructure projects find support among populations". In the case of Utah, LPP embodies the promise of development for Washington County. Having a reliable water supply in the future through pipelines ensures that new settlers and tourists arrive, and the local economy grows. Thus, as in the rest of the world, water infrastructure investment is essential to reduce climate events' economic and social damage, such as floods and droughts.

Infrastructure projects are not simply technical objects placed at the service of collective welfare but represent the crystallization of asymmetrical power relations. Infrastructure selectively distributes benefits and hazards, such as energy, water, knowledge, money, decision-making capacity, poverty, pollution, and disease, to specific populations (Edwards 2010; Appel et al. 2018). This way, infrastructure design, creation, and maintenance shape society. For this reason, it is essential to ask (Appel et al. 2018, p. 2):

“To whom will resources be distributed, and from whom will they be withdrawn? What will be public goods and what will be private commodities, and for whom? Which communities will be provisioned with resources for social and physical reproduction, and which will not? Which communities will have to fight for the infrastructures necessary for physical and social reproduction?”.

The types of benefits Washington County can get from LPP are what the Indigenous nations of the region demand from the federal government, since they require financing to resolve their infrastructure deficit to satisfy their basic needs. Appel et al. (2018) highlight, “By tugging, pulling, and demanding infrastructures to recognize, serve, and subjectify them, publics also make themselves visible as demanding subjects of state care” (p. 23). In the water crisis in the United States, as will be explained in more detail in the next section, the current political struggle consists precisely of defining the priority in which farmers, Indigenous nations, cities, industries, or ecosystems are considered as “subjects of state care.” The creation of water pipelines is political worldwide because it defines (Appel et al. 2018, p. 22):

“... not only who its subjects are, but also how they are collectively and differentially “treated” by the (public or private) institutions that administer infrastructures. Through everyday connections and disconnections, pipes, roads or electricity wires form populations that are unevenly governed and left aside ...”

Consider the case of the Turkey-Northern Cyprus pipeline built in 2015. Water from the Anamur River is transported from the coast of Turkey to the Gecitk y Dam of the Turkish Republic of Northern Cyprus (a state not recognized internationally) to extend the geopolitical control of Turkey under a hydraulic patronage relationship (Mason 2020). The distribution of resources through pipelines is a means of exercising power. In LPP, as in any infrastructure project, its benefits and costs are unevenly distributed. For example, in the case of agriculture, the UDWR, in its Utah Water Plan (2021), recognizes that “there are still many questions about who should bear the costs and who should receive the benefits of agricultural water use optimization” (p. 100). The Colorado River’s water would benefit Washington County’s citizens to varying degrees, especially the water-intensive sectors such as agriculture and golf courses. Still, all its inhabitants would have to bear its economic costs.

Externally, pipelines such as LPP do not solve water shortage problems but redistribute them elsewhere. By using water from the Colorado River system, LPP affects other parts of the region since it impairs the living conditions of various ecosystems and limits the ability of other communities to adapt to climate variability. LPP is not simply buying water but also time, life, and political decision-making capacity. For example, prioritizing this water distribution for southern Utah and not for Indigenous nations reproduces racial structures of exclusion. This problem illustrates how infrastructure projects tend to reinforce historical power relations; pipelines are commonly represented as “critical infrastructure” that promotes interests related to the economy and security of nations to legitimize their construction and block criticism, while hiding the social inequalities and environmental problems that are created (Spice 2018).

The proposal to build LPP leads us to larger questions. Can reliance on technological solutions to water supply problems multiply environmental problems? Instead of reducing Washington County’s vulnerability to drought, could LPP increase it in the medium and long term? In the case of the Turkey-Northern Cyprus pipeline, its defenders stated that this project builds resilience to climate change and reduces demand for water from the island’s aquifers. According to critics, this infrastructure conditions the island to intensive use of water, which encourages agricultural production, thus increasing vulnerability to climate change. In turn, urban expansion due to tourism can have a negative environmental impact by degrading rural landscapes (Mason 2020).

According to Di Baldassarre et al. (2018), creating reservoirs to respond to water supply problems has the secondary effect of increasing demands for water and population growth beyond those originally projected. Consequently, local communities are much more dependent on water infrastructure and, thus, more vulnerable to droughts. Similarly, engineering responses to water scarcity tend to push the problem into the future, such that irrigation efficiency multiplies the water demand (Grafton et al. 2018; Sears et al. 2018). Given the water level reduction in reservoirs due to drought, the southwestern United States has been forced to burn more fossil fuels to compensate for the loss of hydroelectric energy and the increase in demand, which increases global warming and, therefore, extreme droughts (Qiu et al. 2023). These examples illustrate Hornborg’s idea that modern technology displaces environmental problems to other times, spaces, and populations because it is “a strategy to locally save (human) time and (natural) space, at the expense of time and space lost elsewhere in the world-system” (Hornborg 2016, p. 73).

LPP could create and displace engineering problems in the future since Sand Hollow Reservoir, like all reservoirs and dams, has a limited useful life due to the accumulation of sediment. Hoover Dam and Glen Canyon have the same problem. Further, there are more unknown effects since infrastructure consists not of finished and predictable objects but rather fragile entities in permanent development because their construction, maintenance, and monitoring generate unplanned effects. Political, social, and environmental factors constantly affect infrastructure design and purpose (Edwards 2010; Harvey et al. 2017; Calkins, Rottenburg 2017;

Appel et al. 2018). For example, although the operation of Glen Canyon Dam is currently threatened by a lack of water, in 1983 it almost collapsed because its operators filled the dam to a dangerously high level, seeking to produce more hydroelectric power for greater profits (Powell 2010).

Another example of the unintended consequences of infrastructure is the disappearance of wetlands in the United States and Mexico. The Colorado River does not flow freely through its basin because an extensive system of dams controls its water, and in most years its water does not reach the Gulf of California. As a result of this management system, there is less sediment in the river because it is trapped in the reservoirs; sediment was essential to the region's ecology since it carried nutrients for fish and enriched previously flooded soils. The most dramatic impact of the modification of the river has been in the delta of the Colorado. The reduction of sediment and water levels because of overuse in the Lower Basin has been reducing the extent of the delta's disappearing wetlands for several decades.

Each infrastructure project is designed according to the environmental conditions of its time. Mega-dams were created in the context of economic reactivation, expansion of cities in the West, and the climate conditions of the 20th century. Currently, extreme weather events, increased by anthropogenic climate change, challenge the ability of dams to deliver reliable hydroelectric power in periods of severe drought and to be safe in periods of heavy rain. Due to the high cost of maintaining mega-dams, their negative social impacts, their emissions of carbon dioxide and methane, and the large amount of water lost by evaporation from the reservoirs, governments are now considering not building new reservoirs, but rather dismantling them. The rapid reduction of the Colorado River is accelerating the political and scientific debate as to whether its water is sufficient to be stored in Lake Mead and Lake Powell or if, due to its scarcity, it is necessary to prioritize using a single reservoir. In the Colorado River Basin, the infrastructure of the past is in tension with the politics and environmental conditions of the present. In the 21st century, obtaining and extending a stable water supply through pipelines is less secure due to more significant climate variability.

Finally, it is worth clarifying that although the construction of large engineering works such as dams and water pipelines currently faces greater political obstacles, any new form of territorial administration requires some type of infrastructure. Although Utah is now in a dispute over whether the state should build infrastructure or expand its conservation strategies, this opposition is a rhetorical simplification because this distinction is not clear in the real world. The LPP debate is not about whether or not to use infrastructure to solve environmental problems but about what water use should have priority and what type of infrastructure is required for it. On the one hand, conservation involves the installation of measurement technology throughout the region to assess and optimize water use in concert with state goals. As the Colorado River Authority of Utah said, "Conservation is only good to the extent that we can measure." There is no way to validate and legitimize conservation without data on its effectiveness. Therefore, the measurement infrastructure is necessary to make conservation tangible, transparent, and legitimate for public opinion.

On the other hand, due to historical interventions in the Colorado River Basin, the river itself can be considered as infrastructure organized to obtain specific benefits of the water cycle: electric power and water storage. Carse (2012) points out that infrastructure is not a “class of artifact, but a process of relationship-building.” This is to say that dams, locks, and forests are connected and become water management infrastructure through the ongoing work – technical, governmental, and administrative – of building and maintaining the sprawling socio-technical system” (p. 556). From Carse’s analytical perspective, we could say that LPP does not consist of building infrastructure from a natural river but of extending an infrastructural river. This concept implies extending the materiality of its water and the network of technical knowledge, administrative systems, economic benefits, ecological problems, and legal responsibilities anchored to it. Thus, the opposition between infrastructure and conservation is an unstable political demarcation that simplifies a complex debate to win allies in the search for a particular water use in Utah and accelerate the decision-making process.

6. Lake Powell pipeline’s political chess

The development of LPP is a complex political game because the negotiations on the future of the Colorado River operate at two bureaucratic speeds and articulate multiple interests, national actors, and political problems. First, in the southwestern United States, there are widespread obstacles to resolving environmental conflicts and creating responses to interstate water disputes because of political difficulties created by federalism. Second, regional stakeholders in southern Utah seek to secure access to river water even knowing of its decline since they hope to get one last chance to participate in the distribution of their use rights and because of the institutional inertia that defines their capacity for action.

First, water conflicts reveal the political limits of federalism. Although the Bureau of Reclamation is responsible for managing the Colorado River, the autonomy of each state of the basin has prevented effective regional planning, inter-jurisdictional collaboration, and long-term regional planning. While there is a long history of effective cooperation between states (for example, in the Law of the River treaties and the Drought Plans), and they avoid extensive legal battles that would force the intervention of the federal government (threatening their political autonomy); in the negotiations to respond to the Colorado River crisis there is competition between states to defend their historical privileges of access to its water and to avoid major water cuts.

The federalist political structure of the United States, within which the states must operate, can create political obstacles to addressing cross-boundary environmental issues. Therefore, local water supply decisions are often insufficient or fail to address regional water stress problems. The division of powers between the federal government, states, and local governments has generated a lack of leadership and has prevented the development of articulated environmental policies, which is why there is a weak national climate change policy in the country. Congress has broad constraints in designing and implementing environmental policies due to partisan po-

larization and the wide influence of interest groups in candidate choice and public debate, which leads to policy gridlock. These political conditions have prompted states and local governments to take their own climate adaptation paths and goals to respond to the lack of national agreements, obligations, and congressional action (Kraft 2019; Kraft, Vig 2019).

As an example of the challenges of addressing transboundary problems of water among sovereign entities, in May 2023 the lower basin states agreed to conserve a large amount of water to keep the Colorado River system running. But since 2022, the Bureau de Reclamation has tried unsuccessfully to coordinate with the states of the basin a reduction of 2400-4900 MCM of water use. For this reason, to avoid a deadlock in the policy debate, as with the 2007 Interim Guidelines and the 2019 Drought Contingency Plan, the Bureau of Reclamation threatened the states that it would mandate unilateral water cuts in the basin due to the lack of consensus and unified plans for response. This is a political strategy to speed up regional action. The federal government threats have served to neutralize internal conflicts, as according to Fleck and Castle (2022), they “provide political cover for state officials to agree to measures that are not universally supported by their constituents (e.g., “If we didn’t agree to X, the feds would order Y, which would be much worse!”)”. Even so, bureaucratic sluggishness continues to characterize the basin’s response to collective environmental problems due to the vast diversity of interests at stake.



Fig. 4. Glen Canyon Dam. Photo by the author.

The construction of LPP is uncertain in the context of the water crisis of the Colorado River. Although Utah water authorities have been forced to recognize that future Colorado River water development depends only on available water within the 23% agreed in the Law of the River, in 2026 the states must abandon the fixed allocations of water they receive and create a new distribution strategy, which affects the water that Utah will

be able to use in the future. This dynamic will create further disagreements with the states on what mechanisms, hierarchies, and quantities of water-use cuts are necessary to keep dams running. At the same time, Lake Powell's future is unclear for LPP (see Fig. 4); in the next few years, energy production and the water reserve may be prioritized in Lake Mead since there will not be enough water in the basin to fill two large reservoirs.

In this complex panorama, Indigenous nations want to formalize and exercise their water access rights, of which they have been historically deprived. Still, states and water districts claim no more water is available because the water rights these nations can obtain are taken from state allocations. Hence, tribal water rights tend to be unrecognized. Thirty Indigenous nations of the basin have rights to about 26% of the river's annual flow, but even if the courts have defined their water rights, most of them do not necessarily have the infrastructure to use it. Therefore, these rights are undeveloped. Hence, these nations have low access to drinking water. For this reason, Indigenous nations fear that the water rights that correspond to them will be lost in the future, such as the water sought to be used by LPP, which the Ute Indian nation claims in the negotiations of the Colorado River Compact in 2026.

There is a historical distrust of water negotiations with the federal government on the part of indigenous communities. For example, the dispute with the Utes began in the 1950s with the Central Utah Project (CUP), which was designed to transport water from the Colorado River to the Wasatch Front and Utah counties. The water managers of the project agreed to extend these infrastructure works to the Indigenous nation in exchange for using part of their territories. After the first phases of development, the state and the federal government did not comply with the agreement. Although currently there is an institutional commitment to protect the water rights of Indigenous nations, in the 1990s the Bureau determined that the water the Utes sought to obtain did not have a beneficial use, and without consulting the community, passed their rights to the UBWR, which divided these rights of use into different districts and private developers (Penrod 2021).

Seeking to end this legacy of exclusion and place water management at the center of the discussion as a matter of historical justice, the Indigenous nations of the Colorado Basin demand to participate in the negotiations of the Colorado River as sovereign nations since they have legal rights to about a quarter of the river, and because they consider that the basin states do not represent them. Also, wanting to be a part of the solution, they demand to have a vote in the discussions about the region's response to climate change. Currently, there is partial progress on this issue. In 2023, Upper Basin officials proposed including Indigenous nations in collective Colorado River negotiation, and in 2024, the Federal Energy Regulatory Commission created a new veto mechanism that gives Indigenous nations the power to block hydropower projects that affect their territories.

One of the biggest obstacles in discussions about the Colorado River is that there are different levels of concern about current problems and future threats to the water supply. In March 2022, I attended an academic

event in Utah about the future of the Colorado River that allowed me to identify a close relationship between the role of the speakers and the sense of urgency about the water crisis, specifically whether solutions should be developed in the short, medium, or long term. Each type of institutional work generates a range of action, authoritative criticism, and imagination of what is possible. On the one hand, the event attendees who worked close to the states as lawyers, representatives of public institutions, irrigation districts, water authorities, and state scientists affirm that they know the states' institutional limits, possibilities, and imperfections. So, they know how to maneuver and make an imperfect system more flexible since institutions have the discretion to make their regulations operational. In this way, they want to work within the existing system of rules, such as the doctrine of prior appropriation and the Law of the River, because there is predictable order that reduces political conflict. On the other hand, actors far from the state, such as university scientists, Indigenous leaders, and environmental activists, argue that they see the slowness in the state's response to the environmental crisis and the obstacles that generate lobbies by protecting particular economic interests. This type of actor highlights the importance of transforming the political system since its design makes it impossible to respond to the water crisis.

The actors closest to the states seek short-term solutions to the Colorado River crisis, arguing that there is no time to solve structural problems given the rapid reduction of river flow, the current institutional mechanisms that cannot solve several problems at once, and the challenge of articulating political wills around multiple issues. On the other hand, actors furthest from the state seek to discuss medium and long-term solutions because they tend to consider that if the problems of social exclusion of Indigenous nations and environmental protection of the basin are not solved, future solutions will not be effective, considering that these two issues are thought to have caused the current water crisis.

We do not know with certainty how fast the environmental conditions of the Colorado River basin will be transformed by climate change and natural variability, or therefore whether the new actions designed by the basin states and the Bureau of Reclamation will be enough. While there is a range of maneuvers within current laws, if the water supply problems accelerate much more than models suggest, the current policies and mechanisms of planning and collaboration of the region will not be enough to address the water crisis to the point that federalism can spur a struggle for water appropriation. The near future of the American Southwest is fragile.

The second level at which this political game operates is the regional scenario in which the risks of climate change are defined. LPP proponents, as water authorities of the region, justify its construction by stating that this project must use the Colorado River water because climate change will drastically reduce the water supply of Washington County. The environmental dangers of a global threat legitimize a local response. Critics of this infrastructure, such as the Utah Rivers Council, argue that trying to extract more water from the Colorado River denies the reality of climate change since it will negatively affect the river's flow throughout the region.

Interestingly, in Utah, the same conservative politicians who were climate change skeptics in previous years are now mobilizing around this infrastructure project to direct public investment and territorial planning.

The construction of LPP continues to be promoted despite the continuous reduction of the Colorado River because of two factors. First, in the medium and long term, the political actors of Saint George want to be able to participate in the transfer of water rights in the region before there are more significant political constraints. Kuhn explains (Jacobs 2021):

“These large municipal districts are lining up their strategy to make sure as the river continues to diminish because of climate change, they have access to the most senior rights – and those senior rights are agriculture. If you have the pipelines and canals in place, you’re in good shape.”

If Washington County does not obtain access to new water sources and its population continues to increase in the coming years, it may be forced, like Oakley County in Utah in 2021, to establish a moratorium on new construction due to limited water supply. This scenario can be multiplied in the rest of the Southwest United States.

Second, institutional inertia plays a crucial role in the capacity for action and criticism of the water authorities. An essential question in the LPP case is why water authorities insist on building expensive infrastructure projects such as pipelines that generate environmental concerns and broad political disputes. People defend or reject actions on the Colorado River or LPP because they consider this what their community expects from them. If they change their opinion, they risk their reputation by questioning their predecessors’ decisions, knowledge, and financing. In short, the ideals that shape the opinions in environmental conflicts do not circulate freely in the social world but are stabilized by institutional inertia. In an academic debate on the Colorado River previously mentioned, a water authority argued that its job was not to discuss the state’s economic development model or population growth but to guarantee its short-term water supply. These authorities cannot deviate from their states’ legal framework and political guidelines. The legal mandates of their institutions predetermine their range of action.

Understanding water supply issues and the institutional inertia in Utah and worldwide requires analyzing the complex physical and legal connection between water and oil. On the one hand, there is a visible physical link, since oil distribution and using fertilizers and pesticides generate water pollution. In turn, oil accelerates social metabolism because of the machines it drives and the fertilizers it produces, which causes agricultural hyper-productivity, leading to water overconsumption. Finally, oil use releases greenhouse gases into the atmosphere, which multiplies extreme weather events, such as droughts. On the other hand, these two powerful substances have an invisible legal connection since the current institutional perspectives and instruments to address the water crisis are partially configured by the first environmental laws created to address oil pollution in the 70s.

According to Bond (2022), the scientific and legal instruments of the first environmental laws were configured in negotiations with the oil industry seeking to control the impact of oil extraction without compromising its financial profitability. These early environmental regulations were designed to manage environmental problems while avoiding addressing their causes. It is possible to push Bond's ideas further and argue that the logic of the first environmental regulations is still reproduced in subsequent policies, hence the current limitations of institutional strategies to address the water crisis. Oil policy came to frame water policy, enabling and reducing the current political and scientific response capabilities. Oil slowly infiltrates the very depths of our bodies through the contamination of water, air, food, and objects, but also through the regulatory oil regime, which extends into how we understand and manage water.

Utah water authorities may seem conservative in their proposals to respond to the water crisis because they follow the original logic embedded in the framework of environmental policies. In decision-making, they can only see problems and solutions within the context authorized by their legal, economic, and technological frameworks. For this reason, the construction of LPP is not designed to address the structural causes of the water supply problems in Utah. As an example of the inertia that affects institutional decisions, the Legislative Auditor General (2015, p. 3) found that Utah Division of Water Resources:

“... has a challenge to balance the competing elements of its mission. To some extent promoting the full development and utilization of water in the state is at odds with promoting conservation. In fact, in a legislative committee, one member questioned whether Utah should wait to promote conservation until after the state has developed its full allocation of interstate waters. Other policymakers hold the competing view that more focused conservation efforts are needed before investing in large-scale infrastructure projects ...”

In the regional political game, environmental conditions work against LPP. The dramatic images presented by the media about the impacts of drought on farms and reservoirs in the Southwest of the country, especially in the Great Salt Lake, have generated enormous national interest. Reports such as “Utah’s ‘Environmental Nuclear Bomb’” of the *New York Times* in July 2022, warning about the drastic reduction of the lake and the public health impacts of its toxic dust, raised significant concerns about water use in Utah. Recently, the local press has taken a critical position on LPP. In August 2022, an editorial of the *Salt Lake Tribune* invited its readers to think about the long-term future of the Colorado River, which would imply abandoning the construction of LPP because “Lake Powell just isn’t going to have nearly enough water to justify the cost of such a pipeline”. It added, “Utah must prepare itself for two distinct possibilities. Either the United States will abandon and drain Lake Powell, or Mother Nature will. Our state’s power to oppose either is slim at best” (The Salt Lake Tribune 2022).

Despite adverse political and environmental conditions, the Colorado River Authority of Utah maintains that “all options are on the table” to respond to the water crisis in the state, including LPP. In 2022, pro-LPP representatives continued to insist that the LPP should be built, arguing that it is the only way to guarantee Washington County’s future water supply. The associate general manager for the Washington County Water Conservancy District affirmed that: “The Colorado River isn’t going to zero (...) Less water doesn’t mean no water (...) It’s just that we have to be realistic about making sure (the pipeline) can function and operate within the bounds of what Mother Nature gives us and in the bounds of Utah’s allocation of the Colorado River” (Kessler 2022). Similarly, although Governor Cox recognizes the environmental uncertainties of the Colorado River, he assured that he remains committed to supporting this project.

In response to the Great Salt Lake decline, in January 2023, legislators from Utah proposed protecting the lake for five years with money earmarked for LPP and Bear River Development. Although this project was rejected, hopes about the construction of LPP began to disappear. In February, there was a change in the political rhetoric of the LPP. St. George Mayor Michele Randall told the press that while “We are still keeping our fingers crossed on the Lake Powell pipeline”, the city is now focusing on building new reservoirs, reusing water, and expanding conservation. Despite the scientific warnings about the decreasing future of the Colorado River, the polarization around LPP is likely to continue in Utah due to the strong winter of 2022 that, in the spring of 2023, recharged the reservoirs of the region and raised the level of the Great Salt Lake. Finally, in December 2023, various environmental organizations sent a joint letter to request the Department of the Interior to reject LPP. For its part, Washington County Water Conservancy District continues to insist that LPP water is essential to the future of southern Utah.

7. Conclusion

The decrease in the water level of Lake Powell in recent years is a complex environmental sign of the effects of climate change, territorial planning difficulties derived from federalism, the consequences of relying on large infrastructure projects for economic development, and the overuse of natural resources driven by agriculture and the region’s rapid population growth. As Glen Canyon reemerges from among the waters of this artificial lake, scientific and political controversies multiply on how to manage the Colorado River sustainably. Amid this panorama, the proposal to transport the water from this river to southern Utah through the Lake Powell Pipeline is being debated to guarantee the water supply in a region threatened by its future scarcity.

This case study analyzed the history, controversies, implications, and uncertainty in the construction of the Lake Powell Pipeline to show how Utah has been addressing the larger problem of responding to growing demands for water in the face of a well-documented need to reduce water use throughout the basin. To this end, first, a historical panorama of the technological and political intervention that has allowed the management of the Colorado River was presented. The role of hydraulic infrastructure and the Law of the River in shaping

the landscapes of the basin was identified. Second, the arguments for and against LPP were described. On the one hand, proponents argue that this project is necessary to guarantee the future water supply of Washington County since it is threatened by climate change and because conservation strategies will be insufficient to meet the increase in water demand. On the other hand, this project was denounced by its critics since they considered it unnecessary and extremely expensive, its data was misleading, and it could increase the water crisis in the basin.

Third, it was identified that the problems of regional planning intersect the histories of the Colorado River and LPP since the gradual reduction of the river generates broad environmental uncertainties and political debates about its use, which calls into question the construction of LPP. Fourth, the properties of the infrastructures were analyzed to highlight that even as pipelines are essential to satisfy societal needs, they create new forms of inequity through the distribution of benefits and dangers to other regions, times, and populations. For this reason, it was stated that the construction of LPP could lead to the naturalization and reproduction of inequitable forms of access to water. Then, it was highlighted that the LPP controversies are not about the opposition between infrastructure versus conservation but about the legitimate use of water and what kind of infrastructure should be built for it.

Fifth, multiple interests inscribed in the development and opposition to LPP were highlighted, which makes its negotiation a complex political game. Water access problems require regional coordination plans, but the division of administrative authorities by the federalist structure complicates creating unified responses to cross-boundary environmental issues. At the same time, it was argued that the management of the Colorado River basin has enormous political complexity because its water is part of disputes with Indigenous nations that seek to obtain and exercise their historical access rights. This paper also reflected on local interests in constructing the LPP to participate in purchasing senior rights and the effect of institutional legacies as a delimited framework of action in the decision-making criteria of water authorities.

Infrastructure projects are attractive solutions to water supply problems because they can be built in a few years to respond to droughts, generate the illusion of control over nature's threats, and generate short-term electoral and political benefits by creating jobs and guaranteeing access to resources for industries and populations. For this reason, LPP is not an isolated case in the United States. Its controversies exemplify a shared phenomenon worldwide in which priority is given to building local water infrastructure while ignoring the need to create more holistic river basin policies. This happens when decision-makers and citizens ignore the long-term environmental, political, and socio-economic costs of reservoirs and pipelines.

Historically, nations' responses to droughts have been reactive. Instead of risk reduction, there has been a focus on crisis management, which generates dependency on governments and discourages better management of local resources (Wilhite 2011). Currently, the world panorama is changing and is more heterogeneous. Buurman et al. (2017), in their comparative study on drought management in ten cities, found that although

official responses appear reactive, short- and long-term plans are commonly mixed. Nevertheless, they critically highlight that response measures are primarily limited to reducing demand in the short term and increasing supply in the long term. This last aspect is important because a supply-based approach is problematic, as in the LPP case. Expanding water sources generates environmental impacts (for example, excessive exploitation of underground water), political conflicts (shared resources in borders), and physical limitations (contamination in reservoirs that reduces their capacity for use) (Sülün 2023).

Despite the promises of continuous growth, local populations must eventually face the negative consequences of the benefits obtained by their infrastructure because greater economic productivity goes hand in hand with greater environmental deterioration, which is precisely the American Southwest's history. The wealth of this region is directly linked to intensive use of Colorado River water, but economic growth has physical limits. Even the most conservative projections for the river indicate that its reduction will continue in the coming years to the point where there will not be enough water to respond to growing demand. The water crisis in Utah is an environmental bubble about to burst if there is no comprehensive planning that transcends the obstacles generated by federalism to face the climate challenges of the 21st century. In this panorama, it is urgent to redesign the Colorado River Compact in 2026 to create a comprehensive and robust inter-basin management system that allows addressing local conflicts inherent to water management without compromising long-term environmental sustainability objectives.

References

- Appel H., Nikhil A., Akhil G., 2018, Temporality, politics and the promise of infrastructure, [in:] *The Promise of Infrastructure*, N. Anand, A. Gupta, H. Appel (eds.), Durham, Duke University Press, 1-38, DOI: 10.1515/9781478002031-002.
- Bass B., Goldenson N., Rahimi S., Hall A., 2023, Aridification of Colorado River basin's snowpack regions has driven water losses despite ameliorating effects of vegetation, *Water Resources Research*, 59 (7), DOI: 10.1029/2022WR033454.
- Bond D., 2022, *Negative Ecologies: Fossil Fuels and the Discovery of the Environment*, University of California Press, Oakland, 262 pp.
- Bureau of Reclamation, 2011, Interim Report No. 1, Colorado River Basin Water Supply and Demand Study, Boulder City, NV: U.S. Bureau of Reclamation, Lower Colorado Region.
- Buurman J., Mens M.J., Dahm R.J., 2017, Strategies for urban drought risk management: a comparison of 10 large cities, *International Journal of Water Resources Development*, 33 (1), 31-50, DOI: 10.1080/07900627.2016.1138398.
- Calkins S., Rottenburg R., 2017, Evidence, infrastructure and worth, [in:] *Infrastructures and Social Complexity: A Companion*, P. Harvey, C. Bruun Jensen, A. Morita (eds.), Routledge, New York, 253-265.
- Carse A., 2012, Nature as infrastructure: Making and managing the Panama Canal watershed, *Social Studies of Science*, 42 (4), 539-563, DOI: 10.1177/03063127124401.
- Di Baldassarre G., Wanders N., AghaKouchak A., Kuil L., Rangelcroft S., Veldkamp T.I., Garcia M., van Oel P.R., Breinl K., Van Loon A.F., 2018, Water shortages worsened by reservoir effects, *Nature Sustainability*, 1 (11), 617-622, DOI: 10.1038/s41893-018-0159-0.
- Edwards P., 2010, *A Vast Machine: Computer Models, Climate Data, and the Politics of Global Warming*, The MIT Press Cambridge, Massachusetts.

- EPA, 2016, What climate change means for Utah, available online at <https://19january2017snapshot.epa.gov/sites/production/files/2016-09/documents/climate-change-ut.pdf> (data access 06.06.2024).
- Fleck J., Castle A., 2022, Green light for adaptive policies on the Colorado River, *Water*, 14 (1), DOI: 10.3390/w14010002.
- Fleck J., Kuhn E., Schmidt J., 2022, Does the upper Colorado River Basin routinely take shortages in dry years?, available online at <https://www.inkstain.net/2022/07/does-the-upper-colorado-river-basin-routinely-take-shortages-in-dry-years/> (data access 06.06.2024).
- Frankael Z., 2014, Chicken little's new career: How Utah's water development industry shows false fears and misinformation, [in:] *Desert Water: The Future of Utah's Waters Resources*, H. Crimmel (ed.), University of Utah Press, SLC, 98-116.
- Grafton R.Q., Williams J., Perry C.J., Molle F., Ringler C., Steduto P., Udall B., Wheeler S.A., Wang Y., Garrick D., Allen R.G., 2018, The paradox of irrigation efficiency, *Science*, 361 (6404), 748-750, DOI: 10.1126/science.aat9314.
- Harvey P., Bruun Jensen C., Morita A., 2017, Introduction: Infrastructural complications, [in:] *Infrastructures and Social Complexity: A Companion*, P. Harvey, C. Bruun Jensen, A. Morita (eds.), Routledge, New York, 1-22.
- Hornborg A., 2016, *Global Magic: Technologies of Appropriation from Ancient Rome to Wall Street*, Palgrave Macmillan, New York, 201 pp.
- IPCC, 2021, *Climate Change 2021: The Physical Science Basis, Contribution of Working Group I to the Sixth Assessment Report of the Intergovernmental Panel on Climate Change*, Cambridge University Press, Cambridge, United Kingdom and New York, NY, USA.
- Isenberg A., 2006, *Mining California: An Ecological History*, Farrar, Straus & Giroux, 256 pp.
- Jacobs J.P., 2021, As the West bakes, Utah forges ahead with water pipeline, *E&E News*, available online at <https://www.ee-news.net/articles/as-the-west-bakes-utah-forges-ahead-with-water-pipeline/> (data access 06.06.2024).
- Kem C. Gardner Policy Institute, 2022, Utah long-term planning projections. A baseline scenario of population and employment change in Utah and its counties. University of Utah.
- Kessler M., 2022, 'Less water doesn't mean no water' in Washington County even if Lake Powell Pipeline doesn't happen, *St. George News*, available online at <https://www.stgeorgeutah.com/news/archive/2022/04/13/mgk-less-water-doesnt-mean-no-water-in-washington-county-even-if-lake-powell-pipeline-doesnt-happen> (data access 06.06.2024).
- Kraft M., Vig N., 2019, U.S. environmental policy achievements and new directions, [in:] *Environmental Policy: New Directions for the Twenty-First Century*, N.J. Vig, C. College, M.E. Kraft (eds.), University of Wisconsin, Green Bay.
- Kraft M., 2019, Chapter 5: Environmental Policy in Congress, [in:] *Environmental Policy: New Directions for the Twenty-First Century*, N.J. Vig, C. College, M.E. Kraft (eds.), University of Wisconsin, Green Bay.
- Kuhn E., 2020, The Lake Powell pipeline: Asking the bigger questions, available online at <https://qcnr.usu.edu/colorado-river/blog/lake-powell-pipeline-questions> (data access 06.06.2024).
- Kuhn E., Fleck J., 2021, Science be damned. How ignoring inconvenient science drained the Colorado River, *The University of Arizona Press*, 288 pp.
- Lake Powell Pipeline, 2022, <https://lpputah.org/>.
- Legislative Auditor General, 2015, A Performance Audit of Projections of Utah's Water Needs, available online at https://ldwacorp.org/wp-content/uploads/2019/03/2015_UTAH_WATER_NEEDS_by_UT_AUDITOR_GENERAL.pdf (data access 06.06.2024).
- Lukas J., Elizabeth P., 2020, *Colorado River Basin Climate and Hydrology: State of the Science*, Western Water Assessment, University of Colorado Boulder.
- Mason M., 2020, Hydraulic patronage: A political ecology of the Turkey-Northern Cyprus water pipeline, *Political Geography*, 76, DOI: 10.1016/j.polgeo.2019.102086.

- McCool D., 2021, As climate change parches the Southwest, here's a better way to share water from the shrinking Colorado River, The Conversation, available online at <https://theconversation.com/as-climate-change-parches-the-southwest-heres-a-better-way-to-share-water-from-the-shrinking-colorado-river-168723> (data access 06.06.2024).
- Meiners J., 2021, Survey results: How Washington County residents feel about the Lake Powell Pipeline, The Spectrum, available online at <https://www.thespectrum.com/story/news/2021/06/03/how-washington-county-residents-feel-lake-powell-pipeline/5018639001/> (data access 06.06.2024).
- Olalde M., 2022, Why the second-driest state rejects water conservation, The Water Desk, available online at <https://waterdesk.org/2022/01/why-the-second-driest-state-rejects-water-conservation> (data access 06.06.2024).
- Osezua M., Bade S.O., Gyimah E., Tomomewo O.S., 2023, Impact of climate change on the water resources, Lake Powell, United States, American Journal of Water Resources, 11 (3), 103-111, DOI: 10.12691/ajwr-11-3-3.
- Penrod E., 2021, Lake Powell pipeline plans to tap water promised to the Utes. Why the tribe sees it as yet another racially based scheme, The Salt Lake Tribune, available online at <https://www.sltrib.com/news/environment/2021/06/13/lake-powell-pipeline/> (data access 06.06.2024).
- Perdomo J., 2024a, The new tower of babel: Epistemological and political challenges of water measurement in the Southwestern United States, manuscript submitted for publication.
- Perdomo J., 2024b, The struggle to anticipate the future: Political uses, technological approaches and moral debates on climate change, manuscript submitted for publication.
- Powell J., 2010, Dead Pool: Lake Powell, Global Warming, and the Future of Water in the West, University of California Press, Berkeley, 283 pp.
- Qiu M., Ratledge N., Azevedo I.M., Diffenbaugh N.S., Burke M., 2023, Drought impacts on the electricity system, emissions, and air quality in the western United States, Proceedings of the National Academy of Sciences, 120 (28), DOI: 10.1073/pnas.2300395120.
- Schmidt J.C., Yackulic C.B., Kuhn E., 2023, The Colorado River water crisis: Its origin and the future, WIREs Water, 10 (6), DOI: 10.1002/wat2.1672.
- Sears L., Caparelli J., Lee C., Pan D., Strandberg G., Vuu L., Lin Lawell C.-Y., 2018, Jevons' paradox and efficient irrigation technology. Sustainability, 10 (5), DOI: 10.3390/su10051590.
- Smoak G., 2020, "Is the water wet?", Lake Powell Pipeline Part 1 Podcast, available online at <http://zioncanyonmesa.org/podcast-archive/2020/9/2/is-the-water-wet> (data access 06.06.2024).
- Spice A., 2018, Fighting invasive infrastructures. Indigenous relations against pipelines, Environment and Society: Advances in Research, 9, 40-56.
- Sülün E., 2023, Key water challenges in the eastern mediterranean: A call for regional cooperation, Friedrich-Ebert-Stiftung & Peace Research Institute Oslo, available online at <https://library.fes.de/pdf-files/bueros/zypem/20794.pdf> (data access 06.06.2024).
- The Salt Lake Tribune, 2022, Say goodbye to Lake Powell and hello to Glen Canyon National Park, the Editorial Board writes, available online at <https://www.sltrib.com/opinion/editorial/2022/08/28/say-good-bye-lake-powell-hello/> (data access 06.06.2024).
- Udall B., Overpeck J., 2017, The twenty-first century Colorado River hot drought and implications for the future, Water Resources, 53 (3), 2404-2418, DOI: 10.1002/2016WR019638.
- Utah Division of Water Resources, 2021, Utah Water Resources Plan, available online at <https://water.utah.gov/2021waterplan/> (data access 06.06.2024).
- Utah Rivers Council, 2022, <https://utahrivers.org/>.
- Willhite D.A., 2011, Breaking the hydro-illogical cycle: Progress or status quo for drought management in the United State, European Water, 34, 5-18.

A probabilistic model for flood forecasting based on hydrological data in the state of Maranhão, Brazil

Larissa dos Santos Borges^{ID}, Jean Carlos de Almeida Nobre^{ID}, David Lohan Pereira de Sousa^{ID}, Luiz Claudio Fialho Andrade^{ID}

Federal University of Pará, Brazil

Abstract

Investigating critical precipitation phenomena is essential for predicting flood events. In this study, data from 8 hydrological stations in the state of Maranhão in northeastern Brazil were analyzed. The first step involved collecting valid data from the time series of 4 municipalities (Açailândia, Arame, Buriticupu, and Santa Luzia), which were affected by floods due to heavy rainfall in the region. The aim was to use a probabilistic model to predict the occurrence of new floods based on rainfall and river discharge patterns. Atypical precipitation points were identified in boxplots, confirming the correlation between heavy rainfall and floods in 2023. The exponential equations-based model estimated the river discharge during the floods. The Flow Duration Curves (FDC) indicated the probability of events of equal or greater magnitude occurring as follows: Açailândia (10%), Arame (15%), Buriticupu (32%), and Santa Luzia (<5%). Finally, significant trends in the monthly precipitation series were investigated using the Mann-Kendall test.

Keywords

Hydrological series, Floods, Stage-discharge curve, FDC, Mann-Kendall test.

Submitted 7 November 2023, revised 16 December 2023, accepted 9 July 2024

DOI: 10.26491/mhwm/190951

1. Introduction

Floods can have a devastating impact on any region where they occur. Nonetheless, the frequency and severity of these events have increased significantly due to climate change in recent years (Waseem, Rana 2023).

In Brazil, it is estimated that there are approximately 3,000 km² of areas prone to extreme weather events. At least 825 municipalities are considered highly vulnerable to disasters such as landslides and flash floods (Alvalá et al. 2019; Dias et al. 2020). Floods are the most common type of natural disaster worldwide and pose substantial risks to populations (Mishra et al. 2022).

Floods caused by heavy rains have had a drastic impact on the municipalities in the state of Maranhão, located in the northeastern region of Brazil, as indicated by official decrees issued by the Municipal Governments of Açailândia, Arame, Buriticupu, and Santa Luzia (Diário Oficial 2023a, 2023b, 2023c, 2023d).

Some recent research employs boxplots to identify anomalies in precipitation time series (Gogien et al. 2023; Moreira et al. 2023); stage-discharge curves to describe the behavior of rivers (Vishwakarma et al. 2023); flow duration curves (FDC) for optimized water resources management (Ridolfi et al. 2020); and the Mann-Kendall test for detecting trends in rainfall time series (Penereiro et al. 2018; Zhang et al. 2022).

The investigation of intense rainfall phenomena associated with flooding can be conducted through predictive models and proper hydrological data collection (Lima et al. 2019, Lima, Scofield 2021; Alves et al. 2022). In this study, all these tools were combined to develop a probabilistic model that estimates the likelihood of new flood events occurring in four municipalities in Maranhão: Açailândia, Arame, Buriticupu, and Santa Luzia.

2. Material and methods

2.1. Description of the study area

The study area encompasses the municipalities of Açailândia (5806 km²), Arame (2976 km²), Buriticupu (2545 km²), and Santa Luzia (5462 km²), in the state of Maranhão, in northeastern Brazil. These municipalities are in a state of emergency because of extreme precipitation events, as reported by the Ministry of Social Development (Brasil 2023). In the research reported here, hydrological time series data were investigated to develop a probabilistic model for predicting the occurrence of new flood events using data from the National Water and Sanitation Agency (Agência Nacional de Águas e Saneamento Básico – ANA). Figure 1 displays the municipalities and the selected hydrological stations.

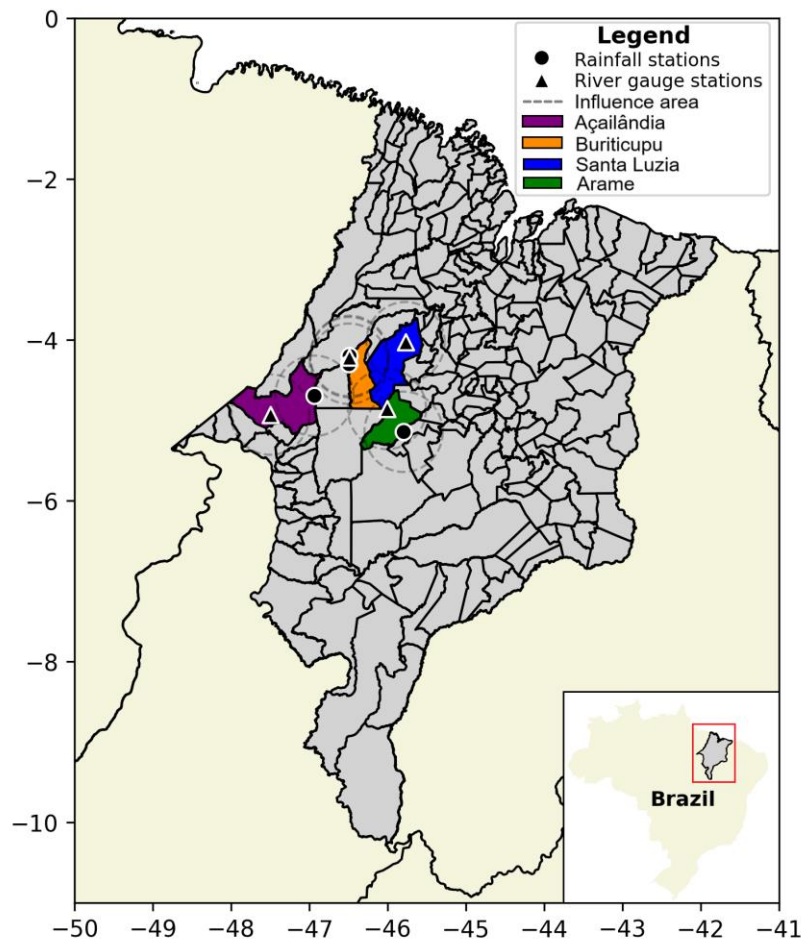


Fig. 1. Geographical location of the study area and spatial distribution of measurement stations.

The selection of stations was based on data availability in the Hydrological Information System (HIDROWEB). If the downloaded file contained data, the sample's consistency was verified through precipitation graphs (mm/day) over time. The goal was to identify the time interval during which the data were available and suitable for analysis; any station that did not provide valid data was discarded. Table 1 presents the stations that met this criterion and were selected for further investigation.

Table 1. Overview of selected hydrological stations.

Municipality	Time series	Station code	Latitude	Longitude	River	Drainage area (km ²)
Açailândia	(1996-2023)	447004 ¹	-4.9308	-47.4967	-	-
	(1979-2023)	330250 ²	-4.6969	-46.9347	Pindaré	5480
Arame	(1983-2023)	445008 ¹	-4.8611	-46.0078	-	-
	(2003-2023)	333330 ²	-5.1447	-45.7953	Grajaú	11400
Buriticupu	(2004-2023)	644019 ¹	-4.2175	-46.4906	-	-
	(2004-2023)	330700 ²	-4.2008	-46.4872	Pindaré	10400
Santa Luzia	(1982-2023)	445001 ¹	-4.0303	-45.771	-	-
	(1979-2023)	330750 ²	-4.2989	-46.4944	Buriticupu	4750

¹Rainfall stations, ²River gauge stations.

2.2. Boxplot

The box plot is an effective graphical tool for detecting atypical precipitation events. It displays the data distribution and allows for the visual identification of outlier values that represent exceptionally high or low precipitation events. The construction of boxplots in this study involved the calculation of several measures.

The median (Quartile 2) is the value that divides the data set in half as follows:

$$Q_2 = \frac{n+1}{2} \text{th value} \quad (1)$$

where n – total number of observations.

In addition to Q_2 , Q_1 (Quartil 1) and Q_3 (Quartil 3) are also required:

$$Q_1 = \frac{n+1}{4} \text{th value} \quad (2)$$

$$Q_3 = 3 \frac{n+1}{4} \text{th value} \quad (3)$$

The interquartile range (IQR) is used to determine the whiskers in the boxplots, calculated as follows:

$$IQR = Q_3 - Q_1 \quad (4)$$

Rainfall values beyond the boundaries represent the outliers. After plotting the graph, the coincidence of these points with flooding events in the municipalities of Maranhão was verified.

2.3. Stage-discharge rating curve

Stage-discharge curves relate the discharge of a river to the water level. These curves are essential in hydrology to understand the behavior of rivers and calculate discharge ($\text{m}^3 \text{s}^{-1}$) at different times. In this study, rating curves were used to assist in predicting a probabilistic model for the recurrence of discharges with magnitude equal to or greater than those of the initial days of flooding in the municipalities (March 18-20, 2023).

The relationship between discharge (Q) and water level (h) in a stage-discharge curve can be represented by an exponential equation in the following form:

$$Q = a(h - h_0)^b \quad (5)$$

where: Q – discharge ($\text{m}^3 \text{s}^{-1}$); h – stage (m), a and b are rating curve constants, h_0 – the stage corresponding to zero discharge (m) (Ramírez et al. 2018).

2.4. Flow Duration Curve (FDC)

The FDC provides a comprehensive graphical representation of the relationship between discharge and frequency (Ma et al. 2023). It was used to indicate the percentage of time when discharges equal to or greater than the reference discharge were observed. Initially, monthly historical discharge data from the stations were collected, and the probability of exceedance was calculated by associating these data with percentiles ranging from 0.05 to 0.95. This range was adopted to emphasize the absence of zero discharge (0%) or absolute discharge (100%) records.

The percentage of time when a specific discharge is equaled or exceeded can be calculated as:

$$Frequency(x) = \frac{n+1-i}{n+1} \times 100 \quad (6)$$

where: $f(x)$ – cumulative frequency for discharge x ; n – total number of observations; i – position of discharge x on the y-axis.

2.5. Mann-Kendall test

2.5.1. Missing Data Index (MDI)

Data consistency is a critical aspect of any hydrological analysis (Becker et al. 2023; Peixoto et al. 2023; Pereira 2023; Tsuha 2023). Therefore, before proceeding with this step, the sample quality in the time series of precipitation was rechecked, adopting a threshold of $\leq 10\%$ of failures (Holender, Santos 2023).

The data provided in HIDROWEB are categorized for quality in each measurement, assigning a number to their category: (0) – blank data (unmeasured), (1) – actual data (measured and verified), (2) – estimated data, (3) – doubtful data (instrumental failures), and (4) – accumulated data (ANA 2002).

The missing data index was calculated as follows:

$$MDI(\%) = \frac{n_0 + n_3}{n_t} \times 100 \quad (7)$$

where: n_0 – number of blank data points; n_3 – number of questionable data points; n_t – sample space.

2.5.2. Sequential test

After qualitative investigation of the data, the non-parametric Mann (1945) and Kendall (1975) tests, as sequenced by Sneyers (1990) and Onoz, Bayazit (2003), were applied in this study to test the significance of a trend present in the pluviometric series.

A time series of a variable y_i consisting of n data points, where $1 \leq i \leq n$, was considered. The procedure involved calculating the sum $t_n = \sum_{i=1}^n m_i$, where m_i is the number of terms preceding y_i and the preceding values y_j are less than y_i ($y_j < y_i$). This procedure was applied to time series with a large number of data points under the null hypothesis H_0 (absence of significant trend).

Based on this premise, it was found that t_n follows a normal distribution, with the mean and variance parameters defined by equations 8 and 9, respectively:

$$E(t_n) = \frac{n(n-1)}{4} \quad (8)$$

$$Var(t_n) = \frac{n(n-1)(2n+5)}{72} \quad (9)$$

Evaluating the statistical significance of t_n with respect to H_0 through a two-tailed test, significance is rejected for high values of $U(t_n)$, a standardized test statistic, defined as:

$$U(t_n) = \frac{(t_n - E(t_n))}{\sqrt{Var(t_n)}} \quad (10)$$

Subsequently, using a standardized normal distribution, the calculation of the probability value (α_1) is done as follows:

$$\alpha_1 = prob(|U| > |U_{tn}|) \quad (11)$$

Acceptance of H_0 occurs when $\alpha_1 > \alpha_0$, with α_0 equal to the significance level of the test. If H_0 is rejected, it implies the presence of a significant trend in the series: $U(t_n) < 0$ indicates a decreasing trend, while $U(t_n) > 0$ indicates an increasing trend.

In the sequential version, $U(t_n)$ is obtained in the forward direction of the series, starting from $i = 1$ to $i = n$. This results in the statistic $-1.65 < U(t_n) < 1.96$, where the values of the two-sided intervals -1.65 to 1.65 and -1.96 to 1.96 are associated with significance levels $\alpha_0 = 0.10$ (10%) and $\alpha_0 = 0.05$ (5%), respectively (Mortatti et al. 2004).

The inflection point in the series can be identified following the same approach as with the inverse series $U^*(t_n)$. The point where $U(t_n)$ and $U^*(t_n)$ intersect provides an approximate estimate of the location of the transition point in the trend. However, this conclusion holds statistical significance only if this change takes place within the two-sided significance interval (Back 2001).

The simplified execution of the steps to obtain the estimated probabilistic model in the present study is shown in Figure 2.

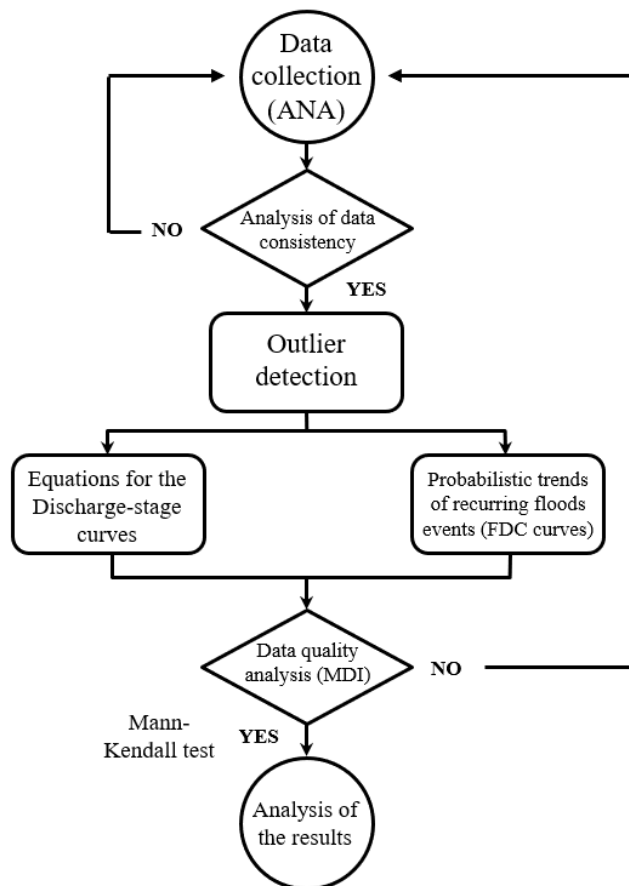


Fig. 2. Flowchart of the methodology used in this study.

3. Results and discussion

Inaccurate or inconsistent information can lead to erroneous conclusions and negatively impact decisions made based on this data. To ensure the reliability of the data used in this research, consistency checks were performed at the beginning of the analysis and before the Mann-Kendall test.

The first step involved verifying the availability of valid data from the pluviometric stations from 1983 to 2023. The results obtained show that Arame (Fig. 3b) and Santa Luzia (Fig. 3d) had data available for the entire series, Açailândia (Fig. 3a) from 1996 onward; in Buriticupu, the station provides data from 2004 forward (Fig. 3c).

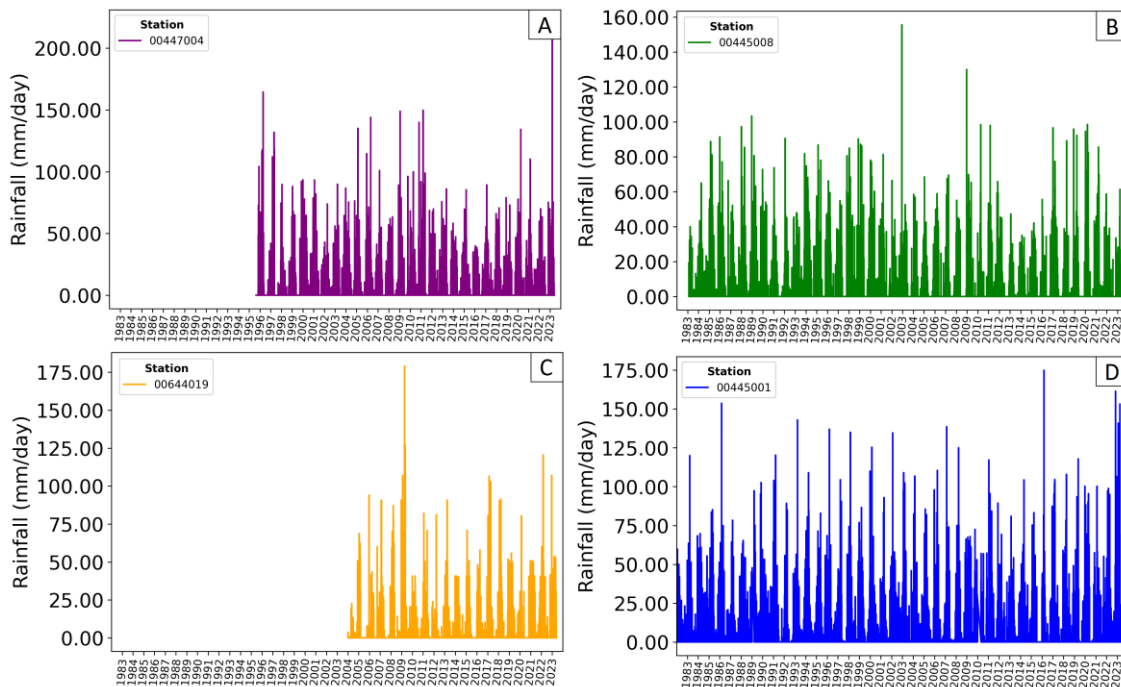


Fig. 3. Available rainfall data from 1983 to 2023 (a) Açailândia, (b) Arame, (c) Buriticupu and (d) Santa Luzia.

Figure 4 shows the box plots for all stations, plotted for each year from 2004 onward. Recent atypical precipitation events were observed, indicated by the outliers (red points).

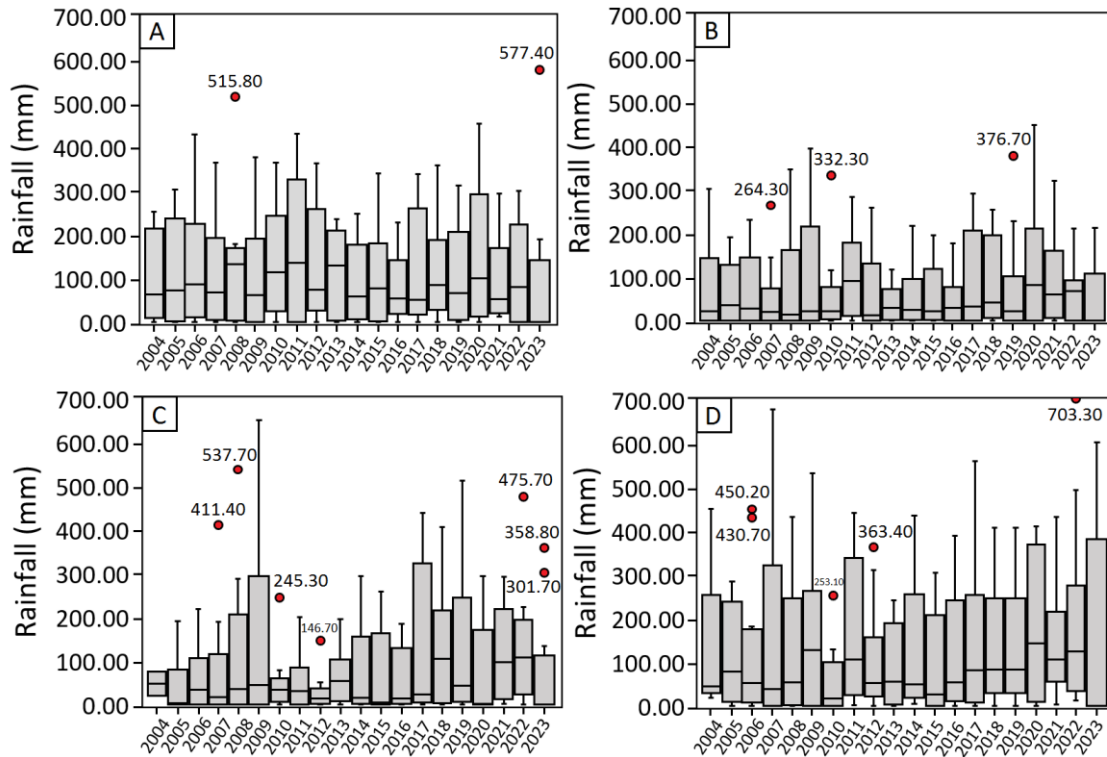


Fig. 4. Total annual rainfall at (a) Açailândia, (b) Arame, (c) Buriticupu and (d) Santa Luzia.

In the municipality of Açailândia (Fig. 4a), extreme precipitation events were recorded in March 2008 and 2023 (515.80 mm, 577.40 mm), coinciding with the onset of flooding events (Mar. 18-20 2023). In Arame (Fig. 4b), the outliers correspond to precipitation in February 2007 (264.30 mm); April 2010 (332.30 mm); and March 2019 (376.70 mm). In Buriticupu (Fig. 4c), rainfall anomalies were identified at various times over the years: in February 2007 (411.40 mm); March 2008, 2012, 2022, and 2023 (537.70 mm, 146.70 mm, 475.70 mm, 301.70 mm, respectively); and April 2010 and 2023 (245.30 mm, 358.80 mm). These records confirm the coincidence of atypical rainfall with flooding events in the municipality. In Santa Luzia (Fig. 4d), the records indicate critical precipitation in March 2006, 2012, and 2022 (430.70 mm, 363.40 mm, 703.30 mm); and April 2006 (450.20 mm). The results reaffirm that March is typically the rainiest month in the state of Maranhão (Cerqueira, Cerqueira 2023).

3.1. Probabilistic model

Figure 5 shows the stage-discharge curves obtained for each municipality, using streamflow data from the respective station. The exponential equations estimating the relationship between discharge (Q [$\text{m}^3 \text{s}^{-1}$]) and water level (h [m]) are provided in the caption.

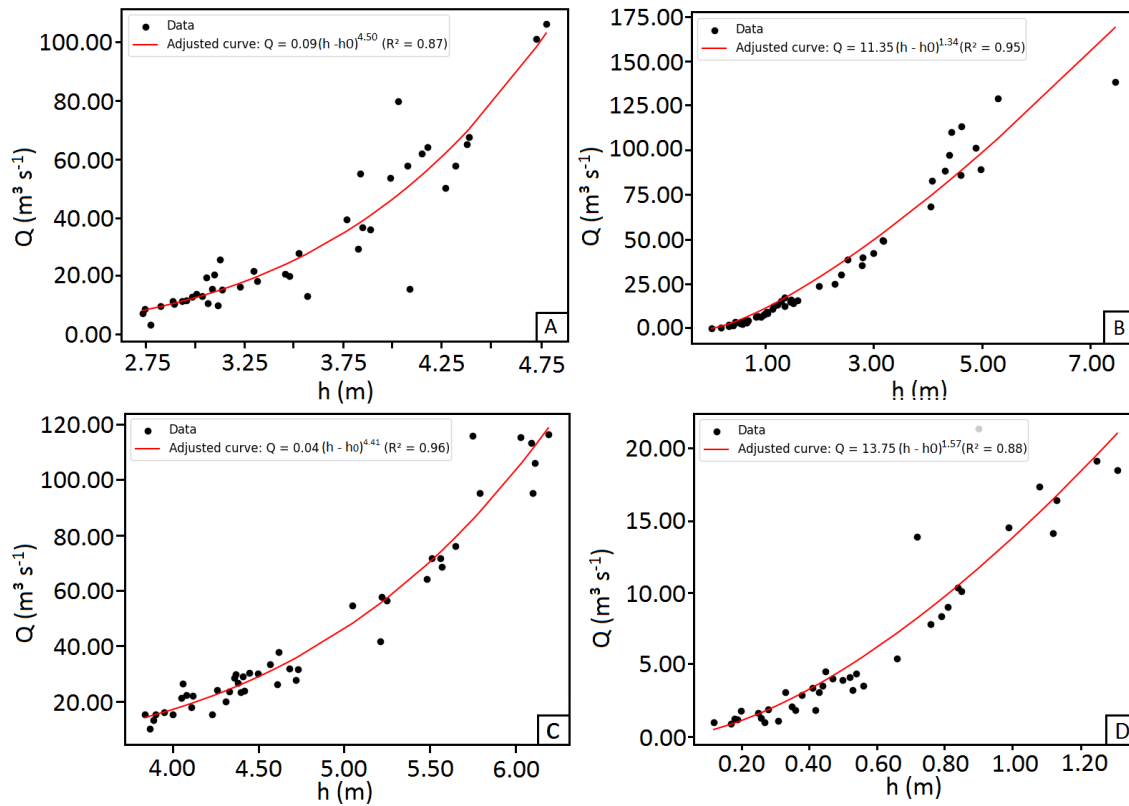


Fig. 5. Stage-discharge curves for (a) Açailândia, (b) Arame, (c) Buriticupu and (d) Santa Luzia.

These equations (Fig. 5) were used to estimate the discharge (Q [$\text{m}^3 \text{s}^{-1}$]) during the first days of flooding in the municipalities (Table 2), at fixed station measurement times (7:00 am and 5:00 pm).

Table 2. Estimated discharge (Q [$\text{m}^3 \text{s}^{-1}$]), measured water level (h [m]), and effective zero discharge level (h_0 [m]) at the onset of flood events.

Date	Time	Municipality	h_0 (m)	h (m)	Q ($\text{m}^3 \text{s}^{-1}$)		
03/18/2023	7:00 a.m.	Açailândia	-0.49	3.93	72.22		
	5:00 pm.			3.97	75.21		
03/19/2023	7:00 am.			4.10	85.59		
	5:00 pm.			4.28	101.76		
03/20/2023	7:00 am.			4.20	94.30		
	5:00 pm.			4.15	89.86		
03/18/2023	7:00 am.			Arame	0.53	3.96	59.20
	5:00 pm.					4.22	65.28
03/19/2023	7:00 am.	4.49	71.76				
	5:00 pm.	4.49	71.76				
03/20/2023	7:00 am.	4.46	71.04				
	5:00 pm.	4.48	71.52				
03/18/2023	7:00 a.m.	Buriticupu	-1.03			4.72	89.58
	5:00 pm.					4.70	88.21

03/19/2023	7:00 am.	Santa Luzia	2.95	4.70	88.21
	5:00 pm.			4.69	87.53
03/20/2023	7:00 am.			4.74	90.96
	5:00 pm.			4.76	92.36
03/18/2023	7:00 a.m.			4.19	19.27
	5:00 pm.			4.19	19.27
03/19/2023	7:00 am.			4.20	20.51
	5:00 pm.			4.20	20.51
03/20/2023	7:00 am.	4.18	20.67		
	5:00 pm.	4.18	20.67		

Using the estimated discharges on flood days as a parameter, the probability of recurring events of equal or greater magnitude was examined through the monthly FDC of the rivers passing through the municipalities in Maranhão, before (solid lines) and after (dashed lines) the onset of floods, as illustrated in Figure 6.

The probability of exceedance in the municipalities can be derived from the data in Table 2 and the FDCs. In the municipality of Açailândia (Fig. 6a), the average probability of exceedance is 10%; about 32% for Buriticupu (Fig. 6b); 15% for Arame (Fig. 6c); and less than 5% for Santa Luzia (Fig. 6d).

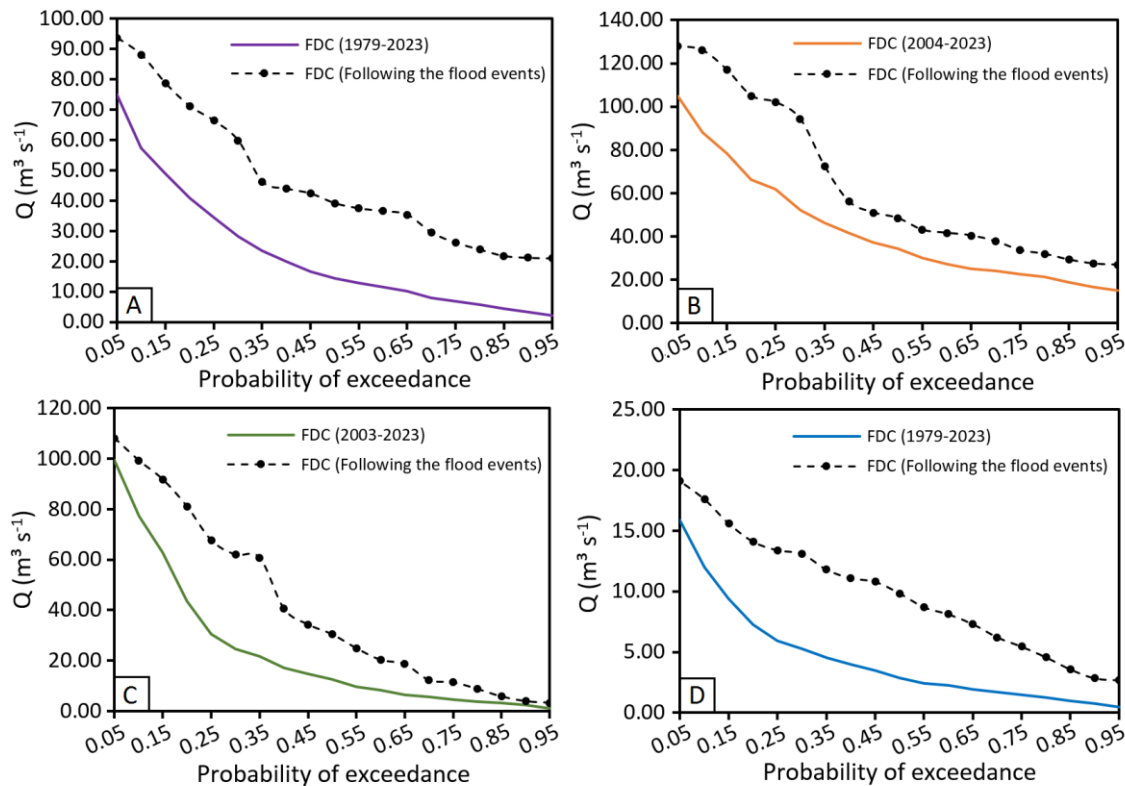


Fig. 6. Flow Duration Curves (FDC) of the monthly flow in different periods for the rivers (a) Pindaré Açailândia, (b) Pindaré, (c) Grajaú and (d) Buriticupu.

3.1.1. Statistical significance

Having established the connection between extreme precipitation events and flooding, data quality was confirmed through the Missing Data Index (MDI) (Table 3), which demonstrated that gaps in the series were within the adopted limit ($\leq 10\%$). Subsequently, a non-parametric test was applied to the monthly precipitation series.

The results of the Mann-Kendall test are presented in Table 4, focusing on two different significance levels: $\alpha_0 = 0.10$ (10%) and $\alpha_0 = 0.05$ (5%). α_1 values equal to or lower than the significance levels confirm a significant trend, depending on the sign of $U(t_n)$ for increasing (+) or decreasing (-) trend.

Table 3. Summary of pluviometric time series data quality metrics.

Time series	Data	Missing	Estimated	Doubtful	Accumulated	Missing Data Index
Açailândia (1996-2022)	14353	307	0.00	29	0	2.34%
Arame (1983-2022)	22,134	470	0.00	93	2	2.29%
Buriticupu (2004-2022)	6602	78	0.00	0	2	1.18%
Santa Luzia (1982-2022)	26,288	903	0.00	1	8	3.42%

Table 4. Summary of monthly Mann-Kendall tests on rainfall.

Month	Açailândia		$U(t_n)$	Arame			
	$Var(t_n)$			α_1	$Var(t_n)$	$U(t_n)$	α_1
Jan	2301.00		-1.42	0.14	6833.67	-2.32	<0.05
Feb	2301.00		0.08	0.93	6833.67	-1.16	0.24
Mar	2058.33		-0.62	0.51	6833.67	-1.61	0.10
Apr	2301.00		-0.69	0.47	7366.67	-1.20	0.22
May	2301.00		-1.00	0.30	6833.67	-1.88	<0.10
Jun	1257.67		1.52	0.13	1833.33	-1.99	<0.05
Jul	125.00		2.77	<0.05	1257.67	0.23	0.82
Aug	165.00		0.93	0.35	333.67	0.44	0.66
Sep	950.00		0.19	0.85	817.00	-0.21	0.78
Oct	1833.33		0.82	0.41	4165.33	-1.86	<0.10
Nov	2058.33		0.40	0.69	4958.33	-0.16	0.85
Dec	2058.33		-0.44	0.63	7366.67	-0.80	0.41
Month	Buriticupu		$U(t_n)$	Santa Luzia			
	$Var(t_n)$			α_1	$Var(t_n)$	$U(t_n)$	α_1
Jan	816.00		3.47	<0.10	12658.67	-0.15	0.88
Feb	815.00		0.84	0.40	13458.67	0.34	0.74
Mar	816.00		2.91	<0.10	13458.67	1.13	0.26
Apr	813.33		0.74	0.46	13458.67	1.16	0.24
May	812.33		0.49	0.62	6833.67	-1.90	<0.10
Jun	788.67		-1.82	<0.10	12658.67	0.55	0.58

Jul	788.67	2.31	<0.05	10450.00	0.16	0.88
Aug	800.33	-1.84	<0.10	7366.67	-0.86	0.39
Sep	812.33	-3.65	<0.05	6833.67	-1.19	0.24
Oct	816.00	1.79	<0.10	10450.00	-1.39	0.16
Nov	817.00	1.40	0.16	11891.00	0.55	0.58
Dec	816.00	1.72	<0.10	12658.67	-0.22	0.82

The values highlighted in bold in Table 4 indicate that $\alpha_1 < \alpha_0$, demonstrating that the null hypothesis of no trend (h_0) can be rejected for these months. The municipalities that showed trends in March were Arame (negative) and Buriticupu (positive).

When $U(t_n)$ exceeds the confidence interval, the trend can be considered significant, and the points of intersection between $U(t_n)$ and $U^*(t_n)$ represent the onset of this trend in the time series, if it occurs within the confidence intervals (Fig. 7).

In the municipality of Açailândia (Fig. 7a), there is a possibility of an increasing trend, becoming significant in July. In contrast, Arame (Fig. 7b) indicates decreasing trends that are significant in March, June, and October. Meanwhile, in Buriticupu (Fig. 7c), there are potential positive trends, with a notable emphasis on March and July. In Figure 7d, Santa Luzia exhibited a significant propensity for growth, starting in February and May.

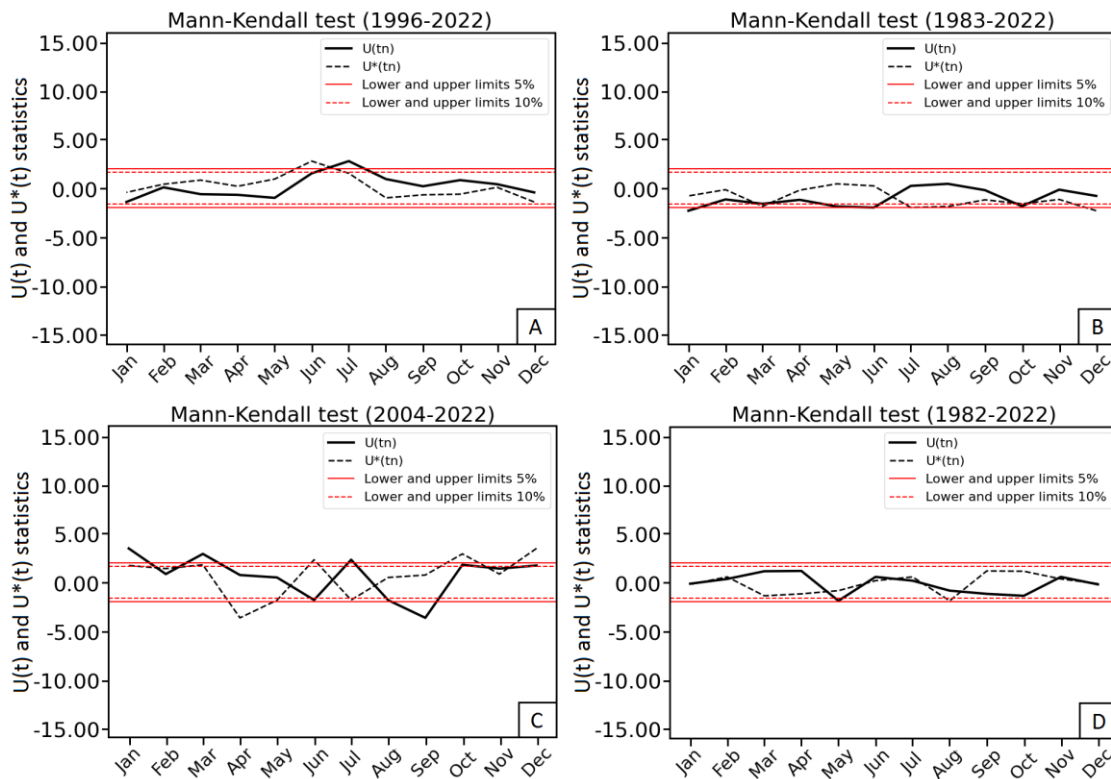


Fig. 7. Monthly rainfall $U(t)$ and $U^*(t)$ statistics for (a) Açailândia, (b) Arame, (c) Buriticupu and (d) Santa Luzia.

4. Conclusions

The results obtained for the municipalities of Açailândia, Arame, Buriticupu, and Santa Luzia highlighted the direct influence of heavy rainfall on the occurrence of flooding events, particularly during February, March, and April. In Açailândia and Buriticupu, extreme precipitation events were recorded in March 2023, with rainfall volumes of 577.40 mm and 301.70 mm, respectively, coinciding with the floods that occurred in March 2023.

The stage-discharge curves obtained provided equations that describe the discharge behavior as a function of water level in each municipality, providing parameters for flood prevention. This relationship was evident through the Flow Duration Curves (FDC), which indicated the probability of events of equal or greater magnitude at different times before and after the onset of floods.

Furthermore, the Mann-Kendall test revealed significant trends in some monthly precipitation series, emphasizing the presence of ascending or descending patterns in rainfall during specific months. These results underscore the critical importance of monitoring precipitation patterns to ensure water resource management and mitigate the impacts of floods in areas susceptible to extreme events.

References

- Alvalá R.C.S., Dias M.C.A., Saito S.M., Stenner C., Franco C., Amadeu P., Ribeiro J., Santana R.A.S. de M., Nobre C.A., 2019, Mapping characteristics of at-risk population to disasters in the context of Brazilian early warning system, *International Journal of Disaster Risk Reduction*, 41, DOI: 10.1016/j.ijdr.2019.101326.
- Alves M.E.P., Fan F.M., Paiva R.C.D. de, Siqueira V.A., Fleischmann A.S., Brêda J.P., Laipelt L., Araújo A.A., 2022, Assessing the capacity of large-scale hydrologic-hydrodynamic models for mapping flood hazard in southern Brazil, *RBRH*, 27, DOI: 10.1590/2318-0331.272220220009.
- ANA, 2002, *HIDRO – Sistema de Informações Hidrológicas, Versão 1.0, Manual do Usuário, Agência Nacional de Águas e Saneamento Básico*.
- ANA, 2005, *HIDROWEB v3.2.7 – Sistema de Informações Hidrológicas, Agência Nacional de Águas e Saneamento Básico*, available online at <https://www.snirh.gov.br/hidroweb/serieshistoricas> (data access 25.07.2024).
- Back A.J., 2001, Aplicação de análise estatística para identificação de tendências climáticas, *Pesquisa Agropecuária Brasileira*, 36 (5), 717-726, DOI: 10.1590/S0100-204X2001000500001.
- Becker A.C.C., Carvalho J.M., Goulart C.B., Ferreira A.H.R., Polli B.A., Ferreira D.M., Bernardo J.W.Y., Bleninger T.B., Fernandes C.V.S., 2023, Zero-dimensional modelling as tool for reservoir water quality planning and management, *RBRH*, 28, DOI: 10.1590/2318-0331.282320220115.
- Brasil, 2023, Ministério do Desenvolvimento Social. Ministro Wellington Dias e governador do Maranhão tratam de ações para atender afetados pelas enchentes no estado, available online at <https://bit.ly/govbrenchentesnomaranhao> (data access 25.07.2024).
- Cerqueira H.D., Cerqueira A.H.M.S., 2023, Avaliação Mensal da Chuva (março de 2023), Núcleo Geoambiental – NuGeo, Universidade Estadual do Maranhão, available online at <https://www.nugeo.uema.br/?p=47742> (data access 25.07.2024).
- Dias M.C. de A., Saito S.M., Alvalá R.C. dos S., Seluchi M.E., Bernardes T., Camarinha P.I.M., Stenner C., Nobre C.A., 2020, Vulnerability index related to populations at-risk for landslides in the Brazilian Early Warning System (BEWS), *International Journal of Disaster Risk Reduction*, 49, DOI: 10.1016/j.ijdr.2020.101742.

- Diário Oficial da Prefeitura de Açailândia, 2023a, Decreto Municipal nº 54, de 21 de março de 2023, Declara estado de Emergência no Município de Açailândia, em decorrência do elevado volume de chuvas, e dá outras providências, Maranhão, Prefeitura Municipal de Açailândia.
- Diário Oficial da Prefeitura de Arame, 2023b, Decreto Municipal nº 06, de 18 de março de 2023, Declara situação de emergência nas áreas do Município afetadas por Chuvas Intensas – COBRADE – 1.3.2.1.4, conforme Portaria MDR nº 260, de 02 de fevereiro de 2022, Maranhão, Prefeitura Municipal de Arame.
- Diário Oficial da Prefeitura de Buriticupu, 2023c, Decreto Municipal nº 009, de 21 de março de 2023, Declara estado de calamidade pública no território do Município de Buriticupu/MA, em virtude de danos causados por chuvas intensas – COBRADE 1.3.2.1.4, conforme a Portaria Federal nº 260, de 02 de fevereiro de 2022, do Ministério do Desenvolvimento Regional, e dá outras providências, Maranhão, Prefeitura Municipal de Buriticupu.
- Diário Oficial da Prefeitura de Santa Luzia, 2023d, Decreto Executivo N° 019, de 20 de março de 2023, Dispõe sobre situação de emergência em razão das áreas afetadas por Chuvas Intensas – Cobrade 1.3.2.1.4 no município de Santa Luzia, e dá outras providências, Maranhão, Prefeitura Municipal de Santa Luzia.
- Gogien F., Dechesne M., Martinerie R., Lipeme Kouyi G., 2023, Assessing the impact of climate change on Combined Sewer Overflows based on small time step future rainfall timeseries and long-term continuous sewer network modelling, *Water Research*, 230, DOI: 10.1016/j.watres.2022.119504.
- Holender B.V., Santos E.B., 2023, Análise de tendência dos eventos de precipitação intensa no Sudeste do Brasil, *Revista Brasileira de Climatologia*, 32, 584-606, DOI: 10.55761/abclima.v32i19.16411.
- Kendall M.G., 1975, Rank Correlation Methods, Charles Griffin, London.
- Lima F.N., Fernandes W., Nascimento N., 2019, Joint calibration of a hydrological model and rating curve parameters for simulation of flash flood in urban areas, *RBRH*, 24, DOI: 10.1590/2318-0331.241920180066.
- Lima G.R.T. de, Scofield G.B., 2021, Feasibility study on operational use of neural networks in a flash flood early warning system, *RBRH*, 26, DOI: 10.1590/2318-0331.262120200152.
- Ma L., Liu D., Huang Q., Guo F., Zheng X., Zhao J., Luan J., Fan J., Ming G., 2023, Identification of a function to fit the flow duration curve and parameterization of a semi-arid region in North China, *Atmosphere*, 14 (1), DOI: 10.3390/atmos14010116.
- Mann H.B., 1945, Non-parametric test against trend, *Econometrica*, 13 (3), 245-259, DOI: 10.2307/1907187.
- Mishra A., Mukherjee S., Merz B., Singh V.P., Wright D.B., Villarini G., Paul S., Kumar D.N., Khedun C.P., Niyogi D., Schumann G., Stedinger J.R., 2022, An overview of flood concepts, challenges, and future directions, *Journal of Hydrologic Engineering*, 27 (6), DOI: 10.1061/(ASCE)HE.1943-5584.0002164.
- Moreira R.M., Santos B.C. dos, Sanches R.G., 2023, Trend analysis of precipitation for protected areas and pasturelands in southwest Amazônia between 1998 and 2019, *Remote Sensing Applications: Society and Environment*, 29, DOI: 10.1016/j.rsase.2022.100901.
- Mortatti J., Bortoletto M.J.J.R., Milde L.C.E., Probst J.-L., 2004, Hidrologia dos rios Tietê e Piracicaba: séries temporais de vazão e hidrogramas de cheia, *Revista de Ciência & Tecnologia*, 12 (23), 55-67.
- Onoz B., Bayazit M., 2003, The power of statistical tests for trend detection, *Turkish Journal of Engineering and Environmental Sciences*, 27, 247-251.
- Peixoto L.O.M., Lima B.A.D., Almeida C.D.C., Fernandes C.V.S., Centeno J.A.S., Azevedo J.C.R.D., 2023, Data imputation of water quality parameters through feed-forward neural networks, *RBRH*, 28, DOI: 10.1590/2318-0331.282320220118.
- Penreiro J.C., Badinger A., Maccheri N.A., Meschiatti M.C., 2018, Distribuições de Tendências Sazonais de Temperatura Média e Precipitação nos Biomas Brasileiros, *Revista Brasileira de Meteorologia*, 33 (1), 97-113, DOI: 10.1590/0102-7786331012.
- Pereira V.B., 2023, Análise de precipitações médias históricas e decenais para determinação de disponibilidade hídrica, com foco na gestão do abastecimento público de água (Dissertação de mestrado), Faculdade de Engenharia de Ilha Solteira, Universidade Estadual Paulista, São Paulo, available online at <http://hdl.handle.net/11449/250226> (data access 25.07.2024).

- Ramírez C.A., Carvajal Y., Bocanegra R.A., Sandoval M.C., 2018, Determinación de relaciones nivel – caudal simple o compleja en un río. Caso del río Cauca, *Ingeniería Y Competitividad*, 20 (2), 45-56, DOI: 10.25100/iyv.v20i2.6354.
- Ridolfi E., Kumar H., Bárdossy A., 2020, A methodology to estimate flow duration curves at partially ungauged basins, *Hydrology and Earth System Sciences*, 24, (4) 2043-2060, DOI: 10.5194/hess-24-2043-2020.
- Sneyers R., 1990, *On the Statistical Analysis of Series of Observations*, Technical Note No. 143, WMO No. 415, World Meteorological Organization, Geneva, 192 pp.
- Tsuha R.T., 2023, Intercaptação de fluxo de água subterrânea (IGF): análise dos possíveis desvios de água da Bacia Hidrográfica do Rio Verde (UGHRI-04) por meio de falhas e fraturas (Dissertação de mestrado), Faculdade de Engenharia de Ilha Solteira, Universidade Estadual Paulista, São Paulo, available online at <http://hdl.handle.net/11449/250503> (data access 25.07.2024).
- Vishwakarma D.K., Kuriqi A., Abed S.A., Kishore G., Al-Ansari N., Pandey K., Kumar P., Kushwaha N.L., Jewel A., 2023, Forecasting of stage-discharge in a non-perennial river using machine learning with gamma test, *Heliyon*, 9 (5), DOI: 10.1016/j.heliyon.2023.e16290.
- Waseem H.B., Rana I.A., 2023, Floods in Pakistan: A state-of-the-art review, *Natural Hazards Research*, 3 (3), 359-373, DOI: 10.1016/j.nhres.2023.06.005.
- Zhang X., Zhao D., Zhao Y., Wen Y., 2022, Analysis of precipitation characteristics and changes of drought and flood disasters on Anhui Province between 1961 and 2020, based on time series, *Water Supply*, 22 (5), 5265-5280, DOI: 10.2166/ws.2022.178.

Flood meteorology, hydrology, and geomorphology of the Upper Godavari River, Western India

Archana D. Patil¹ , Pramodkumar S. Hire² , Gitanjali W. Bramhankar³ , Rajendra P. Gunjal⁴ ,
Vitthal K. Anwat⁵ 

¹RNC Arts, JDB Commerce and NSC Science College, Nashik 422101, India

^{2,3}HPT Arts and RYK Science College, Nashik 422005, India

⁴KRT Arts, BH Commerce and AM Science College, Nashik 422002, India

⁵K.S.K.W. Arts, Science & Commerce College, Nashik 422008, India

Priti R. Khandare⁶

⁶Satish Pradhan Dnyansadhana College, Thane 400604, India

Abstract

Meteorological, hydrological, and geomorphological aspects of large floods on the Upper Godavari River were investigated. Synoptic conditions associated with large floods were analyzed to gain an understanding of flood hydrometeorology in the basin. The study reveals that the southwest summer monsoon dominates rainfall in the Upper Godavari Basin (90% of annual rainfall). Moreover, interannual variability was characterized by increased frequency and magnitude of floods primarily after the 1930s and the majority of large floods were connected with low-pressure systems. Unit discharges (Q_u) and flash-flood magnitude index ($FFMI$) were computed to understand the potential for large floods. The high Q_u (1.13 and 6.00 m³ s⁻¹ km⁻²) are likely to be effective in terms of geomorphic changes in the channel. The greater $FFMI$ values (0.27 and 0.56) indicate the flashy and variable nature of floods and the possibility of significant geomorphic work. Parameters of flood hydraulics and hydrodynamics were computed to estimate the efficacy of infrequent and large-magnitude floods. The highest values for unit stream power (5909.61 W m⁻²) and bed shear stress (609 N m⁻²) reveal the unusually high capacity of the river to erode and transport coarse sediments. The Froude numbers (>1) confirm extremely erosive supercritical flows. High Reynolds numbers indicate exceedingly turbulent flood discharges, capable of accomplishing a variety of geomorphic activities.

Keywords

Meteorology, hydrology, geomorphology, floods, Upper Godavari River.

Submitted 10 June 2023, revised 4 March 2024, accepted 23 July 2024

DOI: 10.26491/mhwm/191702

1. Introduction

India lies at the heart of the classical monsoon region; it is extremely vulnerable to frequent hazards of floods and intense downpours that accompany low-pressure systems (LPS) during the monsoon season (Kale et al. 1994). Such massive floods are critical events, from the standpoint of human impact as well as in terms of geomorphic effectiveness.

The Godavari River has one of the most potent flood regimes in the seasonal tropics (Khandare 2009). Major flood events have been reported for the Godavari River, for instance, in September 1969 (Mujumdar et al. 1970), August 1981 (Pandharinath 1984), August 2006, September 2008 (Khandare 2009) and August 2019. However, information is scant about the causes and effects of such large floods on the Upper Godavari River (UGR). Therefore, the objectives of this paper are to examine the meteorological

aspects of large floods, to understand the hydrological characteristics of floods, and to evaluate the geomorphic impacts of floods on the UGR in terms of hydraulic properties and effects.

2. Upper Godavari Basin (UGB): geomorphic setting

The Godavari River, with 1465 km, is the second longest river in India and the longest among all the rivers in peninsular India. The river rises in the Western Ghat at Bramhagiri near Trimbakeshwar at an elevation of 1287 m in the Nashik District of Maharashtra State (Fig. 1). The river discharges into the Bay of Bengal at Narasapuram in the West Godavari district of the Andhra Pradesh. The total drainage area of the Godavari Basin is 312,813 km². This study represents an attempt to comprehend the meteorological, hydrological, and geomorphological aspects of large floods of the Upper Godavari River (UGR) in the headwater region (UGB = 5085 km²), i.e., from the river's source to Kopargaon Tehsil. The UGB is bounded by the Satmala Range in the north, the Western Ghat Escarpment in the west and the Kalsubai Range in the south. Geologically, the region is underlain by Cretaceous-Eocene Deccan Trap basalt; there are no later formations except the older alluvium of the late Pleistocene (Mujumdar et al. 1970) to late Holocene (Kale 2022). The major tributaries of the Upper Godavari River (UGR) are Dama, Dev, and Umri on the right bank, and Kadva, and Goi on the left bank.

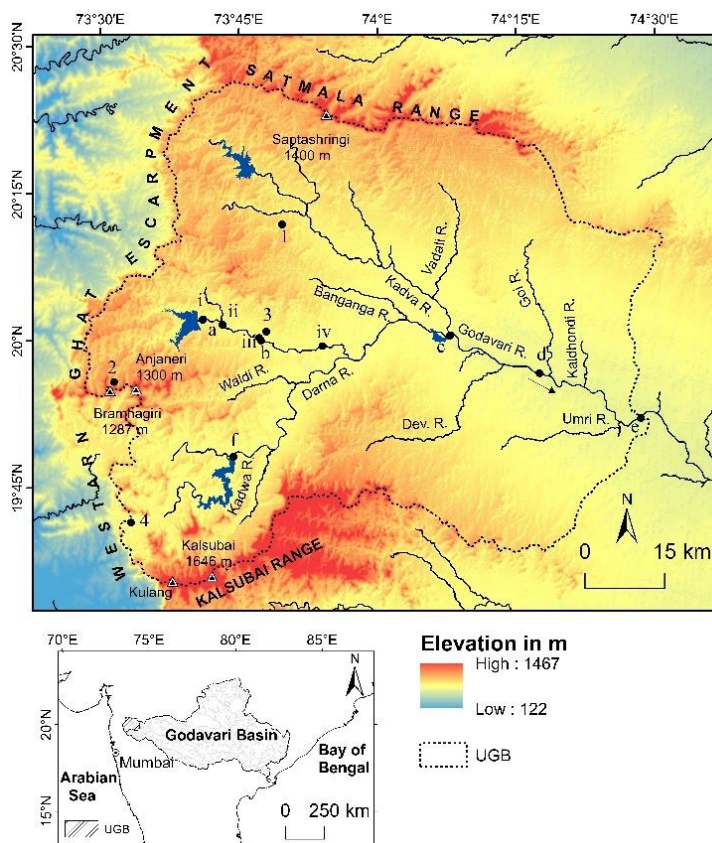


Fig. 1. Physiographic map of the study area: (1) Dindori, (2) Trimbakeshwar, (3) Nashik, (4) Igatpuri; (a) Gangapur Dam, (b) Nashik, (c) Nandur Madmeshwar Dam, (d) Chass, (e) Kopargaon, (f) Darna Dam; (i) Dugaon; (ii) Someshwar, (iii) Sarkarwada, (iv) Odha; UGB – Upper Godavari River.

3. Data source

Rainfall data from four rain gauge stations in the UGB were employed: Dindori, Trimbakeshwar, Nashik, and Igatpuri, with records ranging from 119 to 143 years (1878 to 2019). The data were collected from the India Meteorological Department (IMD), Pune. Data for tracks of low-pressure systems (LPS) from 1891 to 2019 were derived from the e-atlas obtained from IMD, Chennai. The annual maximum series (AMS) stage data were procured from the Centre Water Commission (CWC), New Delhi, Maharashtra Engineering Research Institute (MERI) and Hydrology Department, Nashik, for five gauging sites on the UGR and one site on its tributary, i.e., the Darna River. The AMS gauge records for the UGR are short and discontinuous (24 to 50 years). The cross-sectional surveys were carried out at four sites to compute parameters of hydraulics and hydrodynamics with respect to high flood levels (HFL).

4. Flood meteorology

Rainfall characteristics in monsoonal regions, particularly the distribution in space and time, are important in terms of flood generation. Consequently, one of the core objectives of this paper is to analyze the meteorological data that are currently available and to pinpoint the characteristics of rainfall that lead to significant flooding on the UGB. The UGR is rainfed, as are its tributaries. The southwest monsoon season's heavy to extremely severe rainfall is therefore responsible for all flooding on the river. Excessive and widespread rainfall is caused by a range of flood-producing meteorological conditions. These include LPS originating over the Bay of Bengal and terrestrial depressions, along with active to vigorous monsoon activity. In the following section, the features of flood-generating rainfall and allied synoptic situations are depicted. The UGB is located in an environment typical of southwestern monsoonal tropics, with periodic large-magnitude rainfall. The UGB receives 1780 mm of rain on average per year, with monsoon months, i.e., mid-June to early October, accounting for 90% of the total annual rainfall. The rainiest month is July, followed by August; they contribute 37% and 27% of the basin's total annual rainfall, respectively.

4.1. Interannual rainfall variability and associated floods

Akin to other monsoon-dominated rivers of India, the UGB also shows significant interannual variation in rainfall and, therefore, flood events. Table 1 lists details of the four stations with long-duration rainfall records (>100 years; between 1878 and 2019). Mean annual rainfall of the UGB ranges from 716 mm at Nashik to 3241 mm at Igatpuri. The low coefficient of variation (C_v) (24-33%) of annual rainfall in most parts of the basin demonstrates that interannual variability is not particularly high. The annual rainfall at each site varies greatly (Table 1). For example, the minimum annual rainfall at Nashik was 332 mm in 1984, whereas the maximum annual rainfall at Igatpuri was 6601 mm in 1931.

The coefficient of skewness (C_s) values range from 0.41 to 1.17 and are positive for all of the stations. The Dindori site reveals a relatively high positive C_s value. The positive C_s values indicate episodes of one or two or a few very wet years during the gauged period, for instance, in 1813 (1376 mm), 1981 (1600 mm),

2019 (1371 mm) and 2017 (1819 mm). Given that C_s values have been established based on more than 100 years of data, they are all statistically significant (Viessman et al. 1989).

Table 1. Annual rainfall characteristics of selected stations in the Upper Godavari Basin (UGB) (from 1878 to 2019). Data source: IMD.

Site	Altitude (m ASL)	Record length (years)	R_{max} (mm) [year]	R_{min} (mm) [year]	AAR (mm)	σ	C_s	C_v
Dindori	649	142	1820 [2017]	348 [1986]	791	240	1.17	0.30
Igatpuri	609	140	6601 [1931]	1463 [2015]	3241	772	0.56	0.24
Nashik	593	143	1540 [1883]	332 [1984]	716	234	0.78	0.33
Trimbakeshwar	715	119	4368 [1917]	935 [1998]	2373	574	0.41	0.24

R_{max} – maximum rainfall; ASL – above sea level; R_{min} – minimum rainfall; AAR – average annual rainfall; σ – standard deviation; C_s – coefficient of skewness; C_v – coefficient of variation. See Fig. 1 for site locations.

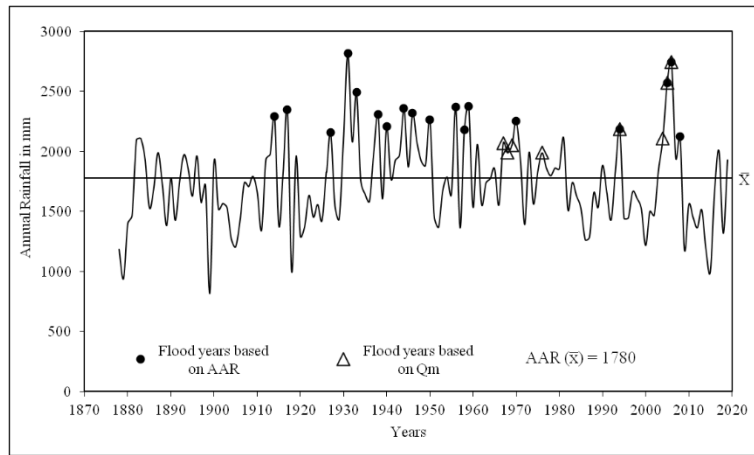


Fig. 2. Interannual rainfall variability and associated floods, UGR (1878 to 2019); AAR = annual average rainfall; Q_m = mean annual peak discharge.

The interannual variability of rainfall is shown as a time series plot in Figure 2 for the rain gauge sites located in UGB. The figure reveals that previous to 1930, rainfall was commonly below average with low interannual variability. In contrast, in many years between 1930 and 1980, above-average annual rainfall was recorded, with high interannual variability. After 1980, rainfall was frequently below average, with moderate interannual variability. In particular, after the 1930s, interannual variability was marked by an increase in the frequency and magnitude of floods on the UGR. Interestingly, similar results and remarkable interannual variability in the rainfall totals have been reported for some of the westward-flowing rivers of India (Kale 1999; Hire 2000; Patil 2018; Pawar, Hire 2018; Pawar 2019; Patil, Hire 2020; Anwat 2022). The time series plot of interannual variability of rainfall and associated floods shows that almost all of the large flood events in the UGR have occurred when rainfall was above average (Fig. 2). To identify the flood years for the UGR, the annual rainfall and discharge data were analyzed by applying equation 1 (Pant, Kumar 1997) and equation 2.

$$R_i \geq AAR + 1\sigma \quad (1)$$

where: R_i is the rainfall of year i , AAR is the long-term mean rainfall, and σ is the standard deviation.

$$Q_i \geq Q_m + 1\sigma \quad (2)$$

where: Q_i is the discharge of year i , and Q_m is the mean annual peak discharge.

4.2. Characteristics of the flood-generating low-pressure systems (LPS)

During all months of the year, except February, the Indian subcontinent is subjected to cyclonic disturbances (such as depressions and cyclonic storms) (Dhar et al. 1984). Attributable to the heavy rainfalls associated with these cyclonic disturbances, floods occur in those rivers whose catchments drain the rainstorm area (Dhar et al. 1984). These floods mark the largest recorded peaks in a flood time series (Kale et al. 1994). Flood-producing rainstorms are associated with Bay of Bengal depressions moving westward, general active monsoon conditions over Madhya Pradesh and Gujarat, and terrestrial depressions, according to earlier and more recent studies of the synoptic conditions associated with rainstorms (Abbi, Jain 1971; Ramaswamy 1987; Hire 2000; Patil 2018; Pawar 2019).

An effort has been made to identify and analyze the LPS tracks that caused the highest discharges in the basin to understand the relationship between LPS and floods in the UGB. The e-Atlas software was used to locate the LPS tracks, and ArcGIS 9.3 was applied to analyze them. The buffer zone was delineated at 500 km from the basin margin, and only LPS tracks that passed through the buffer zone were chosen for the investigation (Patil, Hire 2020) (Fig. 3). According to an assessment of the synoptic conditions associated with the flood-generating LPS, several of the LPS in the UGB were the result of Bay depressions and active monsoon conditions over central India. The association of LPS and consequent floods of the UGB were studied by using the AMS data. Streamflow records available for some sites on the UGR and its tributaries indicate that the LPS can have an immense impact. The systems, which comprise lows, depressions, and cyclonic storms (Dhar, Nandargi 1995), cause extreme stream rise, leading to large floods. Table 2 confirms the prevalence of LPS-linked floods in the UGR in August or September, by which time an average of $\sim 42\%$ of the annual rainfall has been received, and soils are completely saturated, further increasing the magnitude of floods.

In the quadrants to the right of the depression track, the rainfall field is flat. Conversely, large gradients of rainfall subsist in the left quadrants, especially along and west of 80°E . Additionally, the area with the maximum rainfall is in the left front quadrant, 150 km from the center and 50 to 150 km from the depression track (Mooley 1973). The position of the UGB remained in the left front quadrant during transit of the bulk of LPS(s) that traveled WNW or NW (Fig. 3; Table 2), thus resulting in high-magnitude floods. For instance, in 2005 and 2006, LPS caused high flood levels ($Q_i \geq Q_m + 1\sigma$ at Nashik; $633 \text{ m}^3 \text{ s}^{-1}$) on the UGR with 941 and $1034 \text{ m}^3 \text{ s}^{-1}$ discharges, respectively, at the Nashik gauging station. We investigated the relationship between LPS, greatest 24-hr. rainfall, and large floods in the UGB. The highest 24-hr.

rainfall at Nashik station was associated with LPS (Table 3). The September 10, 1969, LPS, which transited from the northwest corner of the UGB, is an excellent example of this kind (Fig. 3). The 24-hr. rainfall measured at Nashik station was 183 mm (16% of the total annual rainfall) (Table 3).

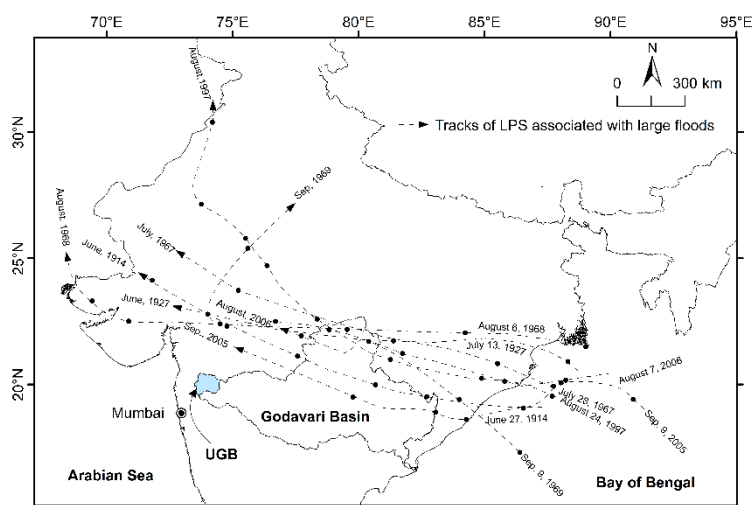


Fig. 3. Tracks of LPS associated with large floods on the UGR (1891 to 2019).

Table 2. Synoptic conditions associated with major floods on the Upper Godavari River.

Month, date and year of flood	Annual rainfall in the basin (mm)	Monsoon rainfall in the basin (mm)	Associated LPS
July 28, 1967	2071 (+16.37%)	1966 (+10.46%)	Bay Depression
August 6, 1968	1990 (+11.80%)	1880 (+05.64%)	Bay Depression
September 9, 1969	2053 (+15.33 %)	1984 (+11.48%)	Bay Depression
August 23, 1997	1664 (-06.49%)	1580 (-11.25%)	Bay Depression
September 23, 2005	2569 (+44.35%)	2481 (+39.39%)	Bay Depression
August 08, 2006	2744 (+54.18%)	2624 (+47.42%)	Bay Depression

Values in brackets represent percentage departure from the mean.

Table. 3 Low-pressure systems and highest 24 hr. rainfall at Nashik station. Data source IMD.

Date	Highest rainfall (mm)	Annual rainfall (mm)	Average annual rainfall (mm) 1878-2019	% of annual rainfall
June 26, 1984	118	999	715	12
July 13, 1927	86	798	715	11
Sept. 10, 1969	183	1145	715	16
Sept.22, 2005	109	1267	715	09
August 8, 2006	114	1233	715	09

5. Flood hydrology

The UGR, similar to other monsoonal rivers of peninsular India, is also subjected to high-magnitude floods at regular intervals. Therefore, it is of paramount importance to know the hydrologic characteristics of floods in terms of magnitude, frequency, and distribution.

5.1. Flood regime characteristics

According to gauge data, mean discharges range between $454 \text{ m}^3 \text{ s}^{-1}$ at Gangapur Dam (GD) and $2178 \text{ m}^3 \text{ s}^{-1}$ at Nandur Madmeshwar Dam (NMD) on the UGR (Fig. 1; Table 4). Historical and modern records show that large floods on the UGR occurred in 1939, 1965 (flood levels marked at Sarkarwada, an old administrative building of the 19th century, Nashik), 1969 (Mujumdar et al. 1970), 1976, 1979, 2004, 2005, 2006, 2008 (Khandare 2009), 2016, and 2019. The highest-ever recorded flood on the UGR at NMD in 1976 was on the order of $9977 \text{ m}^3 \text{ s}^{-1}$. This event, however, was not entirely natural. The unusually high discharge was primarily the result of a sudden release of a large volume of water from the dam. The second largest flood of the UGB occurred on August 10, 2006, with gauged discharge of $8857 \text{ m}^3 \text{ s}^{-1}$ at Kopargaon (Fig. 1). The heaviest 24-hour rainfall, which occurred two days prior to the event, totaled 114 mm, or 9% (Table 3) of the annual rainfall. The other aspects of the UGR's flood regime are presented in the following section.

Table 4. Flood flow characteristics of the Upper Godavari River. Data source: CWC.

Sr. No.	River	Site	A (km^2)	Record length	Q_{min} ($\text{m}^3 \text{ s}^{-1}$)	Q_{max} ($\text{m}^3 \text{ s}^{-1}$)	Q_m ($\text{m}^3 \text{ s}^{-1}$)	Flood Range	Q_{max}/Q_m
1	Godavari	Gangapur Dam (GD)	357	50	20	1886	454	1866	4.15
2	Godavari	Nashik	650	24	31	2288	481	2257	4.76
3	Godavari	Nandur Madmeshwar Dam (NMD)	1664	42	364	9977	2178	9613	4.58
4	Godavari	Chass	5230	25	160	5925	1212	5765	4.89
5	Godavari	Kopargaon	7096	27	128	8857	1822	8729	4.86
6	Darna	Darna Dam (DD)	404	41	142	1891	790	1749	2.39

Q_{min} – minimum annual peak discharge; Q_{max} – maximum annual peak discharge; Q_m – mean annual peak discharge; A – catchment area. See Fig. 1 for the location of the sites.

5.1.1. Interannual variability in annual peak discharges

The temporal patterns of variability in the annual peak discharges at six sites on the UGB are shown in Figure 4. The graphs reveal high interannual variability in the annual peak discharges and the occurrence of one or two extreme events during the gauge period. A large amount of geomorphic work is accomplished by higher flows in the UGB. Floods that generate discharges several times greater than a river's mean flows are more likely to result in considerable geomorphic change (Kochel 1988). This effect can be established merely by estimating the Q_{max}/Q_m ratio. The Q_{max}/Q_m ratio for the UGB ranges from 2.39 to 4.89 (Table 4). Consequently, it can be concluded that maximum annual peak discharges (Q_{max}) are approximately five times larger than average peaks. The significance of higher discharges increases

with flow variability (Wolman, Miller 1960). Such high flows are anticipated to have a significant impact on the geomorphic activities in the channel.

The coefficient of variation (CV), which measures hydrological variability in annual peak discharges, is another useful indicator. The CV , which ranges between 0.54 and 1.28 (Table 5), representing the ratio between the standard deviation (σ) and the mean (Q_m), suggests moderate to high dispersion. The variability in flood flows may be credited to various hydrological events accountable for producing the floods.

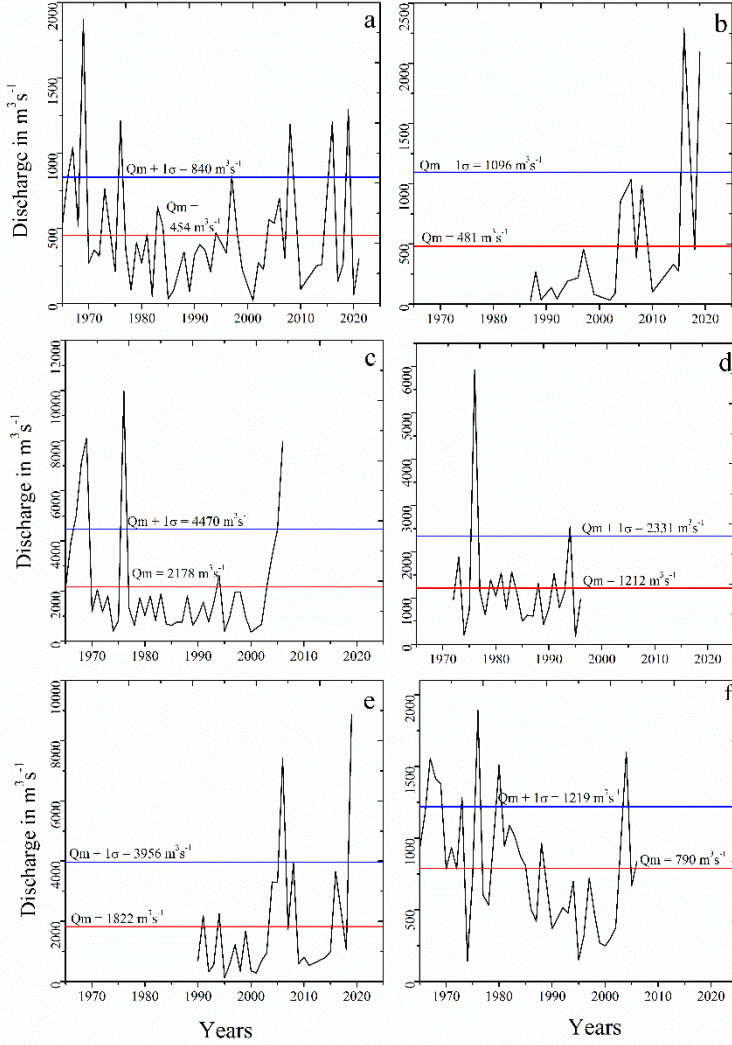


Fig. 4. Interannual variability in annual peak discharges, UGB: (a) Gangapur Dam, (b) Nashik, (c) Nandur Madmeshwar Dam, (d) Chass, (e) Kopargaon, (f) Darna Dam. See Fig. 1 for the location of the sites.

A number of researchers have used Beard's flash flood magnitude index ($FFMI$) to evaluate the variance in flood frequency as an index of the flashiness of floods (Baker 1977). The $FFMI$ values are calculated using the standard deviation of AMS logarithms, as mentioned below.

$$FFMI = \sqrt{\frac{\sum X^2}{N-1}} \quad (3)$$

where: X is $X_m - Q_m$; X_m – annual maximum event; Q_m – mean annual peak discharge; N – number of years of record (X , X_m , and Q_m expressed as \log_{10}).

The *FFMI* of the UGB ranges from 0.27 to 0.56, the mean *FFMI* is 0.4 (Table 6). This *FFMI* value is greater than the mean for the world, i.e., 0.28 (McMahon et al. 1992; Erskine, Livingstone 1999). The high mean *FFMI* indicates that UGR floods are slightly more flashy and variable than the average for world rivers. The *FFMI* further suggests a greater possibility for significant geomorphic changes during large floods.

Table 5. Discharge characteristics of the UGB. Data source: CWC.

Sr. No.	River	Site	Record length	Q_{max} ($m^3 s^{-1}$)	Q_m ($m^3 s^{-1}$)	SD	Cv	Cs	Cs/Cv
1	Godavari	Gangapur Dam (GD)	50	1886	454	386	0.85	1.67	1.96
2	Godavari	Nashik	24	2288	481	615	1.28	2.0	1.56
3	Godavari	Nandur Madmeshwar Dam (NMD)	42	9977	2178	2292	1.05	2.07	1.97
4	Godavari	Chass	25	5925	1212	1119	0.92	3.34	3.62
5	Godavari	Kopargaon	27	8857	1822	2133	1.17	2.19	1.87
6	Darna	Darna Dam (DD)	41	1891	790	429	0.54	0.65	1.20

Q_{max} – maximum annual peak discharge; Q_m – mean annual peak discharge; SD – standard deviation; Cv – coefficient of variation; Cs – coefficient of skewness. See Fig. 1 for the location of the sites.

Table 6. Flash flood magnitude indices (*FFMI*) of the Upper Godavari River. Data source: CWC.

Sr. No.	River	Site	Record length	<i>FFMI</i>
1	Godavari	Gangapur Dam (GD)	50	0.42
2	Godavari	Nashik	24	0.56
3	Godavari	Nandur Madmeshwar Dam (NMD)	42	0.37
4	Godavari	Chass	25	0.32
5	Godavari	Kopargaon	27	0.45
6	Darna	Darna Dam (DD)	41	0.27
7	UGB	Mean value	-	0.40

See Fig. 1 for the location of the sites.

5.1.2. Skewness

The coefficient of skewness (Cs) is the most common statistical moments employed in investigations of flood geomorphology and flood hydrology. Since the AMS data are not normally distributed, it is vital to find the Cs of the data. The values of Cs for all the stations on the UGR are positive, ranging from 0.65 to 3.34 (Table 5). The Cs values computed for other large rivers in India (Sakthivadivel, Raghupathy 1978; Hire 2000) are similar to the skewness values derived for the UGB. The positive Cs values predict the occurrence of one or two (or a few) very large magnitude flows during the gauge period. However, the characteristic of skewness is of doubtful value when applied to less than 50 years of data (Viessman et al.

1989). Subsequently, some hydrologists have also used the ratio Cs/Cv to further consolidate the degree of skewness (Shaligram, Lele 1978). The Cs/Cv ratio for different UGB discharge-gauging sites ranges from 1.20 to 3.62 (Table 5). The Cs/Cv ratios are often greater than 2.0 for the majority of India's large rivers (Shaligram, Lele 1978), demonstrating that peak discharge distribution is not extremely skewed.

5.1.3 Unit discharges (Q_u)

Unit discharge (Q_u) is a crucial indicator of the potential for large floods on a river (Gupta 1988). This ratio divides maximum annual peak discharge (Q_{max}) by the upstream catchment area (A), giving discharge or water yield per unit drainage area ($m^3 s^{-1} km^{-2}$). The Q_u computed for all the sites on the UGB range from 1.13 to $6.00 m^3 s^{-1} km^{-2}$ (Table 7). For the UGB as a whole, the Q_u is $3.64 m^3 s^{-1} km^{-2}$. These unit discharges fall below the world envelope curve of the unit discharges constructed by Baker (1995). In comparison, the unit discharges of natural extreme floods on large peninsular rivers vary from 0.13 to $0.65 m^3 s^{-1} km^{-2}$ (Kale et al. 1997; Hire 2000). In terms of geomorphic changes in the valley and channel, these discharges are likely to be effective (Costa, Connor 1995; Kale et al. 1997).

Table 7. Unit discharges (Q_u) of the Upper Godavari River. Data source: CWC.

Sr. No.	River	Site	A (km ²)	Q_{max} (m ³ s ⁻¹)	Q_u (m ³ s ⁻¹ km ⁻²)
1	Godavari	Gangapur Dam (GD)	357	1886	5.28
2	Godavari	Nashik	650	2288	3.52
3	Godavari	Nandur Madmeshwar Dam (NMD)	1664	9977	6.00
4	Godavari	Chass	5230	5925	1.13
5	Godavari	Kopargaon	7096	8857	1.25
6	Darna	Darna Dam (DD)	404	1891	4.68

A – catchment area; Q_{max} – maximum annual peak discharge. See Fig. 1 for the location of the sites.

6. Flood geomorphology

Flood geomorphology is concerned with the forms, processes, causes, and effects of floods (Baker 1988). Floods are primarily accountable for sculpting the river channel and the landscape in some hydro-geomorphic environments, for instance, the seasonal tropics (Wohl 1992; Gupta 1995). One of the significant themes in flood geomorphology has been the measurement and evaluation of the geomorphic efficiency of floods of various magnitudes. The geometry of river channels is considered to be a key factor in establishing the geomorphic effect of floods (Kochel 1988). To assess the geomorphic effects of floods, cross-sectional surveys were carried out at four sites (Fig. 5a-d) on the UGR to understand the channel geometry/morphology; hydraulic and hydrodynamic parameters of all the stations for respective high flood levels (HFL) have been computed and analyzed (Table 8).

The geomorphic efficacy of a flood, which relates to its capacity to affect the shape of the landscape (Wolman, Gerson 1978), is linked to flood power and the degree of turbulence (Baker, Costa 1987; Wohl 1993; Baker, Kale 1998; Kale, Hire 2004, 2007). Therefore, for identified unusual flood events, boundary

shear stress (τ), stream power per unit boundary area (ω), Froude number (Fr) and Reynolds number (Re) were computed with the help of the following formulas (Equations 4 to 7) (Leopold et al. 1964; Baker, Costa 1987).

$$\omega = \gamma QS/w \quad (4)$$

$$\tau = \gamma RS \quad (5)$$

$$Fr = \bar{V}/(gR)^{0.5} \quad (6)$$

$$Re = \bar{V}R/\nu \quad (7)$$

where: ω is unit stream power expressed in watts per square meter ($W m^{-2}$); γ is the specific weight of clear water ($9800 N m^{-3}$); Q is discharge in $m^3 s^{-1}$; S is the slope, w is the water surface width in m ; τ is the boundary shear stress expressed in Newtons per square meter ($N m^{-2}$); R is the hydraulic radius or mean depth of water in m . Fr – Froude number; \bar{V} – mean flow velocity in $m s^{-1}$; g – acceleration due to gravity ($9.8 m s^{-2}$); Re – Reynolds number; ν – kinematic viscosity ($1 \times 10^{-7} m^2 s^{-1}$ for water temperature of $20^\circ C$; Petts, Foster 1985).

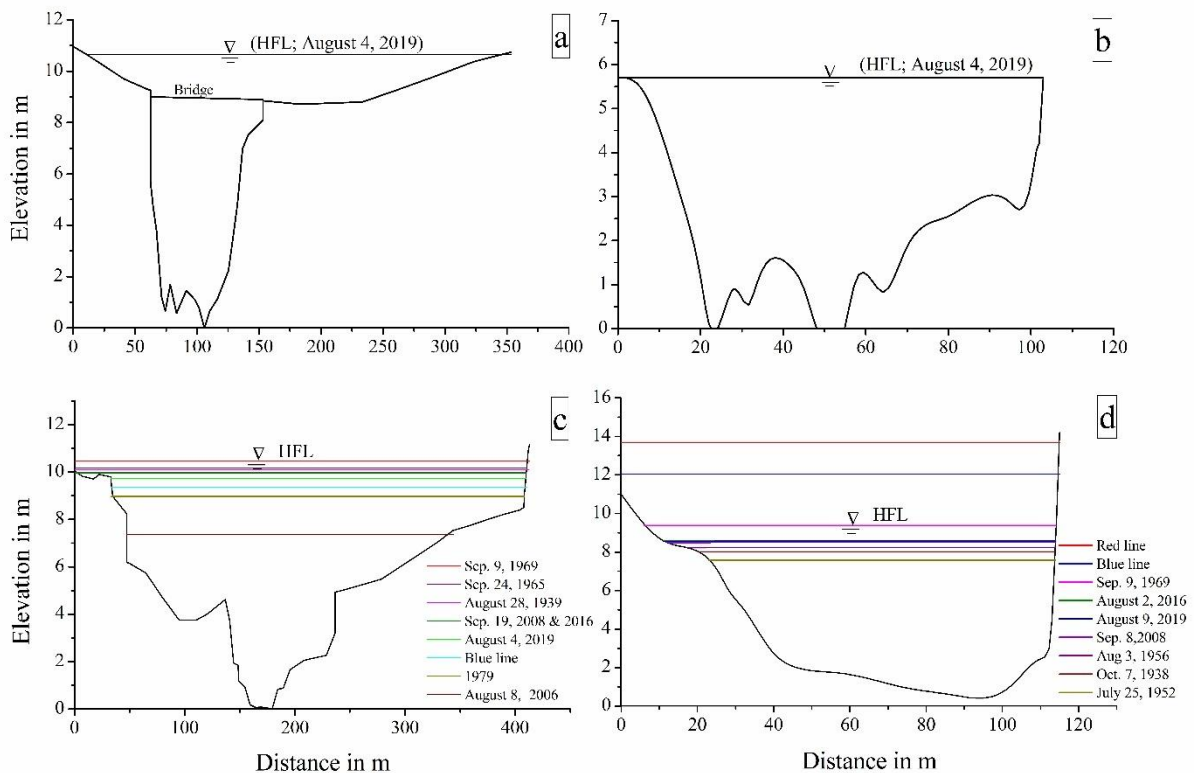


Fig. 5. Cross sections, UGR. (a) Dugaon, (b) Someshwar; (c) Sarkarwada; (d) Odha. See Fig. 1 for the location of sites. HFL – High flood level; Red line = 100-year flood line; Blue line = 25-year flood line.

Table 8. Hydraulic parameters of rare floods on the Upper Godavari River.

Sites on the UGR	DD.MM.YY	Discharge Q ($\text{m}^3 \text{s}^{-1}$)	Width W (m)	Depth D (m)	Slope S	Velocity \bar{V} (m s^{-1})	Shear stress τ (N m^{-2})	Unit Stream Power ω (W m^{-2})	Fr	$Re \times 10^7$	V_c (m s^{-1})
Dugaon	04.08.2019	1583	92	10.65	0.00357	3.12	192.48	600.71	0.43	17.17	11.81
Someshwar	04.08.2019	1894	101.81	5.20	0.012	5.17	423.36	2188	0.87	18.61	10.14
Sarkarwada	28.08.1939	2830.98	102.50	10.09	0.00423	3.97	288.21	1145.35	0.48	27.62	11.65
	24.09.1965	2878.76	102.50	10.16	0.00423	4.00	291.11	1164.68	0.48	28.09	11.67
	09.09.1969	3087.14	102.50	10.46	0.00423	4.11	303.55	1248.99	0.49	30.12	11.76
	1979	2104.96	102.50	9.86	0.00423	3.53	241.35	851.62	0.47	20.54	11.59
	08.08.2006	1410.81	102.50	7.36	0.00423	3.01	189.93	570.78	0.45	13.76	10.83
	19.09.2008	2736.39	102.50	9.95	0.00423	3.92	282.41	1107.08	0.48	26.70	11.61
	19.09.2016	2736.39	102.50	9.95	0.00423	3.92	282.41	1107.08	0.48	26.70	11.61
	04.08.2019	2577.25	102.50	9.71	0.00423	3.83	272.45	1042.70	0.48	25.14	11.54
Odha	07.10.1938	3836.03	87.50	7.50	0.0102	8.60	509.80	4382.28	1.22	43.84	10.88
	25.07.1952	3346.91	87.50	7.10	0.0102	8.14	469.81	3823.51	1.20	38.25	10.75
	03.08.1956	4091.94	87.53	7.80	0.0102	8.82	529.79	4673.03	1.22	46.75	10.97
	09.09.1969	6148.46	104.00	8.90	0.0102	9.69	609.76	5909.61	1.25	59.12	11.30
	03.08.1990	3346.91	87.50	7.10	0.0102	8.14	469.81	3823.51	1.20	38.25	10.75
	19.09. 2008	4587.00	89.50	8.00	0.0102	9.15	559.78	5123.09	1.24	51.25	11.03
	02.08.2016	4724.61	89.50	8.10	0.0102	9.26	569.77	5276.78	1.24	52.79	11.06
	04.08.2019	4724.61	89.50	8.10	0.0102	9.26	569.77	5276.78	1.24	52.79	11.06

Fr – Froude number; Re – Reynolds number; V_c – critical velocity for inception of cavitation.

Critical velocity for inception of cavitation (V_c) is another measure of the erosional power of flows (Equation 8). The V_c in m s^{-1} is given by Baker (1973) and Baker, Costa (1987).

$$V_c = 2.6 (10 + D)^{0.5} \quad (8)$$

where V_c is the critical velocity for the inception of cavitation in m s^{-1} and D is flow depth.

The discharges for the unusual floods on the UGR range from 1410 to 6148 $\text{m}^3 \text{s}^{-1}$ (Table 8). These are large rainfall-runoff floods calculated by indirect methods. From the reconstructed hydraulic data, the stream power per unit area of the UGB ranges from 571 to 5909 W m^{-2} . In comparison, the estimated average unit stream power at a cross-section (alluvial) varies between 322 W m^{-2} on the Godavari and less than 10 W m^{-2} on the Brahmaputra (Kale 1998). Estimation of boundary shear stress for large floods by using Equation (5) indicates that the values for UGR range from 192 to 610 N m^{-2} (Table 8). The estimated values for the Ganga, Yamuna, and Kosi Rivers are 11-25 N m^{-2} , and for the Narmada and Godavari Rivers (as a whole), the shear stress values are $>50 \text{ N m}^{-2}$ (Kale, Gupta 2001). Floods generating shear

stress of 10 N m^{-2} can entrain and transport sediments of about 1 cm and can carry sediments finer than 1 mm in suspension (Komar 1988). The high values of shear stress on the UGR reflect the uncommonly high capacity of the river to entrain and transport coarse sediments.

The analysis further indicates that Froude numbers greater than 1 (supercritical flow) have occurred on the UGR at the deep, narrow bedrock reach at Odha (Fig. 1) for all the flow conditions (Table 8). Intense bedrock scouring, resulting from cavitating flow, is also reflected in erosional features such as polished rock surfaces and potholes (Baker et al. 1988; Kale et al. 1993, 1994) at Odha ($Fr > 1$) and Someshwar sites ($Fr \approx 1$). High values of Reynolds numbers signify that the flood discharges could be exceedingly turbulent, and, therefore, capable of a variety of geomorphic actions. The Odha site (Fig. 1) produced the highest Reynolds number (59.12×10^7) for the September 1969 flood (Table 8), thus, it is probable that this reach experienced very intensive bedrock erosion. The critical velocity for the inception of cavitation (V_c) is a related measure of the erosional power of flows. According to estimates of V_c , no floods have ever exceeded the conditions described by Equation 8 at any of the survey sites on the UGR. However, erosional features, including flute marks, polished rock surfaces, and potholes at various locations at other sites on the UGR, are evidence of severe bedrock scouring by cavitating flow.

The channel bed of the UGR in alluvial reaches is composed of pebbly-cobbly gravel, and of boulders at the Dugaon site (Fig. 1). The sediment-transport equations developed by Williams (1983) were applied to determine the theoretical minimum critical values of bed shear stress (τ), unit stream power (ω), and mean velocity (\bar{V}) that could initiate cobble and boulder movement (Table 8). The equations used in the boulder transport calculations are as follows:

$$\omega = 0.079 dg^{1.27} \quad (9)$$

$$\tau = 0.17 dg \quad (10)$$

$$\bar{V} = 0.065 dg^{0.5} \quad (11)$$

where dg is the intermediate diameter of the grain in mm.

Theoretical estimates indicate that the unit stream power required for moving pebbles (4-64 mm), cobbles (64-256 mm), and a boulder (550 mm) is respectively 16, 90, and 239 W m^{-2} . The corresponding values of boundary shear stress are 11, 44, and 94 N m^{-2} (Williams 1983). A comparison of these theoretical estimates with the calculated values given in Table 9 specifies that, even though sand and pebbles are moved during all flows, floods on the UGR are capable of transporting cobble-sized sediments, and most of the large floods can move large boulders >550 mm in diameter. For instance, a concrete slab of bridge with i-axis of 810 mm was detached by the August 4, 2019 flood, with an estimated discharge of $2577 \text{ m}^3 \text{ s}^{-1}$ (Table 8) on the UGR at Sarkarwada (Fig. 1). This event produced unusually high values of bed shear stress (272 N m^{-2}), unit stream power (1043 W m^{-2}), and mean velocity (3.83 m s^{-1}) relative to the theoretical threshold estimates (Fig. 6, Table 9).

Further, the data computed for maximum velocities at Dugaon and Odha range from 3.12 to 9.69 m s⁻¹ (Table 8), respectively. The maximum surface velocities for very large floods are not available. Nevertheless, for the September 1969 flood, the maximum surface velocity was recorded as 2.47 m s⁻¹ at Paithan (Mujumdar et al. 1970), located in an area of gentle channel slope about 215 km downstream from Odha. According to available data, maximum velocities are much higher than the threshold velocities required for the movement of coarse sediment. It is, therefore, certain that large amounts of coarse sediment are moved during large floods, surpassing the total amount of suspended load transported by moderate flows.



Fig. 6. A view of UGR upstream of Sarkarwada (See location in Fig. 1) on 5th August 2019 (a day after the August 2019 flood). Width of flow 128 m and depth of flow 9.71 m (Photograph taken from Holkar/Victoria Bridge, Nashik).

Table 9. Boulder dimensions at the Dugaon site and the associated theoretical entrainment values.

Site	Distance from source (km)	I-axis (mm)	\bar{V} (m s ⁻¹)	τ (N m ⁻²)	ω (W m ⁻²)	W/D ratio
Dugaon	30	550	1.6	93.5	239	16.57
Panchvati (Sarkarwada)	44	810 (Concrete slab)	5.1	405	1535	39.12

ω – unit stream power in W m⁻²; τ – boundary shear stress in N m⁻²; \bar{V} – mean velocity in m s⁻¹; W/D – width/depth ratio (August 4, 2019 flood).

7. Conclusions

The southwest summer monsoon (mid-June to early October) dominates the rainfall supply of the UGB by producing about 90% of the annual rainfall. Therefore, the annual flow pattern of the UGB is intimately coupled with the patterns of variation in summer monsoon rainfall. The LPS that originate predominantly over the Bay of Bengal boost the magnitude of rainfall and subsequent floods. Human interference, by releasing large volumes of water from the dams, also underlies changes in flow regimes of the UGB. The study further indicates that the interannual variability of rainfall was associated with increased frequency and magnitude of floods, primarily after the 1930s. High interannual variability persists in the annual peak discharges. The more variable the flow, the more significant the higher discharges become.

The maximum annual peak discharges of the UGR are five times higher than average peaks. Therefore, geomorphic activity in the channel is likely to be vital. The slightly flashy and variable nature of floods on the UGR substantiates the possibility of the river experiencing significant geomorphic reworking during large floods. However, unit discharges of the UGR as a whole fall below the world envelope curve of unit discharges constructed by (Baker 1995). The UGR shows high spatial variability in terms of flood hydraulics and hydrodynamics. The higher values for unit stream power and boundary shear stress for rare floods reveal the uncommonly high capacity of the river to erode and transport coarse sediments. The approximate Froude numbers for two sites, as expected, are less than 1, representing that the flows were mainly subcritical. However, Froude numbers >1 for the constricted reach of the bedrock channel at Odha for numerous flood stages revealed that the flows were supercritical. High Reynolds numbers indicate that the flood discharges could be exceedingly turbulent and, therefore, capable of accomplishing a variety of geomorphic activities. According to estimates of the values of critical velocity for the inception of cavitation (V_c), none of the intense floods on the UGR exceeded the conditions required for inception of cavitation. However, erosional features, including flute marks, polished rock surfaces, and potholes at several locations at other sites of the UGR and its tributaries, suggest intense bedrock scouring resulting from cavitating flow conditions. Theoretical estimates of unit stream power, bed shear stress and mean velocity coupled with transported large boulders indicate that the floods on the UGR are competent to move large boulders. The effectiveness of large-magnitude flood events is also evident from the presence of deep, narrow gorges, scablands, polished rock surfaces, inner channels, and waterfalls at several locations on the UGR.

Acknowledgments

The authors are grateful to the Central Water Commission, New Delhi, Maharashtra Engineering Research Institute and Hydrology Department, Nashik, for providing hydrological data and India Meteorological Department, Pune, for supplying rainfall data. The authors are thankful to Snehal Kasar for her support in the field.

References


- Abbi S.D.S., Jain B.C., 1971, A study of major rainstorms of Tapi basin for evaluation of design storm, MAUSAM, 22 (4), 203-212, DOI: 10.54302/mausam.v22i2.4483.
- Anwat V., 2022, Fluvial and Flood Geomorphological Investigations of Bedrock Channel Reaches of The Damanganga River, Ph.D. Thesis, Savitribai Phule Pune University, Pune, 225 pp.
- Baker V.R., 1973, Erosional forms and processes for the catastrophic Pleistocene Missoula floods in eastern Washington, [in:] Fluvial Geomorphology, M. Morisawa (ed.), 123-148
- Baker V.R., 1977, Stream-channel response to floods, with examples from central Texas, Bulletin of the Geological Society of America, 88 (8), 1057-1071, DOI: 10.1130/0016-7606(1977)88<1057:SRTFWE>2.0.CO;2
- Baker V.R., 1988, Flood erosion, [in:] Flood Geomorphology, V.R. Baker, R.C. Kochel, P.C. Patton (eds.), Wiley, New York, 81-95.
- Baker V.R., 1995, Global paleohydrological change, *Quaestiones Geographicae*, 4, 27-35.

- Baker V.R., Costa J.E., 1987, Flood power, [in:] Catastrophic Flooding, V.R. Baker, J.E. Costa (eds.), Routledge, 1-21.
- Baker V.R., Kale V.S., 1998, The role of extreme floods in shaping bedrock channels, [in:] Rivers Over Rock: Fluvial Processes in Bedrock Channels, Geophysical Monograph Series, 107, American Geophysical Union, Washington, D.C., 153-165, DOI: 10.1029/GM107p0153.
- Costa J., Connor J.O., 1995, Geomorphologically effective floods, [in:] Natural and Anthropogenic Influences in Fluvial Geomorphology, Geophysical Monograph, 89, American Geophysical Union, 45-56.
- Dhar O.N., Kulkarni A.K., Mandal B.N., 1984, The most severe rainstorm of India – a brief appraisal, Hydrological Sciences Journal, 29 (2), 219-229, DOI: 10.1080/02626668409490935.
- Dhar O.N., Nandargi S., 1995, On some characteristics of severe rainstorms of India, Theoretical and Applied Climatology, 50, 205-212, DOI: 10.1007/BF00866117.
- Erskine W.D., Livingstone E., 1999, In-channel benches: the role of floods in their formation and destruction on bedrock confined rivers, [in:] Varieties of Fluvial Form, A.J. Miller, A. Gupta (eds.), John Wiley and Sons, 445-475.
- Gupta A., 1988, Large floods as geomorphic events in the humid tropics, [in:] Flood Geomorphology, V.R. Baker, R.C. Kochel, P.C. Patton (eds.), John Wiley and Sons, NY, 301-320.
- Gupta A., 1995, Magnitude, frequency, and special factors affecting channel form and processes in the seasonal tropics, [in:] Natural and Anthropogenic Influences in the Fluvial Geomorphology, Geophysical Monograph Series, 89, American Geophysical Union, 125-136.
- Hire P.S., 2000, Geomorphic and Hydrologic Studies of Floods in Tapi Basin, Ph.D. Thesis, University of Pune, Pune (India), 192 pp.
- Kale V., Gupta, A., 2001, Introduction to Geomorphology, Introduction to Geomorphology. Orient Longman, New Delhi, 274 pp.
- Kale V., Mishra S., Enzel Y., Ely L., Rajaguru S.N., Baker V.R., 1993, Flood geomorphology of the Indian Peninsular rivers, Journal of Applied Hydrology, 6, 49-55.
- Kale V.S., 1998, Monsoon floods in India: a hydro-geomorphic perspective, Memoir Geological Society of India, 41, 229-259.
- Kale V.S., 1999, Long-period fluctuations in monsoon floods in the Deccan Peninsula, India, Journal of Geological Society of India, 53, 5-15.
- Kale V.S., 2022, Holocene regional-scale behavior of the rivers of Indian Peninsula, [in:] Holocene Climate Change and Environment, N. Kumaran, P. Damodara (eds.), Elsevier, 103-129, DOI: 10.1016/B978-0-323-90085-0.00017-6.
- Kale V.S., Ely L.L., Enzel Y., Baker V.R., 1994, Geomorphic and hydrologic aspects of monsoon floods on the Narmada and Tapi Rivers in central India, Geomorphology (1-4), 10, 157-168, DOI: 10.1016/0169-555X(94)90014-0.
- Kale V.S., Hire P., Baker V.R., 1997, Flood hydrology and geomorphology of monsoon-dominated rivers: The Indian Peninsula, Water International, 22 (4), 259-265, DOI: 10.1080/02508069708686717.
- Kale V.S., Hire P.S., 2004, Effectiveness of monsoon floods on the Tapi River, India: Role of channel geometry and hydrologic regime, Geomorphology, 57 (3-4), 275-291, DOI: 10.1016/S0169-555X(03)00107-7.
- Kale V.S., Hire P.S., 2007, Temporal variations in the specific stream power and total energy expenditure of a monsoonal river: The Tapi River, India, Geomorphology, 92 (3-4), 134-146, DOI: 10.1016/j.geomorph.2006.06.047.


- Khandare P.R., 2009, Spatio-temporal aspects of floods on the Godavari River in the Nashik District, MPhil Thesis, Yashwantrao Chavan Maharashtra Open University, Nashik, 131 pp.
- Kochel R.C., 1988, Geomorphic impact of large floods: review and new perspectives on magnitude and frequency, [in:] Flood geomorphology, V. Baker, R. Kochel, P. Patton (eds.), John Wiley and Sons, New York, 169-187.
- Komar P.D., 1988, Sediment transport by floods, [in:] Flood Geomorphology, V.R. Baker, R.C. Kochel, P.C. Patton (eds.), Wiley, New York, 97-112.
- Leopold L.B., Wolman M.G., Miller J.P., 1964, Fluvial Processes in Geomorphology, 2nd edition, Dover Publications, 522 pp.
- McMahon T.A., Finlayson B.L., Haines A.T., Srikanthan R., 1992, Global runoff: continental comparisons of annual flows and peak discharges, Catena Verlag, 166 pp.
- Mooley D.A., 1973, Some aspects of Indian monsoon depressions and the associated rainfall, Monthly Weather Review, 101, 271-280, DOI: 10.1175/1520-0493(1973)101<0271:saoimd>2.3.co;2.
- Mujumdar G.G., Rajaguru S.N., Pappu R.S., 1970, The recent Godavari flood (September 1969) and its relevance to prehistoric archaeology, Bulletin of the Deccan College Post-Graduate and Research Institute, 29 (1-4), 118-134.
- Pandharinath N., 1984, A case study of 1981 flood in the Godavari River, MAUSAM, 35 (2), 195-198, DOI: 10.54302/MAUSAM.V35I2.2004.
- Pant G.B., Kumar K.R., 1997, Climates of South Asia, Belhaven Studies in Climatology, Wiley, 280 pp.
- Patil A., Hire P., 2020, Flood hydrometeorological situations associated with monsoon floods on the Par River in Western India, MAUSAM, 71 (4), 687-698, DOI: 10.54302/mausam.v71i4.58.
- Patil A.D., 2018, Bedrock Channel of the Par River : Its Forms and Processes, PhD Thesis, Tilak Maharashtra Vidyapeeth, Pune, 253 pp.
- Pawar U.V., Hire P.S., 2018, Long term fluctuations and global teleconnections in the monsoonal rainfall and associated floods of the Mahi Basin: Western India, International Journal of Scientific and Technology Research, 5 (1), 237-242.
- Pawar U.V., 2019, An Analytical Study of Geomorphological, Hydrological, and Meteorological Characteristics of Floods in the Mahi River Basin: Western India, PhD Thesis, Tilak Maharashtra Vidyapeeth, Pune, 211 pp.
- Petts G.E., Foster I.D.L., 1985, Rivers and Landscape, Edward Arnold, London, 274 pp.
- Ramaswamy C., 1987, Meteorological Aspects of Severe Floods in India 1923-1979, Meteorological Monography: Hydrology, No. 10, India Meteorological Department, 400 pp.
- Sakthivadivel R., Raghupathy A., 1978, Frequency analysis of floods in some Indian rivers, Hydrology Review, 4, 57-67.
- Shaligram V.M., Lele V.S., 1978, Analysis of hydrologic data using Pearson type III distribution, Hydrology Research, 9 (1), 31-42, DOI: 10.2166/nh.1978.0004.
- Viessman W., Lewis G.L., Knapp J.W., 1989, Introduction to Hydrology, Harper and Row, New York, 612 pp.
- Williams G.P., 1983, Paleohydrological methods and some examples from Swedish fluvial environments I, Cobble and boulder deposits, Geografiska Annaler: Series A. Physical Geography, 65 (3-4), 227-243, DOI: 10.1080/04353676.1983.11880088.
- Wohl E.E., 1992, Bedrock benches and boulder bars: floods in the Burdekin Gorge of Australia, Geological Society of America Bulletin, 104 (6), 770-778, DOI: 10.1130/0016-7606(1992)104<0770:BBABBF>2.3.CO;2.
- Wohl E.E., 1993, Bedrock channel incision along Piccaninny Creek, Australia, Journal of Geology, 101 (6), 749-761, DOI: 10.1086/648272.

- Wolman M.G., Gerson R., 1978, Relative scales of time and effectiveness of climate in watershed geomorphology, *Earth Surface Processes*, 3 (2), 189-208, DOI: 10.1002/esp.3290030207.
- Wolman M.G., Miller J.P., 1960, Magnitude and frequency of forces in geomorphic processes, *Journal of Geology*, 68 (1), 54-74, DOI: 10.1086/626637.

The kinematic and thermodynamic environment during cloud-to-ground lightning occurrence in Poland

Slawomir Sulik 

Faculty of Earth Sciences and Spatial Management, Nicolaus Copernicus University, Toruń, Poland
Skywarn Poland, Warsaw, Poland

Mateusz Taszarek 

Department of Meteorology and Climatology, Adam Mickiewicz University, Poznań, Poland
National Severe Storms Laboratory, Norman, Oklahoma, USA

Abstract

This study identifies convective and kinematic parameters that positively influence elevated values of cloud-to-ground lightning flashes (CGs) in Poland. The analysis used data from the PERUN lightning detection and location system from IMGW-PIB and reanalyses of the ERA5 model from ECMWF for the period 2002-2020. In addition, a spatial-temporal distribution analysis was carried out for the period 1940-2022, covering the key parameters necessary for the appearance of convection. Results showed that thunderstorms most often occur in the summer, but also that there are increasingly favorable conditions for the appearance of organized multicellular systems in the spring. CG flashes most often form in a most-unstable convective available potential energy (MU CAPE) environment of about 1300 J/kg along with vertical wind shear (0-6 km AGL bulk wind shear) of 13-14 m/s. Using the WMAXSHEAR parameter, it was possible to conclude that overlapping CAPE and DLS values of about 500 m²/s² imply increased electrical activity. At the same time, a high correlation with the Hail Size Index (HSI) parameter implies a positive relationship between the occurrence of hailstorms and an increased number of CGs generated in the case of supercells. The research also found a gradual increase in air temperature, MU CAPE, MU Mixing Ratio and the MU WMAXSHEAR parameter for the area under study.

Keywords

Lightning, thunderstorm, convection, climate change, reanalysis data, Poland.

Submitted 23 April 2024, revised 25 June 2024, accepted 30 July 2024

DOI: 10.26491/mhwm/191798

1. Introduction

Thunderstorms in Poland mainly occur in the warmer part of the year. Each year, there are about 150 days with thunderstorms in Poland; their frequency increases from the north to the southeast (Taszarek et al. 2015; Sulik, Kejna 2023). The smallest number of thunderstorm days (TD) per year has been recorded in the region nearest to the Baltic Sea (10-15 TD), while the highest activity occurs in the southeastern part of the country (35-40 TD). Thunderstorm activity in the warmer part of the year increases markedly from May to the end of August (Fig. 1B). Thunderstorms also occur in the cooler part of each year, but their number and electrical activity are nearly negligible.

Speaking of thunderstorms, according to the AMS *Glossary of Meteorology*, a thunderstorm is a phenomenon classified based on the occurrence of lightning, often accompanied by other dangerous phenomena such as strong wind gusts, heavy rainfall, and hail (Byers, Braham 1949). Because the occurrence of thunderstorms is equivalent to the occurrence of lightning, they should be given special attention, as in this study. Earlier studies concerning the spatial distribution and intensity of lightning discharges in Poland have

shown that the greatest electrical activity occurs in central Poland. Each year, the PERUN system records about 480,000 cloud-to-ground lightning flashes in the entire country (Sulik 2022). An increase in the number of lightning flashes each year across the country has also been confirmed (Fig. 1A). The constant activity of thunderstorm phenomena is also evident in the number of days with thunderstorms. Thunderstorm phenomena often contribute to a large number of property losses, usually associated with patchy, local wind gusts in the case of linear formations, or large hailfall associated with supercells (Groenemeijer et al. 2017; Taszarek et al. 2019b; Pilguy et al. 2022).

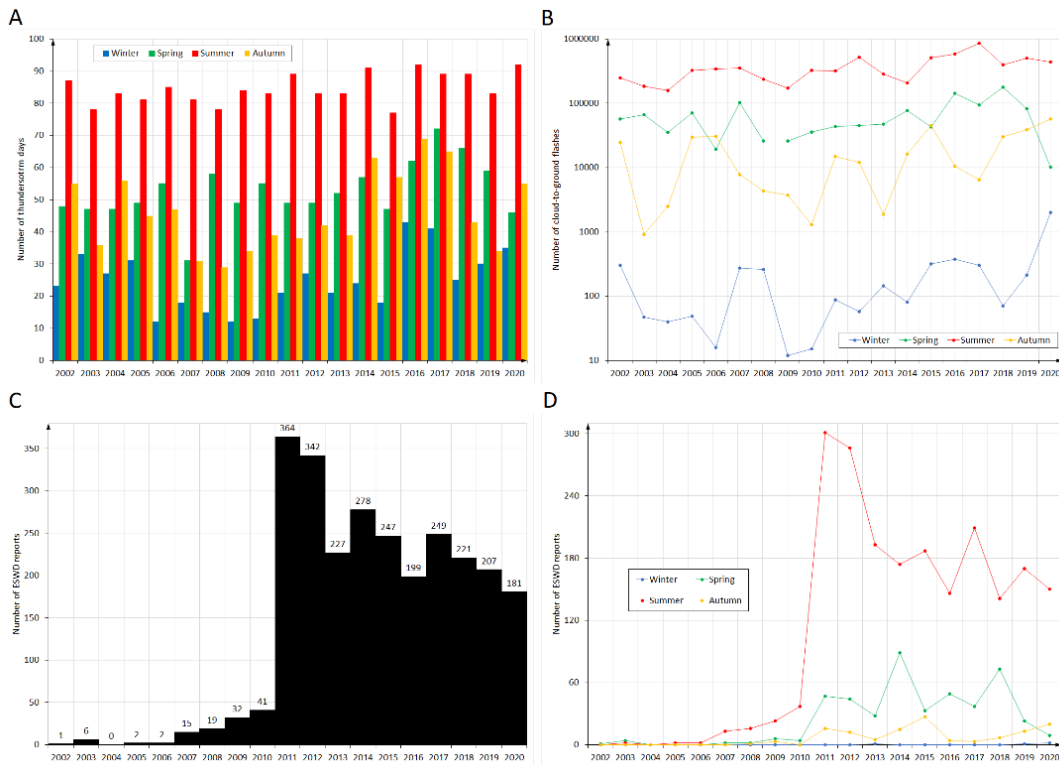


Fig. 1. A. Number of thunderstorm days in Poland by seasons derived from the PERUN lightning detection system; B. Number of cloud-to-ground flashes in Poland by seasons derived from the PERUN lightning detection system; C. Number of damaging lightning reports in Poland derived from the ESWD database; D. Number of damaging lightning reports in Poland by seasons derived from the ESWD database.

The temporal and spatial distributions of days with thunderstorms and their electrical activity can also be seen in reports from the hazardous weather database (ESWD; Dotzek et al. 2009). Thanks to the European Weather Observer (EWOB) system managed by the European Severe Storms Laboratory (ESSL), users of the application can send information about weather events of various types. The reports shown in Figures 1C and 1D reflect a phenomenon known as damaging lightning, which is most often associated with property damage caused by cloud-to-ground lightning. Every year throughout Europe, storms cause millions of euros in damages, and in Poland alone, between 2002 and 2020, 50 people died and 408 were injured by lightning strikes. The relationships of a warming climate to violent atmospheric phenomena are important; this study aims to determine the thermodynamic and kinematic conditions under which thunderstorms generating cloud-to-ground flashes are formed in Poland.

2. Dataset and methodology

2.1. Lightning data

Lightning data were retrieved from the PERUN lightning detection and localization system managed by the Institute of Meteorology and Water Management, National Research Institute (IMGW-PIB). The system is part of the European SAFIR (Surveillance et d'Alerte Foundre par Interferometric Radioelectrique) system, but the Polish part of the system was nicknamed to refer to the Slavic god of lightning, Perun (Gieysztor 2006). The system has been in continuous operation since 2002 and detects intra-cloud, cloud-to-cloud, and cloud-to-ground lightning. Detection system is based on triangulation and applies the technique of detecting the direction finding signal (Bodzak 2006). The entire system currently consists of 13 stations evenly distributed throughout the country (Fig. 2).

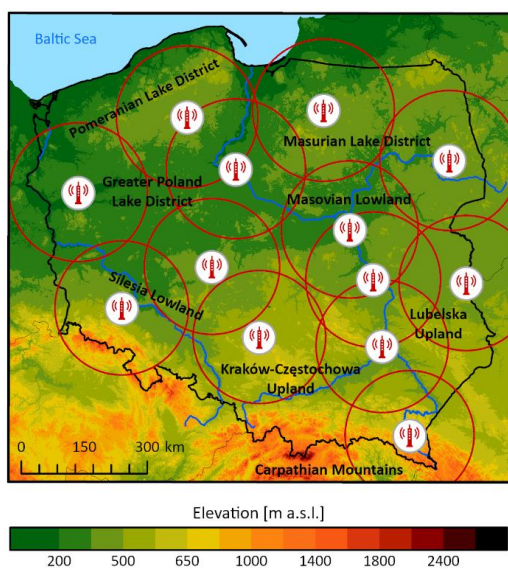


Fig. 2. Hypsometric map of Poland based on the Shuttle Radar Topography Mission Global Coverage (SRTM3; Farr et al. 2007). Symbol points denote the locations of the PERUN lightning detection sensors with 100-km buffer zones (red circles).

Over 95% of the country's coverage area, the precision of discharge detection is less than 1 km. This resolution is being systematically reduced by replacing detectors to enable more precise detection of lightning flashes.

This research is based on a grid of 10×10 km (an area of 100 km^2) so as to address the discharge-area relationship as precisely as possible (Diendorfer 2008). Previous studies on the spatial distribution of lightning in Poland were based on the same grid dimensions (Taszarek et al. 2015; Sulik 2021; Poręba et al. 2022; Sulik 2022). In Europe, the authors used various grid sizes, but the 10×10 km dimensions were most often chosen so that results from different locations around the world would be comparable. The authors of various studies chose different ranges of years, or the dimensions of the base field needed for statistical calculations and the determination of the spatial distribution of the discharges. A number of studies on lightning climatology have been prepared for Europe. The most frequently chosen primary

field was a grid of 10 km × 10 km, 20 km × 20 km, 0.1° × 0.1° (approximately 10 km × 10 km), 0.2° × 0.2° (approximately 20 km × 20 km), and 5 km × 5 km (e.g., Schulz et al. 2005; Soriano et al. 2005; Betz et al. 2009; Biron et al. 2009; Enno 2011; Mäkelä et al. 2011; Novák, Kyznarová 2011; Santos et al. 2012; Feudale et al. 2013; Pohjola, Mäkelä 2013; Wapler 2013; Taszarek et al. 2015; Kotroni, Lagouvardos 2016; Sulik, Kejna 2022). In the United States of America, Koehler (2020) used a grid resolution of 926 m × 926 m and all counts were summed over subsets to yield counts on a coarser grid with 3704 m × 3704 m resolution. As a result, the maximum CG flash values were found over Tampa, Florida. Importantly, several locations in California had no lightning flashes during the 26-yr period.

Because of the low risk of harm from inter-cloud flashes and the system’s errors in detecting them, we decided to use only CG flashes. As shown in a study by Cummins et al. (1998), some CG discharges below 10 kA can often be identified by the system as cloud discharges, so they were removed. Also, if a discharge occurred several times at the same location, it was treated as an error, and only the first flash was taken into account. The whole raw dataset derived from IMGW-PIB was reorganized in the R programming language (R. Core Team 2014) and all maps were prepared in ESRI ArcGIS PRO 3.1.3 software.

2.2. Reanalysis data

Professional Numerical Weather Prediction (NWP) products and, in this case, widely used reanalyses were included in this study. The principle of reanalysis is based on combining data from numerical models with observations made at synoptic stations. Also included are measurements made by automatic stations or, in this case, vertical atmospheric soundings. The result is a coherent dataset based on the laws of physics.

Data assimilation is done by combining previous predictions with new observations to get the most accurate estimate of the state of the atmosphere. Working backward, improved versions of the original observations are used, which, combined with the lack of timely conditions for the release of the model forecast, have a positive effect on the quality of the final product.

We decided to use a proven and accurate reanalysis of convective parameters derived from the ERA5 product managed by ECMWF (ERA5; Hersbach et al. 2020). The study area is all of Poland, so it was necessary to use a wide range of grids so that Poland is completely covered by the reanalysis data.

The ERA5 data were created in a 0.25° grid; the time step is hourly (Table 1).

Table 1. Characteristics of ERA5 reanalysis data used in research.

Data type	Grid
Horizontal grid spacing	0.25° × 0.25°
Projection	Latitude-longitude
Temporal resolution	Hourly
Horizontal coverage	Poland
Timeframe	1940-2022 2002-2020
Total grid points	500,195
Latitude extent	48.75° – 55.25°
Longitude extent	13.75° – 24.50°

To analyze situations in which lightning is generated, specialized parameters were selected to determine the state of the atmosphere at a given time. The standard parameters were air temperature, dew point temperature, convective precipitation, precipitable water amount, or parameters related to humidity at heights of 0-2 km and 2-5 km above the ground surface. Convective parameters related to thermodynamics and kinematics were separated for the most unstable air parcel (MU) along with virtual temperature correction (Doswell, Rasmussen 1994). Thermodynamic and kinematic variables included in the study are convective available potential energy, convective inhibition, lifted condensation level with height and temperature, lifted index, mixing ratio, geopotential height, and bulk wind difference. The specific parameters for analysis are WMAXSHEAR (see Table 2) and hail size index (HSI), which have been used in previous studies related to climatological aspects of convection over Europe. The WMAXSHEAR parameter is used in forecasting severe thunderstorms; it consists of components such as the square root of 2 times CAPE (Convective Available Potential Energy), multiplied by 0-6 km wind shear, as implemented by Taszarek et al. (2020). The HSI parameter developed by Czernecki et al. (2019) is used for predicting large hail precipitation over Europe. The selected convective parameters were chosen to best and most accurately represent the conditions of lightning formation. The list of parameters derived from the ERA5 data is presented in Table 2. In addition, the trends of some variables were calculated for the period 1940-2022 to show the variability over time of the parameters responsible for convection in Poland.

Table 2. List of convective parameters used in research.

Abbreviation	Full name	Units
MUCAPE	most-unstable convective available potential energy	J·kg ⁻¹
MUCIN	most-unstable convective inhibition	J·kg ⁻¹
MULCL H	most-unstable lifted condensation level height	m AGL
MULCL T	most-unstable lifted condensation level temperature	°C
MULI	most-unstable lifted index	K
MUMIXR	most-unstable mixing ratio	g/kg
MUHGT	most-unstable geopotential height	m AGL
MUWMAXSHEAR	square root of 2 times CAPE multiplied by bulk wind difference based on a formula from Taszarek et al. (2017)	m ² /s ²
ISO 0 H	0 Celsius isobar height	m AGL
PW	precipitable water amount (entire column)	mm
RH02	0-2 km above ground level mean relative humidity	%
RH25	2-5 km above ground level mean relative humidity	%
BSEFF	bulk wind difference (shear)	m·s ⁻²
HSI	hail size index formula from Czernecki et al. (2019)	-
T2M	2 m above ground level air temperature	°C
TD2M	2 m above ground level dewpoint temperature	°C
CP	ERA5 1-h accumulated convective precipitation	mm·h ⁻¹

3. Results

3.1. Cloud-to-ground lightning and thunderstorm days

The spatial distribution of lightning and the number of thunderstorm days varies across Poland. The smallest number of TDs occurs in the Baltic Sea area in the north of the country (10-15 days/year), and the largest in the southeastern part (35-40 days/year)(Fig. 3B). On the other hand, if we look at the electrical activity of thunderstorms we can note their greatest distribution in the central part of the country (Kielce Upland through Masovian Lowland)(Fig. 3A). During the 18 years of PERUN's operation, more than 8,626,000 CG strikes were detected and located in Poland.

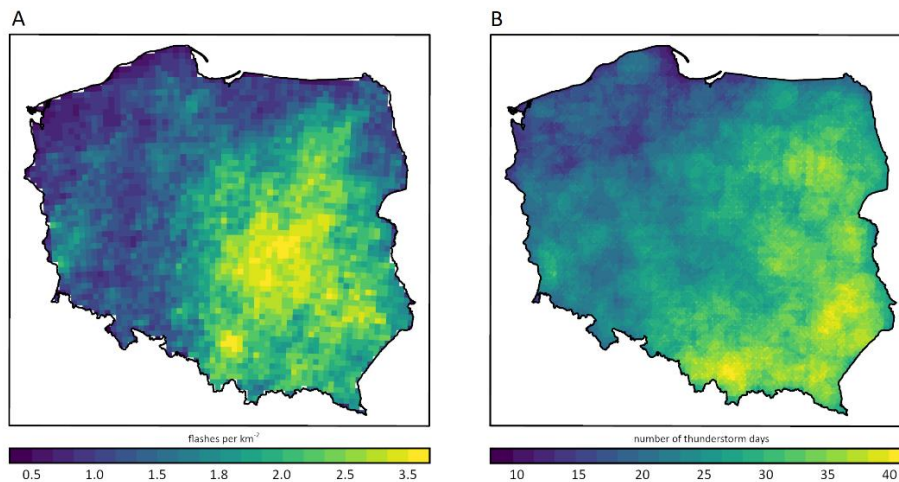


Fig. 3. A. The average annual number of CG lightning flashes per km^2 computed for $10 \text{ km} \times 10 \text{ km}$ grid cells during 2002-2020. B. The average annual number of thunderstorm days during 2002-2020, computed for $1 \text{ km} \times 1 \text{ km}$ grid cells within a radius of 15 km from the bin center. The maps are based on lightning data derived from the PERUN network.

Thunderstorm activity in Poland in terms of the occurrence of TDs and their electrical activity does not deviate from the climatological regularities that characterize the Polish climate (Kejna, Rudzki 2021). Thunderstorms are most numerous from May to the end of August, but their number is also pronounced in September. The period from October to March is the period of least thunderstorm activity, but there are instances of uplift of single convective cells in these months. The electrical activity of thunderstorms during the cooler period of the year is sporadic (Fig. 4). In terms of both the number of CG discharges generated and the number of days with thunderstorms, there is a noticeable increase in both variables especially in June and July. As shown in a study by Poręba et al. (2022) over a similar period of PERUN system operation, the highest hourly thunderstorm activity was during 1400-1500 UTC, and the lowest during 0700-0800 UTC. It is noteworthy that electrical activity during nighttime storms in autumn is greater than in spring and summer.

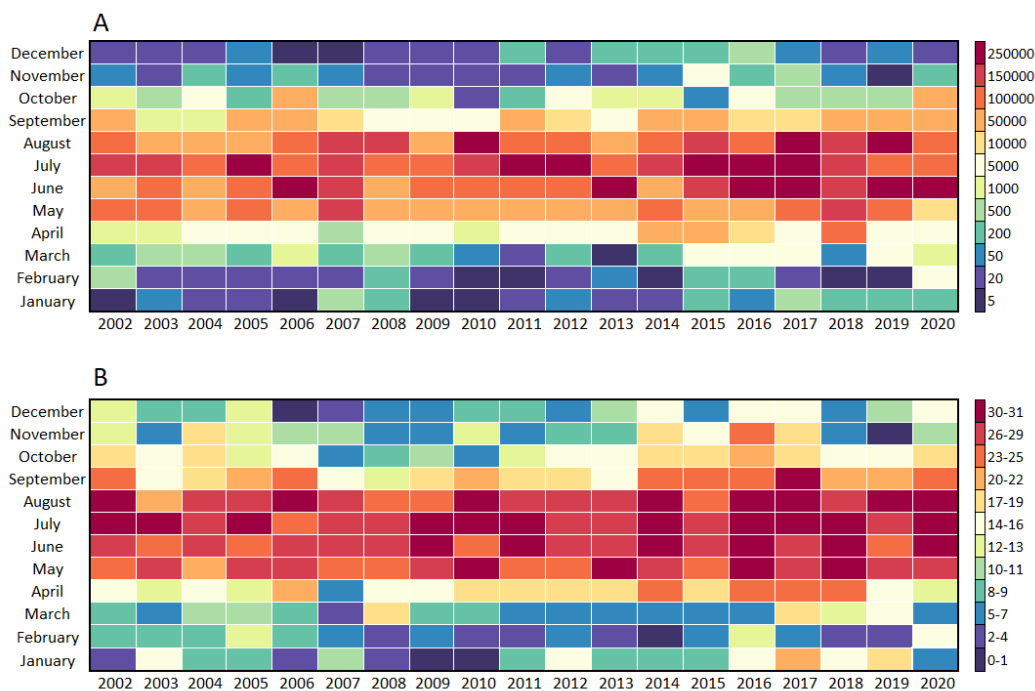


Fig. 4. A. Annual distribution of CG flashes during 2002-2020 by monthly cross-section. B. Annual distribution of TDs during 2002-2020 by monthly cross-section. Based on lightning data derived from the PERUN network.

Considering the distribution of the number of CG discharges during the year, it should be noted that the frequency of discharges varies within and between months that experience thunderstorms. Abnormal numbers of CG discharges are seen primarily in June, July, and August. The days with the highest electrical activity in Poland are summarized below (Table 3). During some days with thunderstorms, the electrical activity of cumulonimbus clouds is very high, and such a distribution can determine the number of discharges recorded by the detection system, which sometimes directly affects the annual distribution. When interpreting the meteorological conditions in which thunderstorms generating elevated CG values arise, it is, therefore, necessary to focus directly on their frequency and the number of days on which extremes of this type occur.

Table 3. The top 8 days with highest electrical activity over Poland during 2002-2020, calculated for $10 \text{ km} \times 10 \text{ km}$ grid cells derived from the PERUN system. Dates are expressed as DD.MM.YYYY.

Date	Number of CG flashes in thousands	Average number of CG flashes per km^2	Highest number of CG flashes in one $10 \text{ km} \times 10 \text{ km}$ grid cell
10.08.2017	154.524	0.50	845
13.06.2019	86.124	0.27	407
02/03.07.2012	80.416	0.25	882
26.06.2006	73.504	0.23	651
19.07.2015	72.030	0.23	325
26.06.2017	69.769	0.22	653
15.08.2008	63.399	0.20	354
11.08.2017	56.510	0.18	482

3.2. Annual variability of CG lighting flash environment

This section of the paper presents the convective conditions under which storm clouds generate ground-based lightning. The convective parameters were derived from ERA5 reanalysis only for thunderstorm days in which at least one CG flash occurred, so convection during the cold period (such as snow convection) was not considered.

The main factors in the build-up of a cumulonimbus storm cloud are favorable thermodynamic and kinematic conditions. Variables relating to thermodynamics are mainly CAPE and Mixing Ratio, which is a measure of the water vapor content of the air (Riemann-Campe et al. 2009). For both CAPE and Mixing Ratio, larger values indicate a more moisture-rich boundary layer, which, along with altitude, may have a greater capacity to release energy through condensation. Even average CAPE values will not be sufficient if there is no initiation of convection positively supported by favorable kinematic conditions. These kinematic conditions can be represented by the Deep Layer Shear (DLS), which is the difference in wind speed at 0-6 km above the ground surface, and the product of the MU CAPE and DLS variables, i.e., WMAXSHEAR developed by Taszarek et al. (2020).

As presented in Figure 5A, CG frequencies $>30,000/d$ occur, although they are not very numerous. Thunderstorms generating $\sim 10,000$ CG/d are the most numerous, and classified as moderate. A section (3.4) of this paper is devoted to this issue. However, when it comes to the thermal and kinematic conditions accompanying the generation of CG discharges, they are most often formed under WMAXSHEAR conditions of about $500 \text{ m}^2/\text{s}^2$. Of course, stronger thunderstorm systems have values as high as $1,000 \text{ m}^2/\text{s}^2$, but these occur sporadically. The highest frequency of thunderstorms is best described by the relationship between DLS and MU CAPE (Fig. 5B). Whereas CAPE values in the range of about 1500 J/kg are elevated values for Poland, it is under such conditions that the potential for generating discharges is favorable. The values of kinematic conditions most often fall in the vicinity of $13\text{-}14 \text{ m/s}$ in the 0-6 km AGL profile. As in the case of the relationship of the number of CG discharges to the WMAXSHEAR index, the key element is the mixing ratio. A mixing ratio in the range of 13 g/kg , superimposed with favorable thermodynamics (WMAXSHEAR above $500 \text{ m}^2/\text{s}^2$), results in increased CG flashes (Fig. 5C). The most important and crucial aspects of storm cloud development take place above the height of lifted condensation level (LCL) and level of free convection (LFC). On the other hand, the layer near the surface also shows variables that indicate an increased potential for CG flashes, which is favorably influenced by an elevated air temperature above 27°C and a dew point temperature around 19°C (Fig. 5D).

In the process of CG formation, an essential component is the moisture contained in the lower troposphere (Farnell, Rigo 2020). The moisture and updraft favorably influence the formation of hail inside the convective core. Therefore, the HSI developed by Czernecki et al. (2019) was used in the study. This parameter determines the potential hail diameter based on remote sensing data and kinematic and thermodynamic conditions in the troposphere. Previous studies have proven that hail is formed inside cumulonimbus clouds when strong ascending currents result in rapid cooling of water droplets in the troposphere

(Allen 2018). As confirmed by studies on supercells and linear systems, the moisture content and thermal gradient in the vertical profile of the troposphere are regulated by vertical wind shear, which simultaneously contributes to updraft velocity. Higher vertical velocity promotes not only lightning but also hail precipitation (Doswell 2001; Coffey, Parker 2015; Lin, Kumjian 2021). Consequently, storm cells, and especially supercells, which typically produce large hail, generate greater amounts of ground discharge. Also, moderate DLS and WMAXSHEAR values are noted in supercell structures (Fig. 6A). Supercell thunderstorms that generate large hail are mainly responsible for heavy rainfall, often exceeding 40 mm/h (Fig. 6B) and tornadoes. Occurrence of a supercell is usually manifested by an increased number of CG flashes. A study performed by Poręba et al. (2022) also showed a positive relationship between supercell composite parameter (SCP) and HSI.

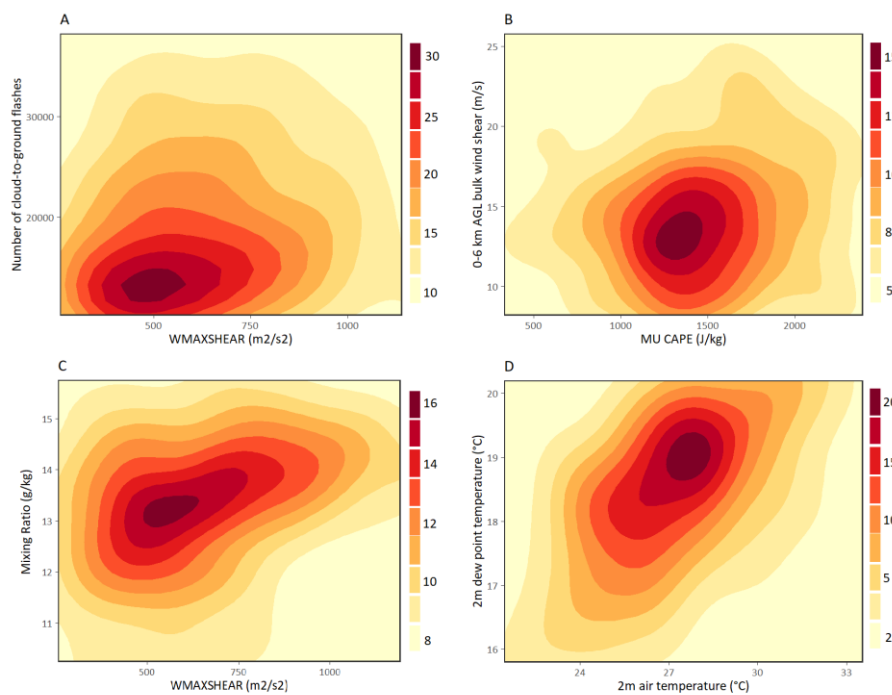


Fig. 5. A. Relationship between the number of CG flashes and WMAXSHEAR. B. Relationship between wind shear and MU CAPE. C. Relationship between mixing ratio and WMAXSHEAR. D. Relationship between 2 m dew point temperature and 2 m air temperature. Computed from PERUN and ERA5 data for thunderstorm days during 2002-2020.

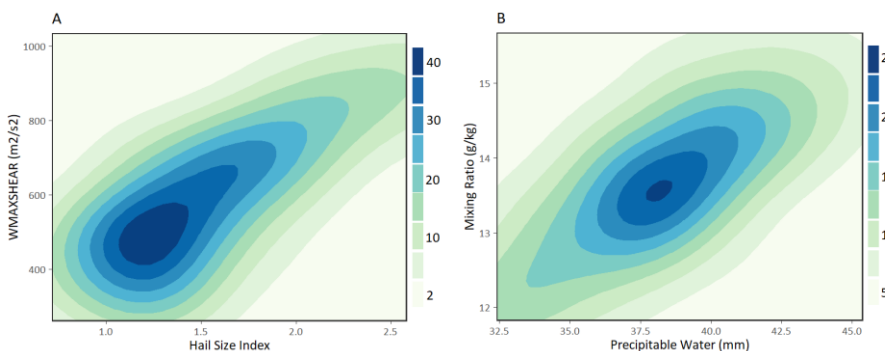


Fig. 6. A. Relationship between WMAXSHEAR and HSI. B. Relationship between mixing ratio and precipitable water amount. Computed from PERUN and ERA5 data for thunderstorm days during 2002-2020.

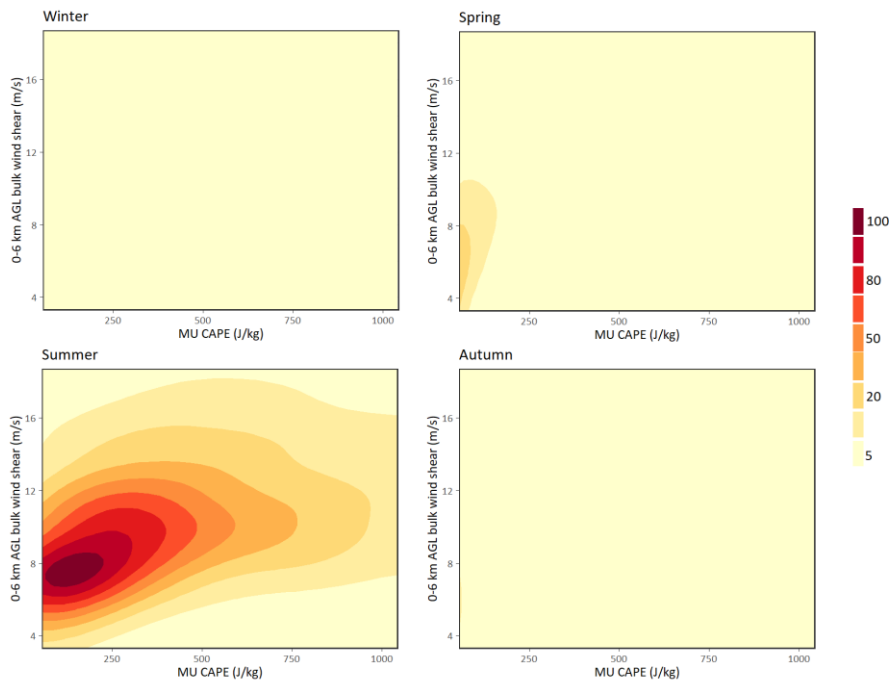


Fig. 7. Seasonal variability of DLS and MU CAPE for thunderstorms over Poland. Derived from ERA5 data.

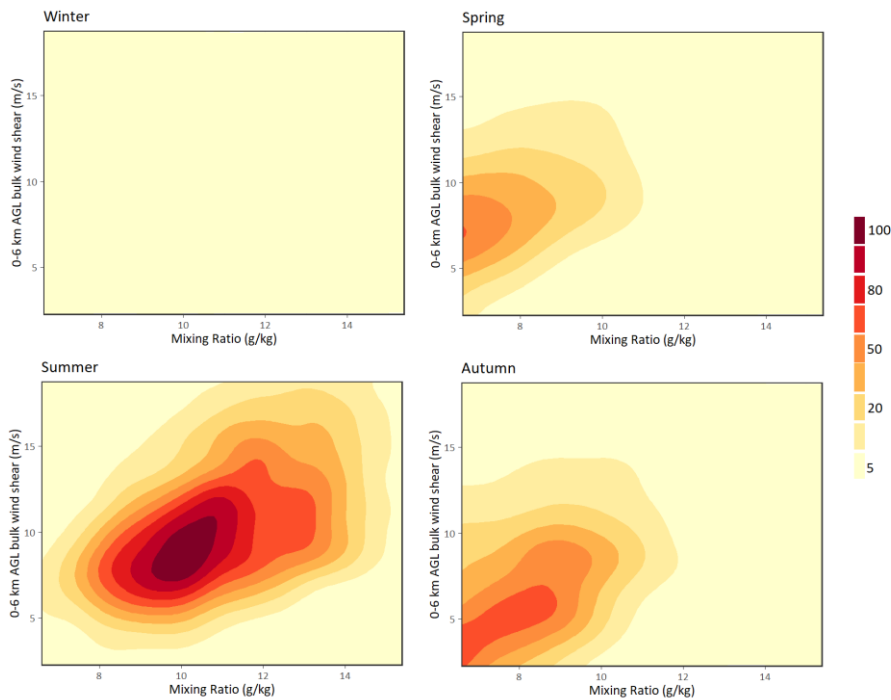


Fig. 8. Seasonal variability of DLS and mixing ratio for thunderstorms over Poland. Derived from ERA5 data.

As mentioned earlier, the most frequent and intense thunderstorm activity in Poland occurs during the warmer period of the year, May through September. This is when the parameters favorable for convection are particularly elevated. In summer, even relatively moderate CAPE values combined with moderate wind shear create the potential for electrical activity. In spring, the relevant thermodynamic and kinematic conditions tend to be lower, and they are virtually nonexistent during autumn and winter. The infrequent

thunderstorms in autumn and winter are manifested mainly in the form of linear convective systems characterized by stronger wind gusts, and less often by an increased number of CG flashes (Celiński-Mysław et al. 2020)(Fig. 7). As for the DLS and mixing ratio during thunderstorms, these variables are also most prominent in summer. The process of discharge formation is closely related to moisture content. As Wang et al. (2018) also note, the larger the moisture deposits in the lower troposphere, the faster the separation of charges in the storm cloud. When relative humidity (RH) increases above 60%, there is a significant increase in CG discharges relative to IC. The distribution and ratio of DLS to mixing ratio by season are shown in (Fig. 8).

3.3. Favorable conditions for deep moist convection

The most important factors enabling the formation of thunderstorms are sufficient moisture, unstable air mass, and wind shear. However, for convection to occur, it must be initiated (Doswell 2001). The factors that initiate convection most often occur in the form of atmospheric fronts during the summer months (Sulik 2021), while in winter, terrain and orographic forcing play a key role (Kolendowicz 2012). Climate change is manifest primarily through increasing air temperature near the earth's surface. Increasingly, heat records are being observed not only in the warm season but also in winter, and systematic air temperature increase is evident throughout the country (Fig. 9).

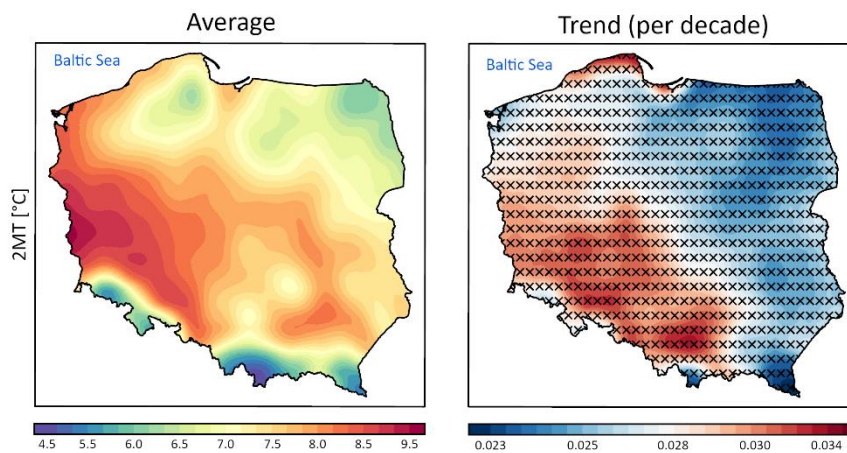


Fig. 9. Spatial distribution of average air temperature from 1940 to 2022. Long-term trends are derived from annual values in hourly resolution and corresponding Sen's slope. X – a statistically significant trend. Computed from ERA5 reanalysis data.

Rising air temperature leads to an increase in the heat capacity of the atmosphere. As a result, larger deposits of moisture can be stored. On the other hand, increasing air temperature can contribute to a decrease in relative humidity, which is essential for the formation of thunderstorms.

To reproduce as accurately as possible the thermodynamic and kinematic conditions for specific values of CG discharges, probabilities of occurrence of a given number of CG were separated. The probability was divided into 3 types: severe, enhanced, and moderate. The severe case refers to the most electrically active

storms, with CG/d >50,000; enhanced is defined as storms with activity of 10,000 -50,000 CG/d; moderate is defined as storms with 5,000 -10,000 CG/d.

By analyzing specific variables over many cases, it is possible to determine parameters favoring the electrical activity of thunderstorms. The most intense thunderstorms are formed in the MU CAPE environment in the range of 1900-2100 J/kg and in the presence of kinematic conditions in the form of DLS from 16 to 20 m/s (Fig. 10). In the cases of enhanced and moderate category storms, a very similar environment is evident in both the values of unstable air mass and wind shear at 0-6 km AGL. These types of thunderstorms can form in the MU CAPE environment, usually above 1000 J/kg, not exceeding 1500 J/kg, with the simultaneous presence of DLS around 11 m/s.

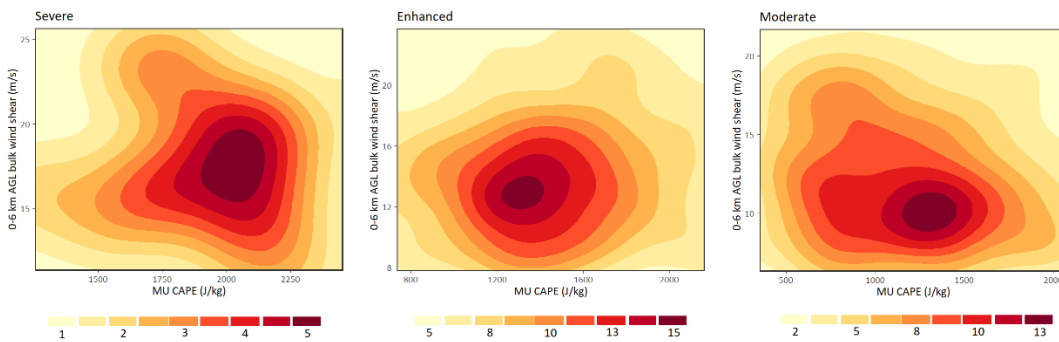


Fig. 10. Relationship between DLS and MU CAPE for the probability of increased electrical activity. Severe = lightning activity >50,000 CG/day. Enhanced =10,000-50,000 CG/day. Moderate = 5,000-10,000 CG/day.

The ratio of mixing of moist air with dry air is similar for the three storm types analyzed, ranging from 13 g/kg to about 15 g/kg in severe storms. However, the greatest differences are in the WMAXSHEAR parameter, where storms generating severe CG values form in conditions ranging from 800 m²/s² to 1300 m²/s². For enhanced and moderate storms, the values of this parameter are between 400-700 m²/s² (Fig. 11).

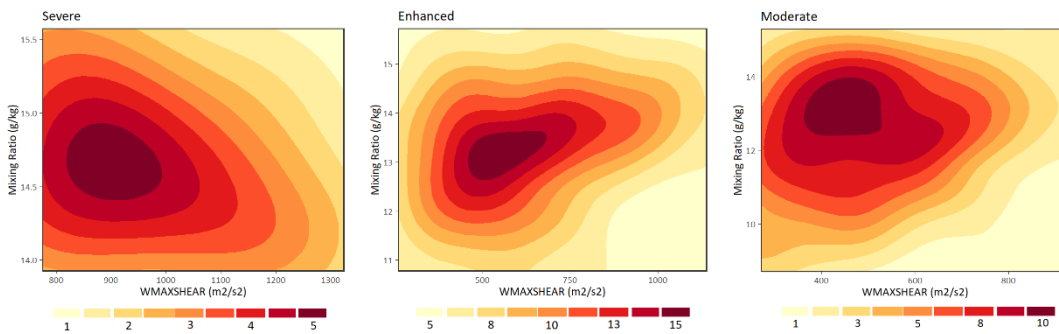


Fig. 11. Relationship between mixing ratio and WMAXSHEAR for the probability of increased electrical activity. Severe = lightning activity >50,000 CG/day. Enhanced =10,000-50,000 CG/day. Moderate = 5,000-10,000 CG/day.

Since thunderstorms are formed in a rather complicated and complex way, the environment in which they form cannot be represented by a single variable. Among the most important are instability, moisture content, and vertical movements. It was therefore decided to present the variables necessary for convection in relation to the number of flashes formed on one panel (Fig. 12). Similar distributions can be observed for humidity-related variables (mixing ratio, dewpoint temperature and precipitable water). Humidity is important because severe thunderstorms usually occur in an environment of elevated dew point. Low values of this variable effectively inhibit the release of latent heat and significantly reduce the threat of organized multicellular systems. Advection of a significant portion of moisture to the boundary layer positively increases the instability of the atmosphere. An additional factor supporting convection is the relatively lifted condensation level (LCL), which, when overlapped with the WMAXSHEAR or DLS parameter, causes an increase in the velocity of the elevated air parcel and the simultaneous release of the energy it contains (Fig. 12 A, B). Convective instability is triggered when dynamic lift from the surface to mid-levels produces moist adiabatic lapse rates of air lifted from the lower troposphere and dry adiabatic lapse rates of air lifted in the middle troposphere. At the same time, strong vertical movements and the presence of fractions of water, ice, and ice crumble cause the formation of hail, which has a strong effect on the formation of lightning.

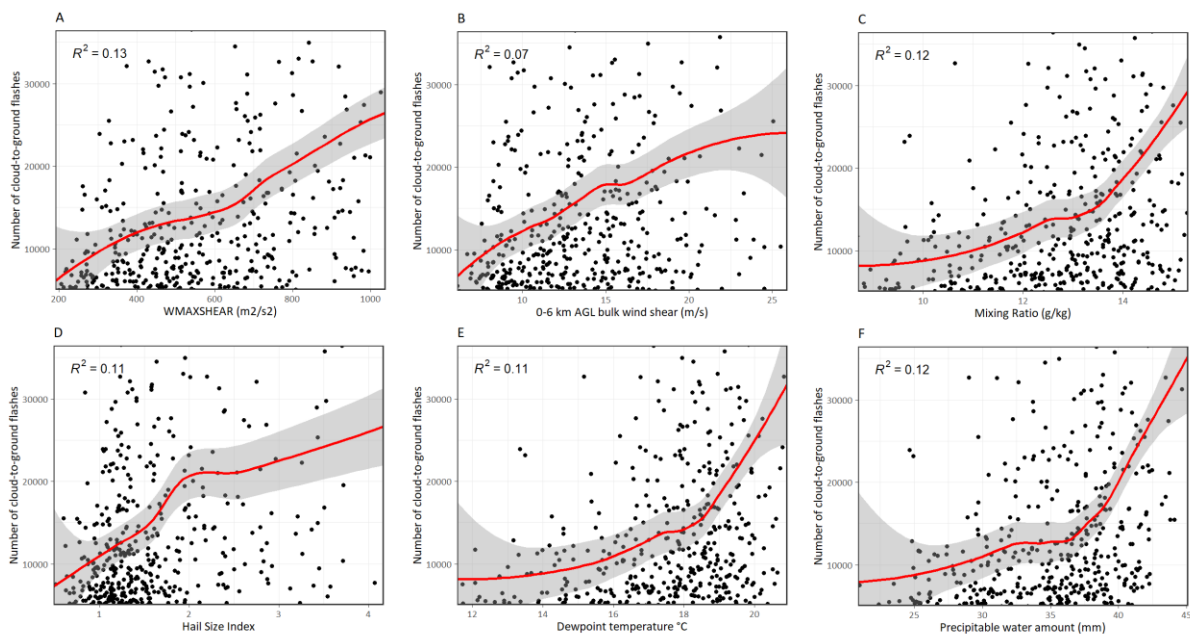


Fig. 12. Relationship between convective parameters and cloud-to-ground lightning flashes A. WMAXSHEAR (product of DLS and MU CAPE); B. DLS (Deep Layer Shear; C. mixing ratio; D. hail size index; E. 2-meter dewpoint temperature; F. Precipitable water. The red line denotes locally-estimated scatterplot smoothing. Grey bands are tolerance range.

Extended storm systems, including supercells, often result in hail. Referring to previous studies, they showed a positive relationship between CG and hail (Soula et al. 2004). The number of discharges increases when hailfall occurs (Lang et al. 2004; Soula et al. 2004). Elevated instantaneous electrical activity

(lightning jump) can also be linked to hail formation inside the convective core (Kane 1993; Williams et al. 1999). In turn, as noted by Changnon (1988), storms of a cold front nature generating hail are characterized by increased electrical activity. Hail production inside the cumulonimbus cloud is therefore crucial for lightning occurrence, and as analysis has shown, HSI (Czernecki et al. 2019) correlates very well with thermodynamic and kinematic parameters (Fig. 13). An unstable air parcel develops when it becomes warmer than its surroundings and at the same time gains lift due to positive buoyancy. An additional factor supporting vertical displacement is wind uplift, that is, the change in wind speed and direction with altitude. Although HSI is well-correlated with CAPE and DLS, the best choice for determining the relationship regarding CG formation and associated hail is the WMAXSHEAR parameter, which contains thermodynamic and kinematic variables (Fig. 13C). As confirmed in an earlier study by Taszarek et al. (2020), the frequency of hazardous convective phenomena is increasing over Europe with the development of WMAXSHEAR and low-level lapse rates.

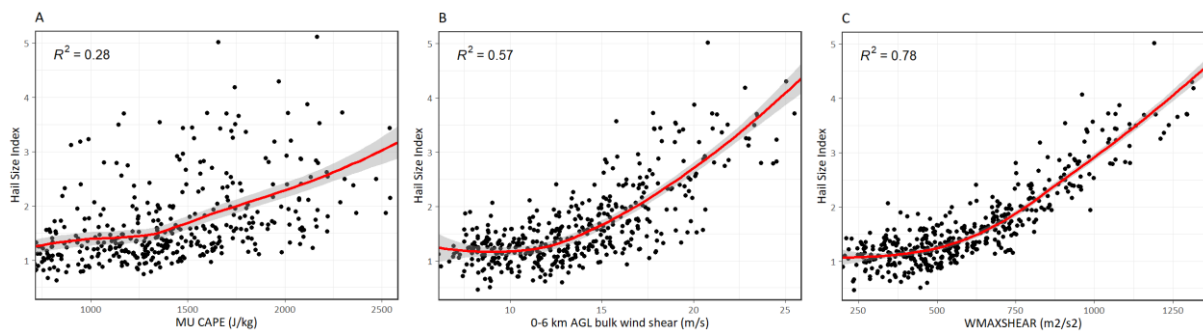


Fig. 13. Relationship between convective parameters and Hail Size Index for A. MU CAPE; B. DLS (Deep Layer Shear); C. WMAXSHEAR (product of DLS and MU CAPE). The red line denotes locally estimated scatterplot smoothing. Grey bands are tolerance range.

3.4. Spatial-temporal changes of convective parameters

Determining the convective conditions that favor the formation of cumulonimbus clouds is crucial to understanding the processes taking place in the troposphere. It is no less important to determine the spatial and temporal changes taking place over the years in a given area. The latest climate report of the Intergovernmental Panel on Climate Change (IPCC 2023) confirmed a statistically increasing trend in air temperature measured at 2 m above ground level. Moreover, global changes are progressing fastest on land. Climate change associated with increasing air temperature is indirectly associated with changes in the convective environment in the higher parts of the troposphere and may favorably influence the development of hazardous storms (Brooks et al. 2003; Taszarek et al. 2017; Taszarek et al. 2020). In Poland, the parameters related to convection over the years correspond to the number of storms. Mixing ratio values in the area of the Tatra Mountains are lower than in the mountainous area of southeastern Poland (Fig. 14). Higher elevations result in greater dry stability and thus can foster increasingly steep vertical air temperature gradients.

However, the increase in air temperature also leads to a decrease in relative humidity and, thus, deeper and deeper mixing of the boundary layer (Byrne, O’Gorman 2016). However, it is important to keep in mind that the mere presence of an unstable air parcel is not sufficient; rather, for convection to occur, the processes that initiate it must also be present. Vertical wind shear is extremely important in terms of the organization and evolutionary potential of uplifted storm cells (Allen et al. 2015; Pucik et al. 2015); in this study, it was vectorized by the difference in wind speed and direction between the ground surface and a height of 6 km because typically the highest updraft velocities in storm clouds occur in this layer. The overlap of potential energy along with vertical air movement indicates a continuous increase in these parameters at the scale of Poland, and a systematic increase even greater than the alarming increase in air temperature (Fig. 15).

As shown in the study by Taszarek et al. (2020), an increase in WMAXSHEAR indicator is also evident in northwestern Europe, which may be the reason for the shift in the jet stream due to the weakening thermal gradient between the mid-latitudes and the Arctic (Pena-Ortiz et al. 2013; Coumou et al. 2015). In addition, the climatology of the WMAXSHEAR factor for Europe clearly indicates that severe storms most often occur in summer in the corridor from northeastern Spain through parts of Central Europe, Italy or the Balkan Peninsula (Taszarek et al. 2020). In contrast, in spring, positive trends were recorded for most of Europe (including Poland), which confirms that favorable conditions for deep convection are also increasingly common in spring. These changes may be mainly due to an increase in convective potential energy and moisture using constant DLS values.

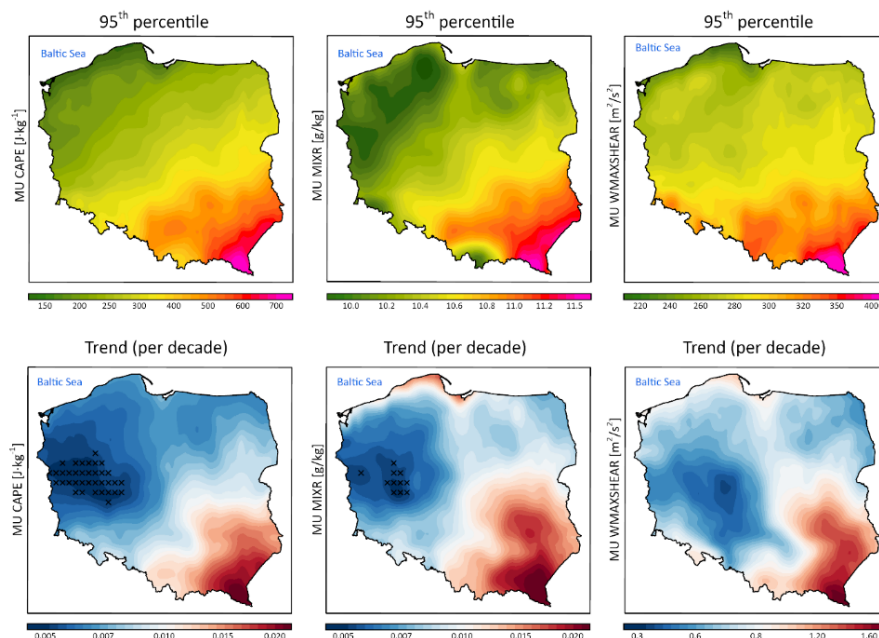


Fig. 14. 82-yr climatology of 95th percentile MU CAPE, MU mixing ratio and MU WMAXSHEAR for Poland. Long-term trends are derived from annual values in hourly resolution and corresponding Sen’s slope (values denote change per decade).

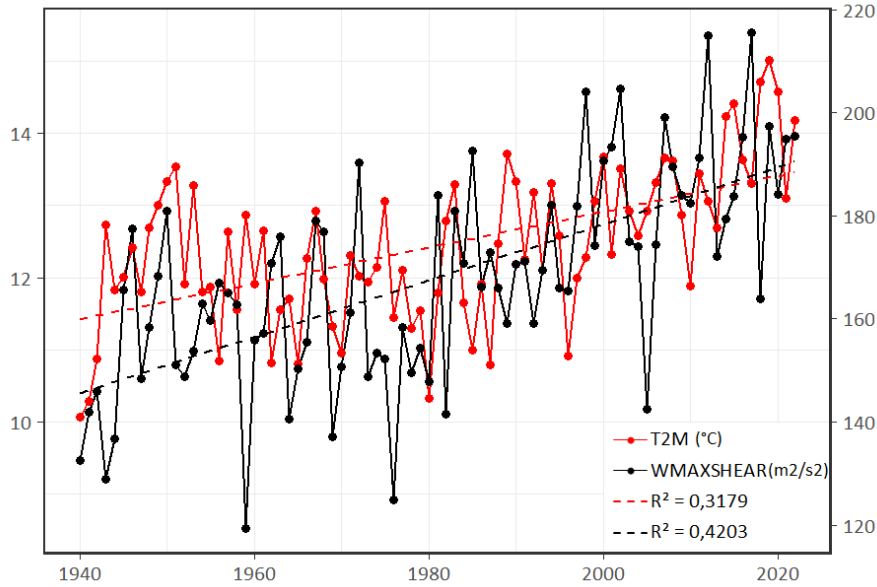


Fig. 15. Time-course distribution of 2 m air temperature [T2M] and 0-6 km AGL wind shear with CAPE [WMAXSHEAR] for Poland. The dashed line indicates a trend for two factors.

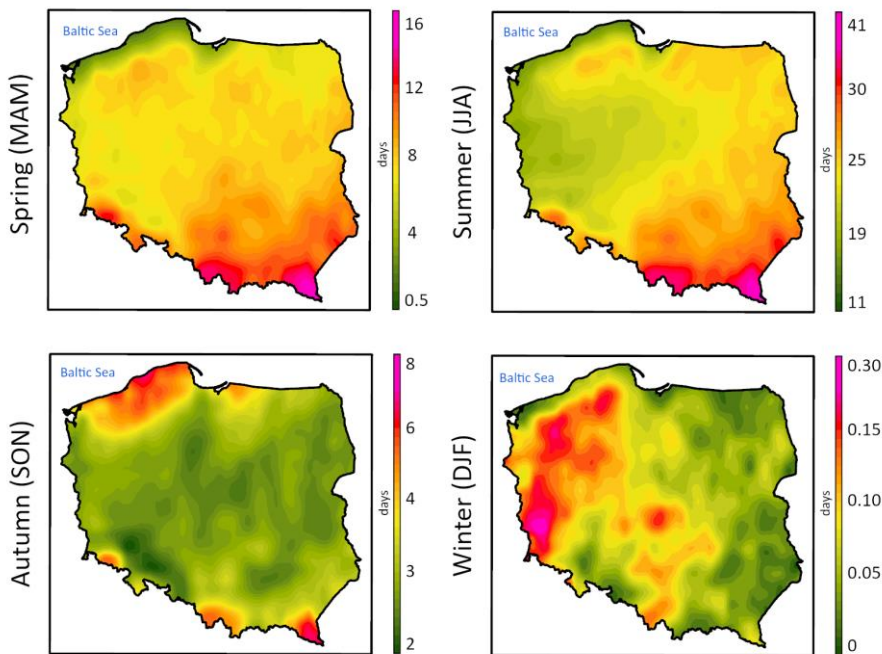


Fig. 16. 82-yr climatology of thunderstorm days in Poland for seasons. A thunderstorm environment is expected when CAPE > 150 J/kg and CP > 0.1 mm/h. Computed from ERA5 reanalysis data.

Knowing the convective and kinematic conditions, it was decided to simulate and reconstruct the number of days with thunderstorms for the period 1940-2022 based on ERA5 data (Fig. 16). The spatial distribution by season is very similar to the spatial distribution of the number of days with thunderstorms calculated using data from the PERUN lightning detection and localization system for 2002-2020. In summer and spring, the number of days with thunderstorms increases toward the southeast, while in autumn thunderstorms mainly occur in close proximity to the Baltic Sea. This is related to the increased temperature of

the sea and the simultaneous possibility of convection over land (Sulik, Kejna 2023). In winter, the occurrence of thunderstorms in Poland is local and is mainly associated with the western circulation, which provides an influx of unstable air masses from the north (Konarski et al. 2008). Winter is also a period when dangerous phenomena can be observed in thunderstorms formed as linear systems with embedded scour lines (Celiński-Mysław et al. 2020).

4. Discussion and final remarks

Each year, about 150 days with thunderstorms are recorded throughout Poland. Storm cells generate various amounts of lightning, and their number and spatial distribution are slightly different each year (Sulik 2022). From 2002-2020, the PERUN system detected and located more than 8 million CG flashes, which were used in this study. The intensity of generated flashes and their number associated with storm cells were necessary to reconstruct the convection environment in which CG flashes are generated. Data from ERA5 reanalysis were used for this task. As a result of the analysis of thermodynamic and kinematic conditions for the generation of CG lightning by cumulonimbus clouds in Poland, the following conclusions can be stated:

- 1) The average number of days with thunderstorms is about 30. The least number of days with a thunderstorm occurs in the northwest (10-15 days) and the most in the southeast (35-40).
- 2) Each year, there is an average of about 480,000 CG flashes.
- 3) 96% of all detected CG flashes have a negative current.
- 4) The highest electrical activity occurs in central Poland.
- 5) The highest number of thunderstorm days and electrical activity are in July.
- 6) From 2002-2020, there were 8 days with thunderstorms, during which the sum of CG flashes exceeded 50,000.
- 7) CG flashes are most common in WMAXSHEAR environments of $\sim 500 \text{ m}^2/\text{s}^2$.
- 8) MU CAPE values in the range of 1,000 to 1,500 J/kg, combined with DLS in the vicinity of 13 m/s, are very favorable for the potential to generate CG flashes.
- 9) The chance of increased electrical activity increases when the air temperature is $\sim 28^\circ\text{C}$, and the dew point is above 18°C .
- 10) The WMAXSHEAR parameter positively correlates with mixing ratio in the range of 12-14 g/kg.
- 11) WMAXSHEAR correlates very well with HSI, which translates into increased generating of CG flashes.
- 12) A steady long-term increase in the WMAXSHEAR can be noted.
- 13) An additional positive aspect of the occurrence of elevated CG is supercells characterized by strong updraft speed, rotation, and the potential to precipitate large hail.

A detailed study covering the area of a country compared to the whole of Europe shows regional dependencies in the formation of CG on a local scale. Also noteworthy is the fact that forecasting hazardous weather phenomena such as severe wind gusts, torrential rainfall, or large hail is extremely important but is

still quite challenging due to the changing climate. The tasks of forecasting and delineating areas at risk of hazardous weather events also include assessing the likelihood of lightning. Despite the continuous development of technology, warnings issued, and forecasts, there are still reports of people killed or injured by lightning, especially during the storm season, as evidenced by data from the ESWD database. Improving knowledge related to the environment in which CG flashes are formed will allow even more precise determination of the area at risk and greater protection of the population.

References

- Allen J.T., 2018, Climate change and severe thunderstorms, Oxford Research Encyclopedia of Climate Science, Oxford University Press.
- Allen J.T., Tippett M.K., Sobel A.H., 2015, An empirical model relating U.S. monthly hail occurrence to large-scale meteorological environment, *Journal of Advanced Modeling Earth Systems*, 7 (1), 226-243, DOI: 10.1002/2014MS000397.
- Betz H.D., Schumann U., Laroche P. (eds.), 2009, Principles, Instruments and Applications: Review of Modern Lightning Research, Springer, 641 pp., DOI: 10.1007/978-1-4020-9079-0.
- Biron D., 2009, LAMPINET – Lightning detection in Italy, [in:] Principles, Instruments and Applications: Review of Modern Lightning Research, H.D. Betz, U. Schumann, P. Laroche (eds.), Springer, 141-159.
- Bodzak P., 2006, Detekcja i lokalizacja wyladowań atmosferycznych, Instytut Meteorologii i Gospodarki Wodnej, 135 pp.
- Brooks H.E., Lee J.W., Craven J.P., 2003, The spatial distribution of severe thunderstorm and tornado environments from global reanalysis data, *Atmospheric Research*, 67-68, 73-94, DOI: 10.1016/S0169-8095(03)00045-0.
- Byers H.R., Braham R.R., 1949, Glossary of Meteorology, American Meteorology Society, The Thunderstorm. U.S. Government Printing Office, p. 287.
- Byrne P., O’Gorman P.A., 2016, Understanding decreases in land relative humidity with global warming: conceptual model and GCM simulations, *Journal of Climate*, 29 (24), 9045-9061, DOI: 10.1175/JCLI-D-16-0351.1.
- Celiński-Myslaw D., Palarz A., Taszarek M., 2020, Climatology and atmospheric conditions associated with cool season bow echo storms in Poland, *Atmospheric Research*, 240, DOI: 10.1016/j.atmosres.2020.104944.
- Changnon S.A., 1988, Climatology of thunder events in the conterminous United States. Part I: Temporal aspects, *Journal of Climate*, 1 (4), 389-398.
- Coffer B.E., Parker M.D., 2015, Impacts of increasing low-level shear on supercells during the early evening transition, *Monthly Weather Review*, 143 (5), 1945-1969, DOI: 10.1175/MWR-D-14-00328.1.
- Coumou D., Lehmann J., Beckmann J., 2015, The weakening summer circulation in the Northern Hemisphere mid-latitudes, *Science*, 348 (6232), 324-327, DOI: 10.1126/science.126176.
- Cummins K.L., Murphy M.J., Bardo E.A., Hiscox W.L., Pyle R.B., Pifer A.E., 1998, A combined TOA/MDF technology upgrade of the U.S. National Lightning Detection Network, *Journal of Geophysical Research. Atmospheres*, 103 (D8), 9035-9044, DOI: 10.1029/98JD00153.
- Czernecki B., Taszarek M., Marosz M., Pórolniczak M., Kolendowicz L., Wyszogrodzki A., Szturc J., 2019, Application of machine learning to large hail prediction – The importance of radar reflectivity, lightning occurrence and convective parameters derived from ERA5, *Atmospheric Research*, 227, 249-262, DOI: 10.1016/j.atmosres.2019.05.010.
- Diendorfer G., 2008, Some comments on the achievable accuracy of local ground flash density values, Proceedings of 29th International Conference on Lightning Protection, Uppsala, Sweden, ICLP Centre.
- Doswell C.A., 2001, Severe convective storms – An overview, [in:] Severe Convective Storms, C.A. Doswell (ed.), Meteorology Monographs, American Meteorology Society, 50, 1-26.
- Doswell C.A., Rasmussen E.N., 1994, The effect of neglecting the virtual temperature correction on CAPE calculations, *Weather Forecasting*, 9 (4), 625-629, DOI: 10.1175/1520-0434(1994)009<0625:TEONTV>2.0.CO;2.

- Dotzek N., Groenemeijer P., Feuerstein B., Holzer A.M., 2009, Overview of ESSL's severe convective storms research using the European Severe Weather Database ESWD, *Atmospheric Research*, 93 (1-3), 575-586, DOI: 10.1016/j.atmosres.2008.10.020.
- Enno S.E., 2011, A climatology of cloud-to-ground lightning over Estonia, 2005-2009, *Atmospheric Research*, 100 (4), 310-317, DOI: 10.1016/j.atmosres.2010.08.024.
- Farr T.G., and Coauthors, 2007, The Shuttle Radar Topography Mission, *Reviews of Geophysics*, 45, RG2004, DOI: 10.1029/2005RG000183.
- Farnell C., Rigo T., 2020, The lightning jump algorithm for nowcasting convective rainfall in Catalonia, *Atmosphere*, 11 (4), DOI: 10.3390/atmos11040397.
- Feudale L., Manzato A., Micheletti S., 2013, A cloud-to-ground lightning climatology for north-eastern Italy, *Advances in Science and Research*, 10 (1), 77-84, DOI: 10.5194/asr-10-77-2013.
- Gieysztor A., 2006, *Mitologia Słowian*, Wydawnictwo Uniwersytetu Warszawskiego, 407 pp.
- Groenemeijer P., Tomáš P., Alois M.H., Antonescu B., Riemann-Campe K., Schultz D.M., Kühne T., Feuerstein B., Brooks H.E., Doswell C.A. III, Koppert H.-J., Sausen R., 2017, Severe convective storms in Europe: Ten years of research and education at the European Severe Storms Laboratory, *Bulletin of the American Meteorological Society*, 98 (12), 2641-2651, DOI: 10.1175/BAMS-D-16-0067.1.
- Hersbach H., Bell B., Berrisford P., Biavati G., Horányi A., Muñoz Sabater J., Nicolas J., Peubey C., Radu R., Rozum I., Schepers D., Simmons A., Soci C., Dee D., Thépaut J.-N., 2020, ERA5 hourly data on single levels from 1979 to present, Copernicus Climate Change Service (C3S) Climate Data Store (CDS).
- IPCC, 2023, *Climate Change 2021: The Physical Science Basis*, the Working Group I contribution to the Sixth Assessment Report, available online at <https://www.ipcc.ch/report/sixth-assessment-report-working-group-i/> (data access 30.07.2024).
- Kane J.R., 1993, Lightning-rainfall relationships in an isolated thunderstorm over the mid-Atlantic states, *National Weather Digest*, 18 (3), 2-14.
- Kejna M., Rudzki M., 2021, Spatial diversity of air temperature changes in Poland in 1961-2018, *Theoretical and Applied Climatology*, 143 (3-4), 1361-1379, DOI: 10.1007/s00704-020-03487-8.
- Koehler T.L., 2020, Cloud-to-ground lightning flash density and thunderstorm day distributions over the contiguous United States derived from NLDN measurements: 1993-2018, *Monthly Weather Review*, 148 (1), 313-332, DOI: 10.1175/MWR-D-19-0211.1.
- Kolendowicz L., 2012, Synoptic patterns associated with thunderstorms in Poland, *Meteorologische Zeitschrift*, 21 (2), 145-156, DOI: 10.1127/0941-2948/2012/0272.
- Konarski J., Gajda W., Dziewit Z., Barański P., 2008, Severe winter thunderstorm in Poland, case study, [in:] 20th International Lightning Detection Conference; 2nd International Lightning Meteorology Conference, 21-25 April, Tucson, USA, 8 pp.
- Kotroni V., Lagouvardos K., 2016, Lightning in the Mediterranean and its relation with sea-surface temperature, *Environmental Research Letters*, 11 (3), DOI: 10.1088/1748-9326/11/3/034006.
- Lang T.J., Miller L.Y., Weisman M., Rutledge S.A., Barker III L.J., Bringi V.N., Chandrasekar V., Detwiler A., Doesken N., Helsdon J., Knight C., Krehbiel P., Lyons W.A., MacGorman D., Rasmussen E., Rison W., Rust W.D., Thomas R.J., 2004, The severe thunderstorm electrification and precipitation study, *Bulletin of the American Meteorological Society*, 85 (8), 1107-1126, DOI: 10.1175/BAMS-85-8-1107.
- Lin Y., Kumjian M.R., 2021, Influences of CAPE on hail production in simulated supercell storms, *Journal of Atmospheric Sciences*, 79 (1), 179-204, DOI: 10.1175/JAS-D-21-0054.1.
- Mäkelä A., Rossi P., Schulz D.M., 2011, The daily cloud-to-ground lightning flash density in the contiguous United States and Finland, *Monthly Weather Review*, 139 (5), 1323-1337, DOI: 10.1175/2010MWR3517.1.
- Novák P., Kyznarová H., 2011, Climatology of lightning in the Czech Republic, *Atmospheric Research*, 100 (4), 318-333, DOI: 10.1016/j.atmosres.2010.08.022.

- Pena-Ortiz C., Gallego D., Ribera P., Ordonez P., Alvarez-Castro M.D.C., 2013, Observed trends in the global jet stream characteristics during the second half of the 20th century, *Journal of Geophysical Research. Atmosphere*, 118 (7), 2702-2713, DOI: 10.1002/jgrd.50305.
- Pilguy N., Taszarek M., Kryza M., Brooks H., 2022, Reconstruction of violent tornado environments in Europe: High-resolution dynamical downscaling of ERA5, *Geophysical Research Letters*, 49 (11), DOI: 10.1029/2022GL098242.
- Pohjola H., Mäkelä A., 2013, The comparison of GLD360 and EUCLID lightning location systems in Europe, *Atmospheric Research*, 123, 117-128, DOI: 10.1016/j.atmosres.2012.10.019.
- Poreba S., Taszarek M., Ustrnul Z., 2022, Diurnal and seasonal variability of ERA5 convective parameters in relation to lightning flash rates in Poland, *Weather and Forecasting*, 37 (8), 1447-1470, DOI: 10.1175/WAF-D-21-0099.1.
- Pucik T., Groenemeijer P., Ryva D., Kolar M., 2015, Proximity soundings of severe and nonsevere thunderstorms in Central Europe, *Monthly Weather Review*, 143 (12), 4805-4821, DOI: 10.1175/MWR-D-15-0104.1.
- R Core Team, 2014, R: A language and environment for statistical computing, R Foundation for Statistical Computing, Vienna, Austria, available online at <https://www.r-project.org/> (data access 30.07.2024).
- Riemann-Campe K., Fraedrich K., Lunkeit F., 2009, Global climatology of convective available potential energy (CAPE) and convective inhibition (CIN) in ERA-40 re-analysis, *Atmospheric Research*, 93 (1-3), 534-545, DOI: 10.1016/j.atmosres.2008.09.037.
- Santos J.A., Reis M.A., Sousa J., Leite S.M., Correia S., Janeira M., Fragoso M., 2012, Cloud-to-ground lightning in Portugal: Patterns and dynamical forcing, *Natural Hazards Earth System Science*, 12 (3), 639-649, DOI: 10.5194/nhess-12-639-2012.
- Schulz W., Cummins K., Diendorfer G., Dorninger M., 2005, Cloud-to-ground lightning in Austria: A 10-year study using data from a lightning location system, *Journal Geophysical Research*, 110 (D9), DOI: 10.1029/2004JD005332.
- Soriano L.R., De Pablo F., Tomas C., 2005, Ten-year study of cloud-to ground lightning activity in the Iberian Peninsula, *Journal of Atmospheric and Solar-Terrestrial Physics*, 67 (16), 1632-1639, DOI: 10.1016/j.jastp.2005.08.019.
- Soula S., Seity Y., Feral L., Sauvageot H., 2004, Cloud-to-ground lightning activity in hail-bearing storms, *Journal of Geophysical Research. Atmospheres*, 109 (D2), DOI: 10.1029/2003JD003669.
- Sulik S., 2021, Formation factors of the most electrically active thunderstorm days over Poland (2002-2020), *Weather and Climate Extremes*, 34, DOI: 10.1016/j.wace.2021.100386.
- Sulik S., 2022, A cloud-to-ground lightning density due to progressing climate change in Poland, *Environmental Challenges*, 9, DOI: 10.1016/j.envc.2022.100597.
- Sulik S., Kejna M., 2022, Spatial diversity of cloud-to-ground lightning flashes in the Kujawsko-Pomorskie Voivodeship (Poland), 2002-2019, *Geographia Polonica*, 95 (1), 5-23, DOI: 10.7163/GPol.0224.
- Sulik S., Kejna M., 2023, Comparison of thunderstorm days in Poland based on SYNOP reports and PERUN Lightning Detection System, *Miscellanea Geographica*, 27 (3), 134-146, DOI: 10.2478/mgrsd-2023-0019.
- Taszarek M., Allen J., Púčik T., Groenemeijer P., Czernecki B., Kolendowicz L., Lagouvardos K., Kotroni V., Schulz W., 2019a, A climatology of thunderstorms across Europe from a synthesis of multiple data sources, *Journal of Climate*, 32, 1813-1837, DOI: 10.1175/JCLI-D-18-0372.1.
- Taszarek M., Brooks H.E., Czernecki B., 2017, Sounding-Derived Parameters Associated with Convective Hazards in Europe, *Monthly Weather Review*, 145, 1511-1528, DOI: 10.1175/MWR-D-16-0384.1.
- Taszarek M., Czernecki B., Koziol A., 2015, A cloud-to-ground lightning climatology for Poland, *Monthly Weather Review*, 143 (11), 4285-4304, DOI: 10.1175/MWR-D-15-0206.1.
- Taszarek M., Pilguy N., Orlikowski J., Surowiecki A., Walczakiewicz S., Pilorz W., Piasecki K., Pajurek Ł., Pólrólniczak M., 2019b, Derecho evolving from a mesocyclone – A study of 11 August 2017 severe weather outbreak in Poland: Event analysis and high-resolution simulation, *Monthly Weather Review*, 147 (6), 2283-2306, DOI: 10.1175/MWR-D-18-0330.1.
- Taszarek M.T., Allen J., Púčik T., Hoogewind K.A., Brooks H.E., 2020, Severe convective storms across Europe and the United States. Part II: ERA5 environments associated with lightning, large hail, severe wind, and tornadoes, *Journal of Climate*, 33 (23), 10263-10286, DOI: 10.1175/JCLI-D-20-0346.1.

- Wang P., Shi J., Hou J., Hu Y, 2018, The identification of hail storms in the early stage using time series analysis, *Journal of Geophysical Research. Atmospheres*, 123 (2), 929-947, DOI: 10.1002/2017JD027449.
- Wapler K., 2013, High-resolution climatology of lightning characteristics within Central Europe, *Meteorology and Atmospheric Physics*, 122, 175-184, DOI: 10.1007/s00703-013-0285-1.
- Williams E., Boli B., Matlin A., Weber M., Hodanish S., Sharp D., Goodman S., Raghavan R., Buechler D., 1999, The behavior of total lightning activity in severe Florida thunderstorms, *Atmospheric Research*, 51 (3-4), 245-265, DOI: 10.1016/S0169-8095(99)00011-3.